

TECHNICAL UNIVERSITY OF CIVIL ENGINEERING BUCHAREST DOCTORAL SCHOOL

Research Report no. 2

Displacement response spectra for crustal and intermediate-depth ground motions

PhD candidate: Paul Olteanu

Adviser: Prof. Radu Văcăreanu

Contents

Ir	ntroduc	tion	5
1	Sha	llow and intermediate depth earthquakes	5
	1.1	Shallow earthquakes	7
	1.2	Intermediate depth earthquakes	11
2	Gro	und motion prediction equation for displacement response spectrum ordinates	13
	2.1	Database. The processing of records. Ground types	14
	2.2	Ground motion prediction equation	18
	2.2.	1 Moderate - strong national set of records	23
	2.2.	2 The set of digital records	28
	2.2.	3 Data set containing whole database	29
	2.3	Testing the attenuation model	30
3	Nor	llinear displacement spectra	34
	3.1	Database	36
	3.2	Hysteretic model	38
	3.3	Results	39
	3.3.	1 Amplification coefficient values	39
	3.3.	2 Influence of soil type	42
	3.3.	Influence of earthquake magnitude	42
	3.3.	4 Epicentral distance influence	43
	3.3.	5 Functional form for median values	44
	3.3.	6 Inelastic displacement spectra for a given seismic scenario	46
C	onclus	ions	48
A	cknow	ledgements	49
A	pendix		50
	Regre	ssion coefficients for the 1977 – 1990 earthquakes set	50
R	eferen	res	61

Table of figures

FIG. 1-1 TECTONICAL MAP OF THE EARTH, (NASA, 2002)	6
FIG. 1-2 SEISMOGENIC ZONES AFFECTING ROMANIA, (BIGSEES, 2017)	7
Fig. 1-3 Crustal (22.11.2014) vs. subcrustal quake (25.04.2009), $M_W = 5.4$, INCERC station	9
Fig. 1-4 Crustal (22.11.2014) vs. subcrustal quake (25.04.2009), $M_W = 5.4$, Giurgiu station	10
FIG. 1-5 LOCATION OF EPICENTRES FOR SUBCRUSTAL EARTHQUAKES IN ROMPLUS CATALOG, (INFP, 2017) LE	EFT. NW-
SE TRANSVERSAL SECTION AND POSITION OF HYPOCENTRES FOR EVENTS WHICH OCCURRED BETWEEN 1	982 AND
1989, Oncescu și Bonjer cited in (Frohlich, 2006) right	11
Fig. 1-6 Seismic tomography – CALIXTO experiment, cited in (Ismail-Zadeh, Mueller & Schuber	RT, 2005)
Fig. 1-7 Epicentre locations for earthquakes with $Mw \geq 6.3$ recorded in 20^{th} century, left. Evolutions	
MOMENT MAGNITUDE WITH FOCAL DEPTH (LUNGU, ALDEA, ARION & VĂCĂREANU, 2003), RIGHT	13
FIG. 2-1 ORIGIN, GROUND TYPE, MAGNITUDE AND EPICENTRAL DISTANCE DISTRIBUTION OF THE RECORDS IN DA	
Fig. 2-2 Ground types for Romanian territory and and neighbouring countries, adapted	
(Trendafiloski, Wyss, Rosset, & Marmureanu, 2009), based on USGS (Allen & Wald, 2007)	
Fig. 2-3 Distance metrics for GMPE.	
Fig. 2-4 Correlation of spectral displacement with epicentral and hypocentral distance for	
GROUND TYPE C, 1977, 1986, 1990 EARTHQUAKES RECORDED IN ROMANIA	
Fig. 2-5 Spectral displacement as a function of moment magnitude for $T=1.0s$, $150 \text{km} < D_{\text{epi}} < 0.05$	
GROUND TYPE C, MODERATE-LARGE NATIONAL RECORDS 1977, 1986, 1990. LINEAR (LEFT) AND QU.	
SHAPE (RIGHT).	
FIG. 2-6 DISPLACEMENT SPECTRA FROM 4 TH OF MARCH 1977 EARTHQUAKE FOR TWO SITES: INCERC BUCHAR	
CHIŞINĂU	
Fig. 2-7 Displacement spectra for 4.03.1977, 31.081986. 30.05.1990 Earthquakes recorded at 1	INCERC
BUCHAREST	
$Fig.\ 2-8\ Simulated\ vs.\ computed\ displacement\ spectra\ for\ 4.03.1977,\ 30.05.1990\ earthquakes\ recomputed\ displacement\ spectra\ for\ 4.03.1977,\ 30.05.1990\ earthquakes\ for\ 4.03.1977,\ 30.05.1990\ earthquakes\ for\ 4.03.1977,\ 30.05.1990\ earthquakes\ for\ 4.03.1990\ earthquakes\ for\ 4.03.1977,\ 30.05.1990\ earthquakes\ for\ 4.03.1990\ earthquakes\ for\ 4.03.199$	
INCERC, AND ONEȘTI SITES, ATTENUATION MODEL WITHOUT QUADRATIC TERM	
$Fig.\ 2-9\ Displacement\ demand\ as\ a\ function\ of\ magnitude\ and\ ground\ type\ C,\ type\ B\ respective Lorentz and\ ground\ type\ C,\ type\ B\ respective\ Lorentz and\ ground\ type\ C,\ type\ B\ respective\ Lorentz and\ ground\ type\ C,\ type\ B\ respective\ Lorentz and\ ground\ type\ type\ type\ type\ Lorentz and\ ground\ type\ t$	
Fig. 2-10 Displacement spectra for three epicentral distances, ground type C and B \dots	
FIG. 2-11 SIMULATED DISPLACEMENT SPECTRA FOR 4.03.1977, 31.08.1986 EARTHQUAKES, INCERC SIT	
QUADRATIC TERM	
FIG. 2-12 SIMULATION EREN SITE, 1986 EARTHQUAKE	
Fig. 2-13 Simulation of a seismic event with $M_{\rm w} = 7.50$, $D_{\rm epi} = 150$ km, median values, three sets	30
FIG. 2-14 NORMALIZED RESIDUALS (UP), QQ PLOT (DOWN)	
FIG. 2-15 INTER-EVENT RESIDUALS DEPENDENCE ON MAGNITUDE, WHOLE DATABASE	
FIG. 2-16 DEPENDENCE WITH DISTANCE OF INTRA-EVENT RESIDUALS, WHOLE DATABASE	32
Fig. 3-1 Elasto-plastic system and corresponding elastic system, after (Chopra, 2012)	
FIG. 3-2 DISTRIBUTION BY ORIGIN, GROUND TYPE, MAGNITUDE AND DISTANCE OF RECORDS IN THE DATABASE	
FIG. 3-3 DISTRIBUTION BASED ON EPICENTRAL DISTANCE AND PGA OF DATABASE RECORDS	
Fig. 3-4 Modified Takeda with stiffness degradation, (Utility Software for Data Processing, 20	
FIG. 3-5 INELASTIC AMPLIFICATION COEFFICIENTS, MEDIAN VALUES, GROUND TYPE B AND C (LEFT), DETAIL	
FIG. 3-6 INELASTIC AMPLIFICATION COEFFICIENTS, MEDIAN VALUES, GROUND TYPE B (LEFT) AND C (RIGHT)	
Fig. 3-7 Amplification coefficients, median values \pm 1 Σ , soil B (left) and C (right)	
Fig. 3-8 Σ_{C} variation with period, $\mu=3$. Ground type C	
Fig. 3-9 Soil influence, $\mu = 4$. Soil type B, left; type C right	
FIG. 3-10 EARTHQUAKE MAGNITUDE INFLUENCE, GROUND TYPE C	43
Fig. 3-11 Epicentral distance influence, ground type C, $\mu = 2.0$ and $\mu = 4.0$.	43
FIG. 3-12 C(T, M) SURFACE, SOIL TYPE B.	44
Fig. 3-13 Amplification coefficient – prediction vs. observed – soil type C and $\mu = 3.0$	45

Table list

Table 1-1 Crustal seismic zones, according to BIGSEES catalogue (Văcăreanu, Pavel, Aldea, Aric)N &
Neagu, 2015)	8
TABLE 2-1 DATABASE STRUCTURE, ACCORDING TO ROMPLUS CATALOG AND K-NET & KIK-NET NETWORKS	15
TABLE 2-2 GROUND TYPES ACCORDING TO EUROCODE 8 (CEN, 2004)	17
TABLE 2-3 MAGNITUDE SCALING OF DISPLACEMENT SPECTRA, INCERC SITE	24
TABLE 3-1 FUNCTIONAL FORM'S COEFFICIENTS, GROUND TYPE B	44
TABLE 3-2 FUNCTIONAL FORM'S COEFFICIENTS, GROUND TYPE C	45
TABLE A-1 SET 1, GROUND TYPE B, ORIGINAL GMPE (WITHOUT QUADRATIC TERM)	51
TABLE A-2 SET 1, GROUND TYPE C, ORIGINAL GMPE (WITHOUT QUADRATIC TERM)	52
TABLEA-3 SET 1, GROUND TYPE B, WITH QUADRATIC TERM	53
TABLE A-4 SET 1, GROUND TYPE C, WITH QUADRATIC TERM	54
Table A-5 Set 2, Ground type B	56
Table A-6 Set 2, Ground type C	58
TABLE A-7 SET 3, GROUND TYPE B	59
Table A-8 Set 3, Ground type C	60

Introduction

Romanian seismic design code P100-1/2013 (MDRAP, 2013), along with historical data which span 1000 years, leads to the conclusion that all of the Romanian territory is exposed to seismic hazard. Both probabilistic seismic assessment and deaggregation of seismic hazard studies (Văcăreanu, Pavel, Aldea, Arion & Neagu, 2015) conducted on numerous locations in the country showed that Vrancea sub crustal seismic source governs seismic hazard for a wide range of periods, even on sites located inside shallow crustal seismogenic zones.

To better describe the input data for displacement based design a study on relative displacement response spectrum was conducted. The chosen approach was, in the first phase, to construct an elastic response spectrum and then to generate inelastic displacement spectra from the elastic spectrum. For the first phase an attenuation law was developed, which generates spectral ordinates for a specific seismic scenario. In the second phase, the spectral coordinates are amplified by a coefficient which depends on the hysteretic model, system ductility and vibration period.

In the first part of the report some of the main features of both shallow and intermediate depth earthquakes are highlighted.

The second part is aimed at the development of the ground motion prediction equation for displacement response spectrum, taking into account both inter-event and intra-event variability. The equation was tested according to methodologies available in the literature and then some of the past seismic events where retrodicted using the equation.

The last part is devoted to the generation of the inelastic displacement spectra, using the coefficient method. The variability associated with this coefficient and the variability of the attenuation law is propagated to the inelastic displacement spectrum, leading to a probabilistic displacement demand, for a specific seismic event.

1 Shallow and intermediate depth earthquakes

Most of the earthquakes occur at the boundary zones of the tectonic plates. There, because of the relative motion tendency, the energy accumulates and plates deform until plate material fails and triggers the release of energy and sudden movement of the plates.

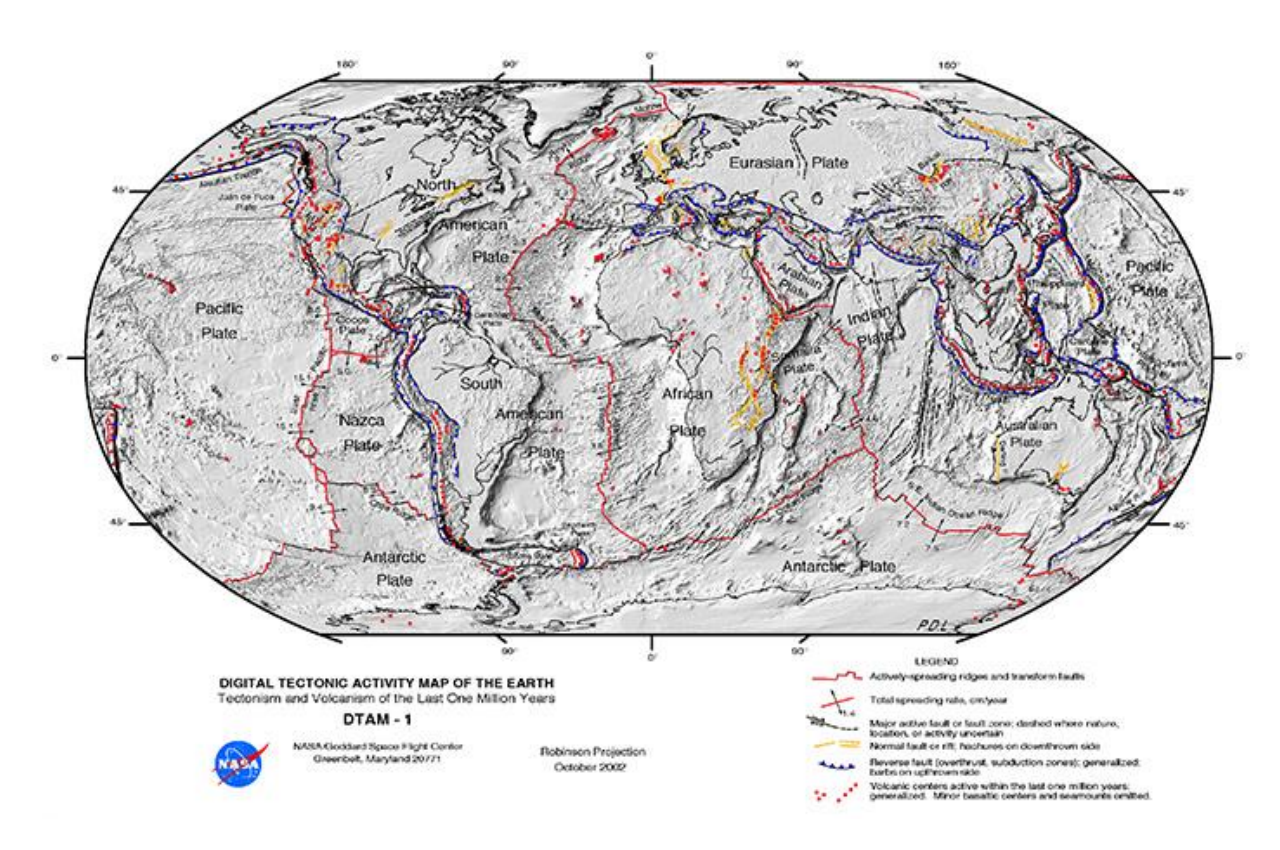


Fig. 1-1 Tectonical map of the Earth, (NASA, 2002)

Intraslab earthquakes occur away from the boundaries of the tectonic plates, in the so called stable continental regions. They take place less often than those produced along the boundaries and their intensity is usually small. Nevertheless, some of them have large magnitudes and can have devastating effects on environment and structures. For instance, in central US there is the New Madrid seismic source which generated three earthquakes with magnitudes exceeding 7.0 between 1811 and 1812. Currently, US design codes assign this region larger peak ground acceleration values than those given for California.

Depending on their depth, the earthquakes can be crustal (or shallow) with depths smaller than 60km, intermediate depth (or subcrustal) with focal depths at 60-300km and deep focus earthquakes with depths exceeding 300km. Focal mechanism of intermediate depth and deep focus earthquakes is not fully understood and is a subject of debate between researchers worldwide. Usually, subcrustal earthquakes occur in subduction zones, in the descending tectonical plate and are associated with volcanic activity. The pressure and temperature at these depths shouldn't normally allow the accumulated energy for two reasons. First, mechanical resistance of the rocks increases with depth and confinement and the shear stress which initiate rupture should be very large. Secondly, the temperatures which supposed to exist at these depths would rather lead to plastic flow of the rock than to brittle fracture. The first theory which tried to explain focal mechanism for deep earthquakes claimed that the rock suffers a phase transition between a loose phase and a more compact one. Following this transition an implosion would be produced which will trigger the earthquake. Another theory suggests that intermediate and deep focus earthquakes

are caused by dehydration of minerals with high content of water. Pore pressure rises and cancels the normal effect, which leads to a decrease of resistance and friction force. Therefore strength capacity is diminished and brittle failure can occur (Frohlich, 2006).

The main features which differentiate subcrustal from crustal earthquakes are the absence of surface waves (or their limitation in terms of intensity and duration), the pronounced presence of body waves and a smaller number of aftershocks.

1.1 Shallow earthquakes

As mentioned above, the entire territory of Romania is exposed to seismic hazard. Seismogenic areas producing crustal earthquakes are shown in the figure below.

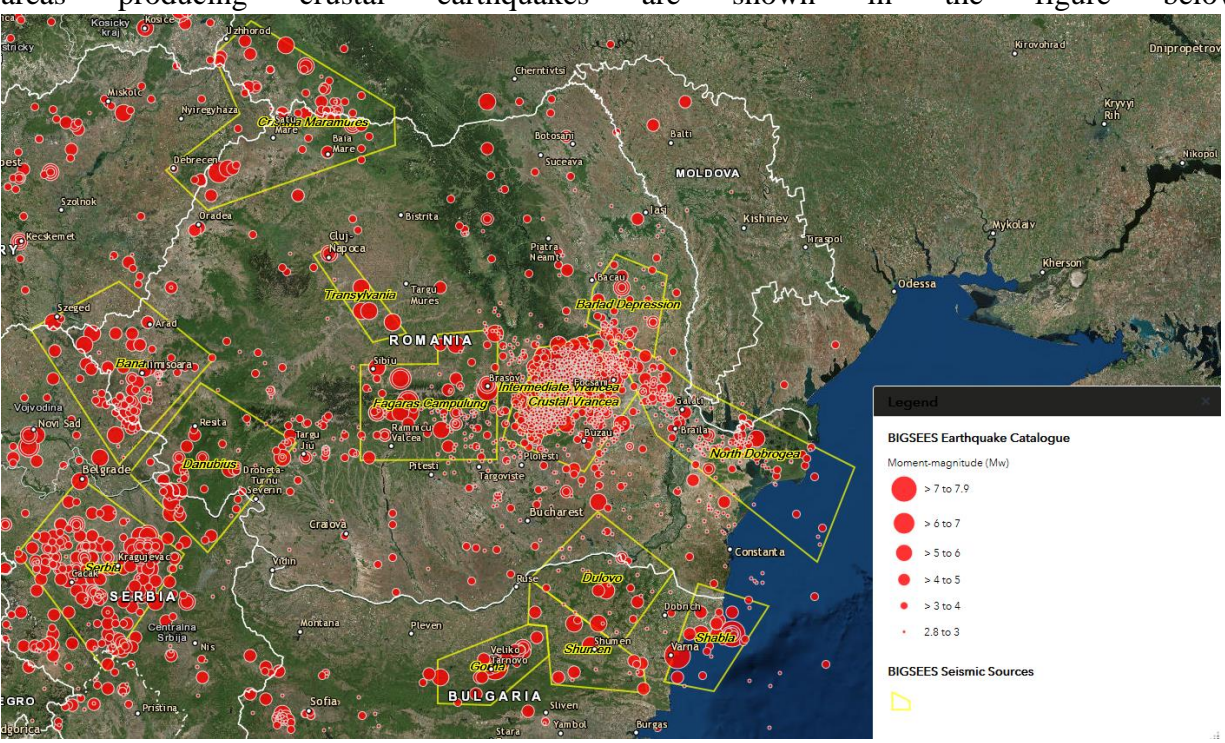


Fig. 1-2 Seismogenic zones affecting Romania, (BIGSEES, 2017)

The most significant zones are: Făgăraș – Câmpulung, Vrancea crustal, Banat, Crișana – Maramureș and Bârlad Depression.

The seismic catalog developed under the BIGSES project, which is based on the Romplus catalog, the SHEEC catalog obtained from the SHARE project and the DACEA project catalog, contains information about all seismic sources affecting the territory of the country. Some of the features of these crustal sources are taken from (Văcăreanu, Pavel, Aldea, Arion & Neagu, 2015) and shown below.

Seismic	Number of	Maximum
source	events	magnitude
Banat	57	6.4
Bârlad	40	5.8
Depression	40	3.6
Crișana	57	6.6
Danubius	54	6.0
Făgăraș	31	6.8
Pre-		
Dobrogean	54	5.7
Depression		

Seismic source	Number of events	Maximum magnitude	
Serbia	122	6.6	
Transilvania	11	6.2	
Vrancea crustal	40	6.2	
Dulovo	21	7.1	
Shabla	17	7.8	
Gorna	46	7.4	
Shumen	19	6.7	

Table 1-1 Crustal seismic zones, according to BIGSEES catalogue (Văcăreanu, Pavel, Aldea, Arion & Neagu, 2015)

A seismic hazard analysis for a site can be done in three ways: deterministic, probabilistic or neodeterministic. Probabilistic seismic hazard analysis, devised by Cornell in 1968, has several important benefits over the other two: it takes into account all identified seismic sources, earthquakes of any possible magnitude occurring at any distance from the site, and the uncertainties associated with all the parameters mentioned. One of the tools derived from probabilistic seismic hazard analysis is the deaggregation of the seismic hazard. In this way, it can be estimated the contribution of earthquake magnitudes, source to site distance and number of standard deviations from the median for a given spectral acceleration value. In (Văcăreanu, Pavel, Aldea, Arion, & Neagu 2015) are given the results of deaggregation analyses for some of the large cities in Romania. Unless the site is located near or inside a crustal seismic zone, the hazard is dominated by the Vrancea intermediate source. Even though the site is within the outlines of a crustal seismogenic region, seismic hazard is controlled for spectral periods greater than 1s also by Vrancea intermediate depth source (Pitești and Turda cities).

Theoretically, because of the lower credible magnitude of magnitude for crustal sources, crust earthquakes should have a lower content of long periods when compared to subcrustal events of magnitude close to their maximum credibility magnitude (e.g. a crust earthquake magnitude 6.1 produced by the Vrancea crustal area will have a lower content of lower frequencies than a quake with M > 7 produced by the Vrancea intermediate source).

Below are shown side by side acceleration and displacement response spectra for two earthquakes both having the same magnitude, $M_w = 5.4$, a shallow one (recorded on November $22^{nd}\ 2014$, with a focal depth of 40.9km) and an intermediate depth one (109.6km) for two sites, INCERC București and Giurgiu. Epicentral distances are 178km for the crustal earthquake and 145km for the subcrustal quake.

It can be seen from the adjacent figures that, despite the fact that the earthquakes have the same magnitude, the subcrustal earthquake involves higher acceleration values, so the seismic waves are attenuated differently at medium and large epicentral / hypocentral distances. For the INCERC station, the acceleration spectrum of the intermediate earthquake is well above that of the crust earthquake for periods of less than 1-2 s.

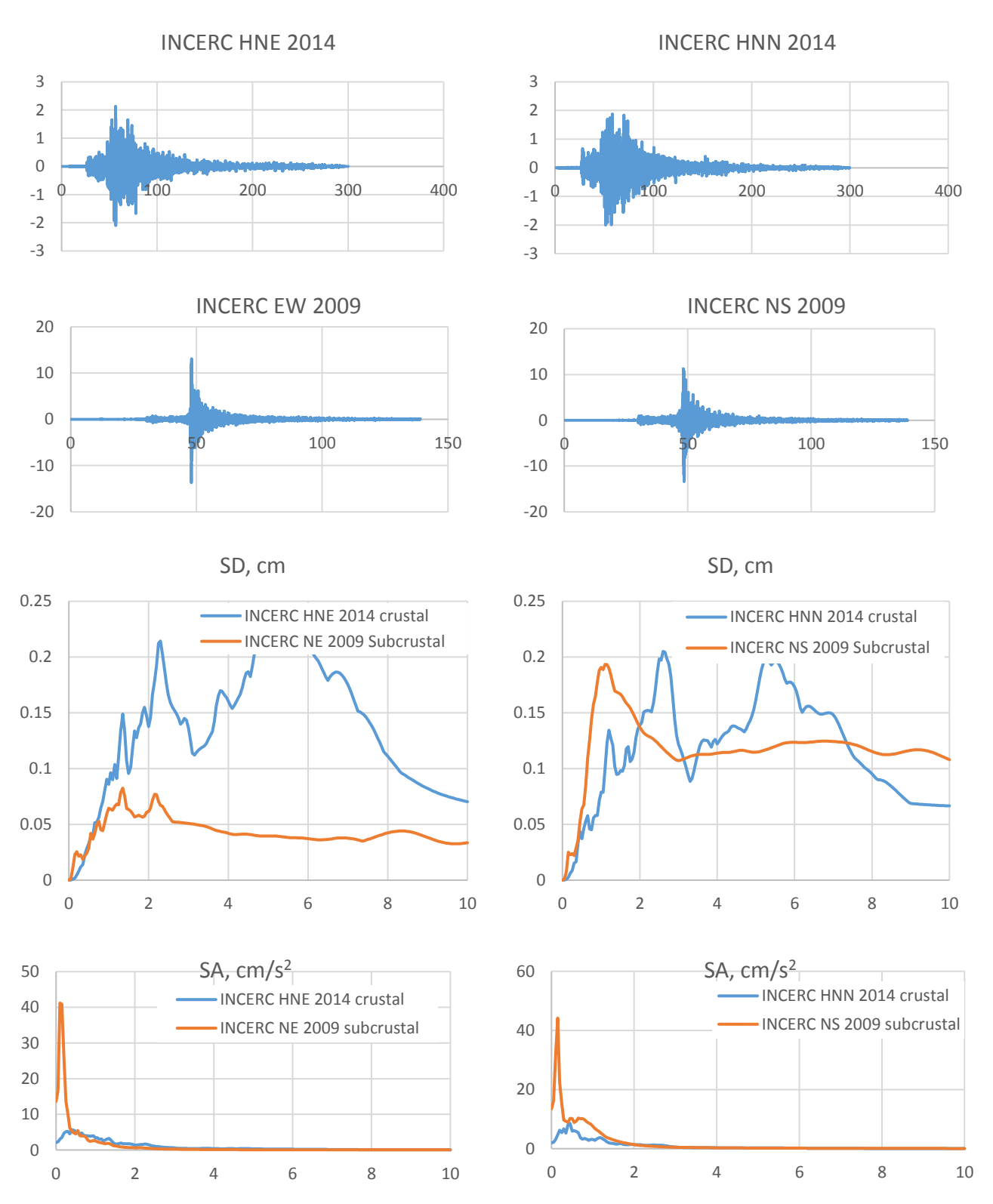


Fig. 1-3 Crustal (22.11.2014) vs. subcrustal quake (25.04.2009), $M_W = 5.4$, INCERC station

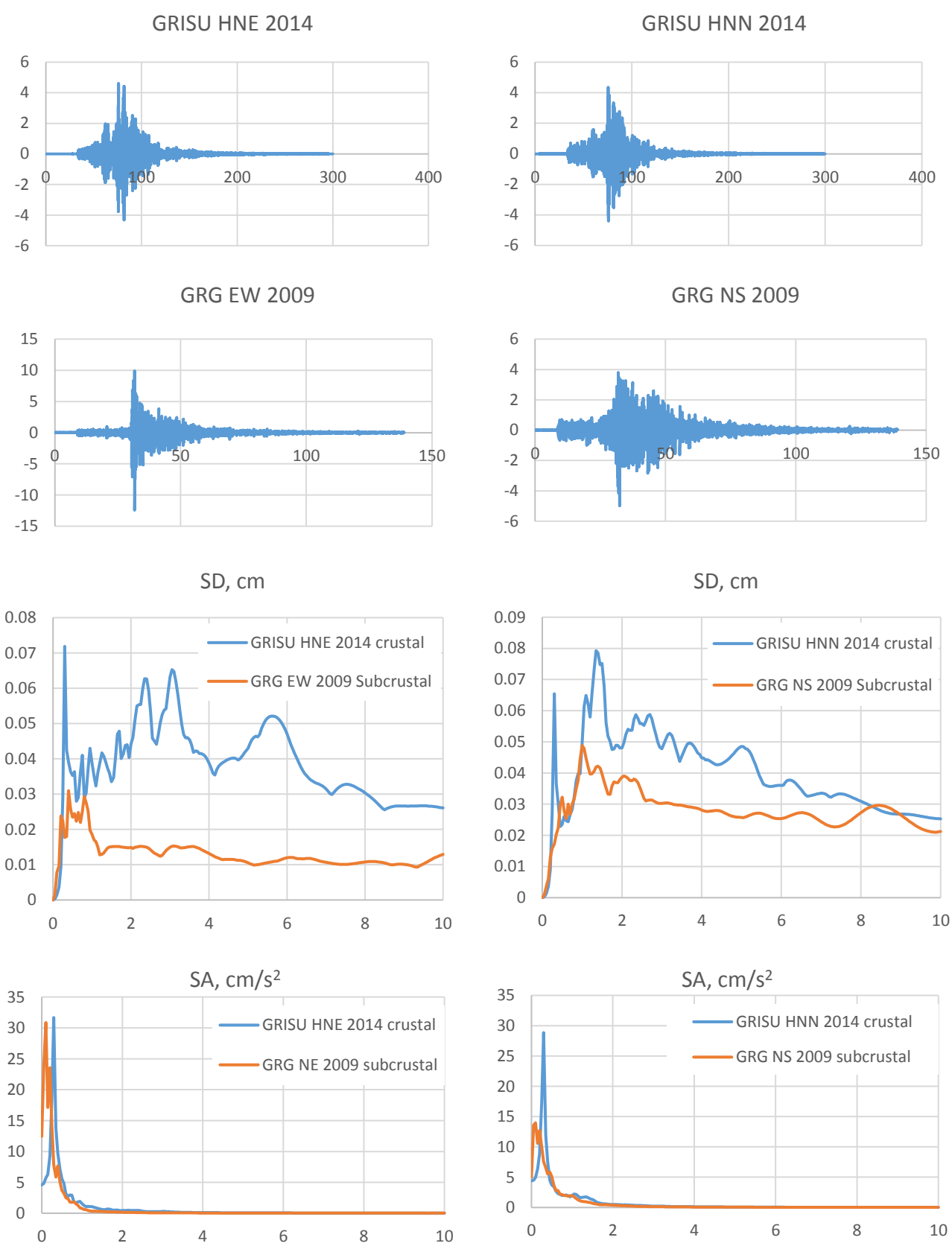


Fig. 1-4 Crustal (22.11.2014) vs. subcrustal quake (25.04.2009), $M_W = 5.4$, Giurgiu station

For Giurgiu station, acceleration spectra have approximately the same shape and size. Here too we can see an amplification of the acceleration values for the crustal earthquake, while for the intermediate depth the values respect the natural tendency of attenuation.

For the displacement spectra, both stations and horizontal components, the spectral ordinates of the shallow quake are above those of the intermediate one for almost all periods. A possible explanation would reside in the different types of waves generated by the two quakes. The crustal event should have a high content of surface waves – Rayleigh, Love – (Frohlich, 2006) which would entail superficial stratification in other manner than body waves would. In this way large amplifications could occur as compared with those of the subcrustal earthquake, which radiates mainly body waves (P and S). For Giurgiu station, the peaks of the displacement spectra occur at the same periods for both types of quakes but usually have different values. There seems to be a small tendency of shift towards right (period elongation) for the crustal quake, maybe a sign of nonlinear behaviour of superficial stratification.

1.2 Intermediate depth earthquakes

Vrancea subcrustal seismic source is the most important seismogenic source from the country and has prompted the interest of a large number of renowned seismologists in the last 30-40 years, including M. Oncescu, F. Wenzel, A. Ismail-Zadeh, and A. Soloviev. Intermediate depth seismic source Vrancea generates on average three or four large events in a century and their effects are felt at large distances. For this reason, this source is present from the first half of the 20th century in Western seismic catalogs.

The seismogenic region is NE-SW oriented, intermediate depth earthquakes occurring mainly between 70-110km and 130-160km. Below 160km the activity suddenly ceases.

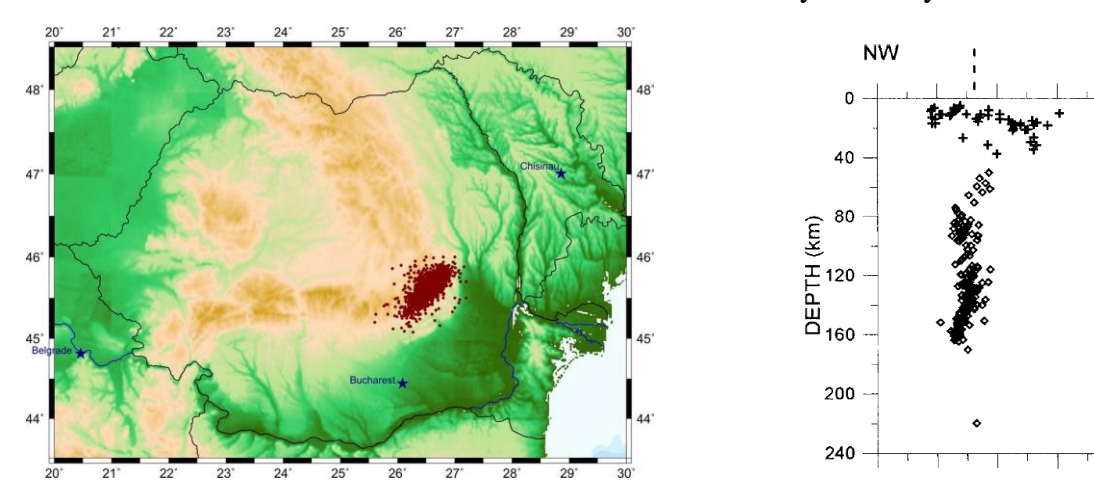


Fig. 1-5 Location of epicentres for subcrustal earthquakes in ROMPLUS catalog, (INFP, 2017) left. NW-SE transversal section and position of hypocentres for events which occurred between 1982 and 1989, Oncescu şi Bonjer cited in (Frohlich, 2006) right.

Intermediate depth earthquakes usually occur in subduction zones where two tectonic plates are in contact, one slipping and sinking underneath the other. Earthquakes can be classified (Sucuoglu & Akkar, 2014) as interface earthquakes (located in the contact zone of the two plates) and interplate

SE

earthquakes (located in the slab sinking at high depths). For Vrancea seismic zone there is evidence that subduction ceased 10 million years ago (Frohlich, 2006). Since 1970s, the researchers hypothesized that the intermediate depth seismicity in the Vrancea area is related to the dipping of a portion of a tectonic plate into the mantle (asthenosphere). This would be the last stage of the subduction phenomenon. The nature of the plate (oceanic or continental) is for the time being a subject of debate among seismologists.

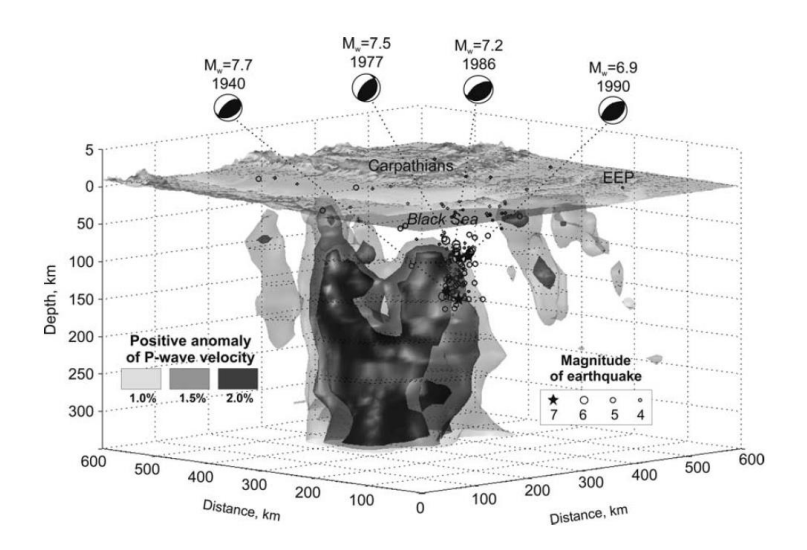


Fig. 1-6 Seismic tomography - CALIXTO experiment, cited in (Ismail-Zadeh, Mueller & Schubert, 2005)

The fact that there is a low seismic activity, located at depths of 40-70km, has led to the idea that the plate fragment is already detached from the continental crust. The fragment, originally quasi-horizontal, has reached a nearly vertical position, is colder and denser than the surrounding environment and descends under the action of gravity. The bottom of the descending fragment is located at a minimum depth of 350km[†]. Interaction between gravitational forces, buoyancy, viscous and friction forces produces in the descending body shear forces large enough to trigger earthquakes (Ismail-Zadeh, Mueller & Schubert, 2005).

The epicentres of the subcrustal Vrancea earthquakes are located inside a small rectangular region, with dimensions of about 80x40km. There is a tendency of increasing magnitude with increasing depth. This phenomenon was explained by the increasing resistance of the asperity cell along with the increase of the depth of the lithostatic pressure. There is also present a marked NE – SW mobility of the epicentres of intermediate depth earthquakes generated by Vrancea source, which causes localization of effects towards Bucureşti or Moldova (Lungu, Aldea, Arion & Văcăreanu, 2003).

-

[†] It is the lowest depth of seismic tomography conducted in 1999 within the CALIXTO project (Ismail-Zadeh, Mueller & Schubert, 2005).

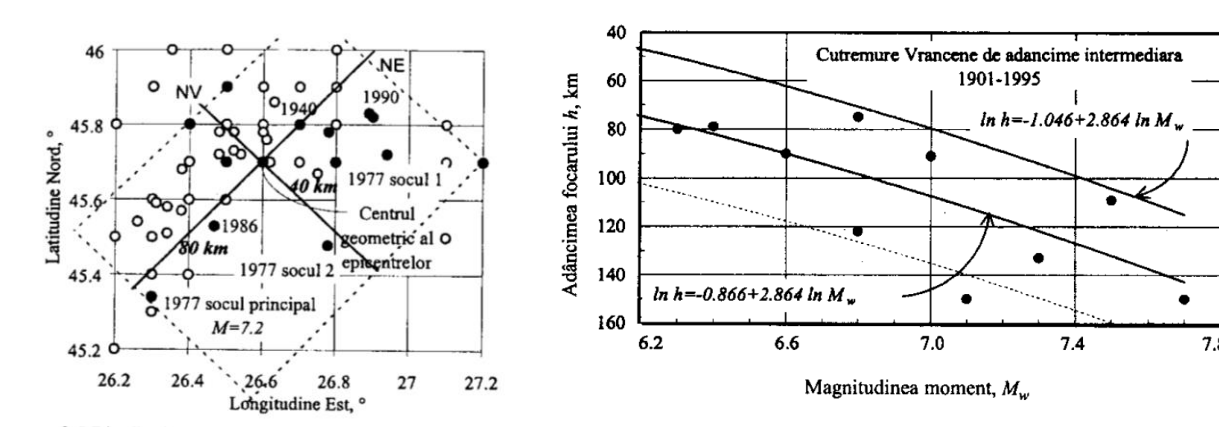


Fig. 1-7 Epicentre locations for earthquakes with $Mw \ge 6.3$ recorded in 20^{th} century, left. Evolution of moment magnitude with focal depth (Lungu, Aldea, Arion & Văcăreanu, 2003), right.

Regression relations that correlate the magnitude of the earthquake with the length of the rupture surface and the surface area of the rupture (Wells & Coppersmith, 1994) can provide the maximum magnitude of the source. In (Lungu, Aldea, Arion & Văcăreanu, 2003) are given the maximum values for the surface rupture length -150-200km – and for surface rupture area -8000km^2 . These values lead to a maximum credible magnitude of $Mw \approx 8.1$. According to regression equations cited in the above mentioned publication, the focal depth of the maximum credible earthquake would be located at a depth between 140 and 170km.

2 Ground motion prediction equation for displacement response spectrum ordinates

Ground motion prediction equations (GMPE) represents quantitatively the way in which a parameter of the seismic movement decreases with increasing source-site distance. They are typically empirically developed, starting from a functional form that mathematically expresses how the parameter of interest varies with distance, magnitude, and other parameters considered important. Using a database of records representative for the site, and then using regression techniques, one can determine the coefficients of the functional form.

The first GMPE was obtained by Esteva and Rosenbluth and published in 1964, while in 2016 there were available more than 400. The vast majority of prediction equations use the peak ground acceleration as a parameter of interest for the seismic motion. In the 1990s the concepts of *Performance Based Design* and *Displacement Base Design* were devised, through which a better control on the structural behaviour can be achieved. These concepts have as a start point the idea that the damage caused by earthquakes to building structures is better related to the peak relative displacements than to peak accelerations. Although GMPE for peak ground displacement where available since 1974 – Orphal & Lahoud for California cited in (Douglas, 2016) – only in 2004 (Faccioli, Paolucci & Rey, 2004) made significant efforts towards the development of GMPE for relative displacement response spectrum.

The reason why it was considered appropriate to obtain the displacement spectra by direct processing of the records and not by their derivation from the accelerations response spectra is that

the displacement spectra vary more strongly with moment magnitude than the acceleration spectra. Moreover, the shape and ordinates of the displacement spectra are much more sensitive to the way acceleration processing/correction was performed than the acceleration spectrum ordinates.

The purpose of this chapter is to develop a GMPE for the relative displacement spectrum applicable in Romania, a territory largely exposed to the seismic hazard generated by the Vrancea subcrustal source.

2.1 Database. The processing of records. Ground types

In order to develop a GMPE, a database containing strong motion records for each soil class was compiled. The databank used for this study contains 272 ground motion records (544 horizontal components) generated by 15 intermediate depth earthquakes. A number of nine earthquakes where produced by Vrancea subcrustal source (235 records), while six were recorded in Japan. The database contains earthquakes with magnitudes $5.2 \le M_w \le 7.4$ with focal depths in the range 66-154km. From the total number of records, 169 were from stations located on type C ground (62%), the remainder being recorded on ground type B. Digital records add to 57% of the total number and are generated by earthquakes having $5.2 \le M_w \le 7.1$. Therefore, most earthquakes in the database, with $M_w > 7.0$, were analogical recorded in Romania.

Because of the small number of ground motion recorded on firm ground (rock or rock-like formation including at most 5 m of weaker material at the surface and $V_{s30} > 800 \text{m/s}$, type A according to Eurocode 8) and scarcity of strong ground motions behind the Carpathian Arch (Transylvania), they were not selected in the database. Thus, the GMPE is valid in the area located in front of the Carpathian Arch: Moldova, Muntenia and Dobrogea on ground types B and C.

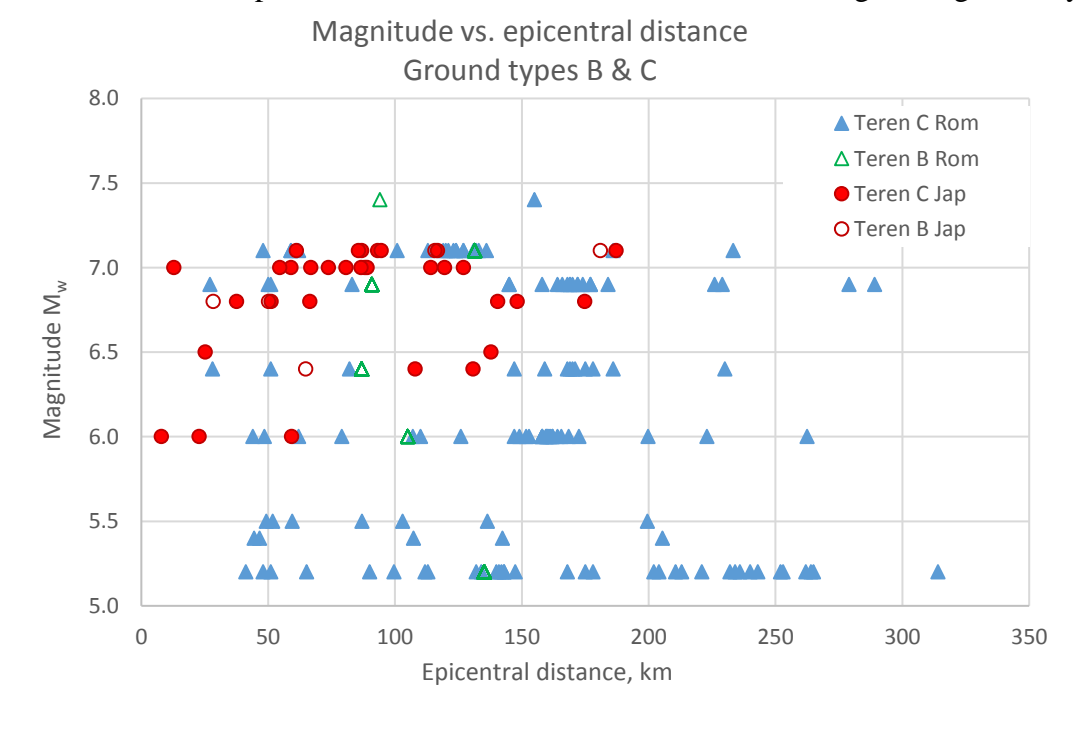


Fig. 2-1 Origin, ground type, magnitude and epicentral distance distribution of the records in database

The decision to include non-Romanian records was taken as a result of the lack of high quality (digital) national records for earthquakes with $Mw \ge 6.0$. Recommendation of researchers John Douglas and Julian Bommer (Văcăreanu, Pavel, Aldea, Arion & Neagu, 2015), is to use records from other countries, especially when there are not enough local records. Furthermore, it is desirable to extend the databases with "import" records to obtain GMPE, especially when † local records do not cover the full range of magnitudes and distances for which the attenuation model is desired.

The Japanese earthquakes (Strong Motion Seismograph Networks (K-NET, KiK-net), 2017) have focal depth in the range of 66-122km and magnitudes $6.0 \le M_w \le 7.1$. Unfortunately, the database of the two networks does not include records for seismic events with $M_w > 7.1$ for depths between 60 and 200km.

Date	Time	Latitude (N)	Longitude (E)	Focal depth (km)	M_{w}	Number of horizontal components	Obs
1977/03/04	19:21:54	45.77	26.76	94	7.4	4	RO
1986/08/30	21:28:37	45.52	26.49	131.4	7.1	70	RO
1990/05/30	10:40:06	45.83	26.89	90.9	6.9	92	RO
1990/05/31	00:17:48	45.85	26.91	86.9	6.4	66	RO
2004/10/27	20:34:36	45.84	26.63	105.4	6.0	92	RO
2005/05/14	01:53:21	45.64	26.53	148.5	5.5	14	RO
2005/06/18	15:16:42	45.72	26.66	153.7	5.2	14	RO
2009/04/25	17:18:48	45.68	26.62	109.6	5.4	10	RO
2013/10/06	01:37:21	45.67	26.58	135.1	5.2	108	RO
2001/12/02	22:02:00	39.40	141.26	122	6.4	6	JAP
2003/05/26	18:24:00	38.81	141.68	71	7.0	24	JAP
2005/07/23	16:35:00	36.58	140.14	73	6.0	6	JAP
2008/07/24	00:26:00	39.73	141.63	108	6.8	16	JAP
2011/04/07	23:32:00	38.20	141.92	66	7.1	18	JAP
2013/02/02	23:17:00	42.70	142.23	102	6.5	4	JAP

Table 2-1 Database structure, according to ROMPLUS catalog and K-NET & Kik-net networks

In (Faccioli et al., 2007), (Cauzzi & Faccioli, 2008) attention is drawn to the sensitivity of the displacement spectra to the quality of the recording (digital vs. analog) and the way the accelerograms are processed. Analogue records obtained during seismic movements are affected by various types of errors (due to instrumentation and digitization, among others) that affect recording quality, especially in high frequency (> 20Hz) and low (<0.5Hz) frequencies. Low frequency errors affect the history of velocities and displacements, while high frequency errors particularly affect the peak ground acceleration. To limit the effect of these errors, various

15

[†] For instance, when the GMPE should cover seismic events considered possible from the hazard analysis near the upper limit but which have not yet occurred or have occurred and there are no records.

corrections and filters are used. Filtering removes the errors, but with them it eliminates the useful information present in the filtered frequency range (Borcia, 2008).

The analog records were obtained in a form already processed, the waveforms were not further adjusted. The methodology used for filtering is described in (Borcia, 2008). The filtering procedure is not uniformly applied, the filter is of the Ormsby type and the cutting thresholds are 0.15-0.25Hz for low frequencies and 25-28Hz for high frequencies. The digital records were processed by applying a fourth order Butterworth filter with the lower threshold at 0.05Hz while the higher is at 50Hz.

Seismic design codes take into account the nature of the ground on the site through the measurable parameters of the soil characteristics. Topographic and underground stratification effects are only considered by assigning a soil type. In the United States, Europe and Japan, the parameter that decides the belonging of a plot to a particular category is the average shear wave velocity in the first 30 meters from the free surface, $v_{s,30}$. If this parameter is not available, the blow counts in the standard penetration test can be used, N_{SPT} . The average shear wave velocity is calculated with the following equation:

$$v_{s,30} = \frac{30}{\sum_{i=1,N} \frac{h_i}{v_i}}$$
 Ec. 2-1

where h_i and v_i denote the thickness and speed of the shear waves in the i^{th} layer of the total N layers of the first 30m from ground surface.

The national design code for seismic design, P100-1/2013, (MDRAP, 2013) uses the classification of ground types following the approach of Lungu (1997), cited in (Lungu, Văcăreanu, Aldea & Arion, 2000). Control periods T_C și T_D are evaluated according to the following relationships for locations exposed to moderate or strong earthquakes.

$$T_{C} = 2\pi \frac{EPV}{EPA}$$
, Ec. 2-2
$$T_{D} = 2\pi \frac{EPD}{EPV}$$

where EPA, EPV, EPD denote the averaged values using a mobile window of 0.4s of the ordinates of the acceleration, velocity and displacement spectra (Lungu et al., 1996).

P100-1/2013 code recommends for important structures (importance classes I and II) to carry out studies to characterize field conditions on the site: the shear and compression wave velocity profile, v_s and v_p , for strata up to the base rock or minimum for the first 30m, the terrain stratification (thickness, density, type), the weighted average value v_s on the considered stratification. Then the soil is classified according Eurocode 8.

Ground Type	Profile	$v_{s,30}$ (m/s)	N _{SPT} (blows/30cm)	c _u (kPa)
A	Rock or other rock-like geological formation, including at most 5 m of weaker material at the surface.	> 800	-	-
В	Deposits of very dense sand, gravel, or very stiff clay, at least several tens of metres in thickness, characterised by a gradual increase of mechanical properties with depth.	360 - 800	> 50	> 250
С	Deep deposits of dense or medium-dense sand, gravel or stiff clay with thickness from several tens to many hundreds of metres.	180 - 360	15 - 50	70 - 250
D	Deposits of loose-to-medium cohesionless soil (with or without some soft cohesive layers), or of predominantly soft-to-firm cohesive soil.	< 180	< 15	< 70
E	A soil profile consisting of a surface alluvium layer with v_s values of type C or D and thickness varying between about 5 m and 20 m, underlain by stiffer material with $v_s > 800$ m/s.			

Table 2-2 Ground types according to Eurocode 8 (CEN, 2004)

In this study, Eurocode 8 (CEN, 2004), terminology was used. This allows classification based on the weighted average shear wave's velocity for layers located in the first 30m. It has the advantage that it is a proven method (used in countries like US, Japan), is recommended by national seismic design code, and can be applied relatively easily. Within the BIGSEES project it was created a database containing stratifications, compression waves velocities, etc. Most boreholes measurements were conducted in the 1970's, and information on shear wave velocities is no longer available (Neagu, Arion, Aldea, Văcăreanu & Pavel, 2017). There is a small number of boreholes with depths between 13m-153m, located in Bucharest for which there are complete data.

In (Allen & Wald, 2007) a methodology is proposed to obtain information on shear wave velocity using topographic slope data. The latter were taken over during space shuttle Endeavour's mission in 2000. The US researchers have found a correlation between the topographic slope and the data recorded by $v_{s,30}$ in several locations in the United States, Taiwan, Italy, Puerto Rico, New Zealand and Japan. The conclusion of the study is that the $v_{s,30}$ data from the slope topography survey can be used to describe the field conditions at regional level.

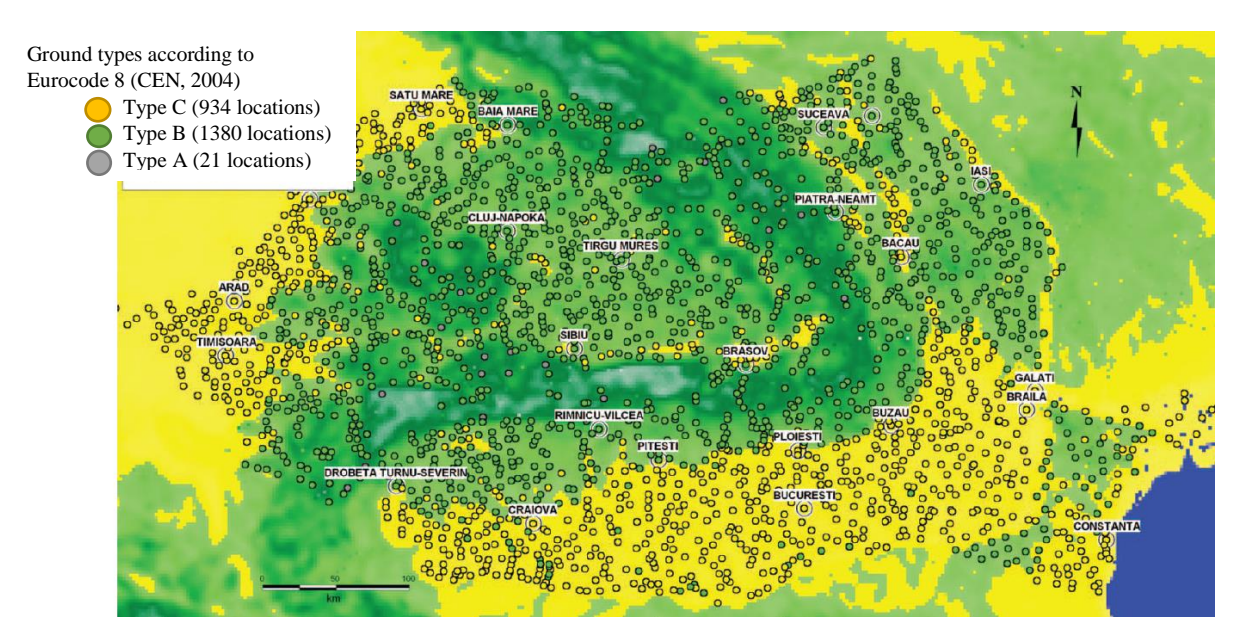


Fig. 2-2 Ground types for Romanian territory and and neighbouring countries, adapted after (Trendafiloski, Wyss, Rosset, & Marmureanu, 2009), based on USGS (Allen & Wald, 2007)

Studies by Neagu and Aldea, cited in (Neagu, Arion, Aldea, Văcăreanu & Pavel, 2017), using data from 19 bore holes in Bucharest showed a good correlation between values given by (Allen & Wald, 2007) study and field measurements. The differences between the two data sets are on average of 12% (the slope method slightly underestimating the shear wave velocity), with a maximum difference of 28%. In spite of all these differences, ground type classification is the same for both methods for the sites surveyed.

In this study, the values of the shear velocities for the first 30m for the locations where the waveforms were recorded, are according to (Allen & Wald, 2007) and available on United States Geological Survey website, (USGS, 2017). Japanese sites, are usually assigned $v_{s,30}$ values (Strong Motion Seismograph Networks (K-NET, KiK-net), 2017). However, some sites do not have boreholes extending to the depth of 30m, so the values for $v_{s,30}$ were determined using the methodologies described in (Boore, 2004) and using the database files available in (Boore D. , 2017).

2.2 Ground motion prediction equation

The coefficients of the attenuation model for relative displacement response spectrum ordinates where determined using two stage regression analysis, following the methodology given in (Joyner & Boore, 1993). Two stage regression is used in order to uncouple magnitude and distance scaling. The method is used extensively in determining the coefficients of attenuation laws, along with the algorithm given by Abrahamson & Youngs (1992). Together with the two-step regression, Joyner and Boore introduced a single-stage regression method in the same article, the coefficients controlling magnitude dependence and distance dependence being determined simultaneously. Both methods are based on maximizing the likelihood of the set of observations.

The first step of the two stage regression algorithm consists in determining the coefficients which give the distance dependence, and an array of deviations (for each record). In the second step

coefficients expressing magnitude dependence are determined by maximizing the likelihood of the set of observations.

The functional form of the GMPE, (Joyner & Boore, 1993), is:

$$\lg(SD) = a + b(M_W - 6) - \lg \sqrt{D_{epi}^2 + h^2} + c \sqrt{D_{epi}^2 + h^2} + \varepsilon_r + \varepsilon_e$$
 Ec. 2-3

where SD (cm) is the spectral ordinate of relative displacements (as a geometrical mean of two perpendicular horizontal components) for 5% damping, M_w is moment magnitude of the earthquake, D_{epi} (km) is the epicentral distance, a, b, c and h are coefficients which are determined through regression, ϵ_r is an independent random variable normal distributed which takes values for every record, ϵ_e is an independent random variable normal distributed with values for every earthquake and lg denotes base 10 logarithm. Random variable ϵ_r has the mean equal to 0 and variance σ^2_r , represents the variability between seismic stations (intra-event), while random variable ϵ_e has 0 mean and variance σ^2_e , representing the variability between seismic events (interevent). Total variance is:

$$\sigma = \sqrt{\sigma_r^2 + \sigma_e^2}$$
 Ec. 2-4

Original functional form (Joyner & Boore, 1993) uses Joyner-Boore distance (the shortest distance from the seismic station to the vertical projection of the ruptured surface) as metric instead of D_{epi} which was used in this study. Because Joyner-Boore distances are not available for intermediate depth earthquakes generated by Vrancea source, epicentral distance was chosen as predictor variable.

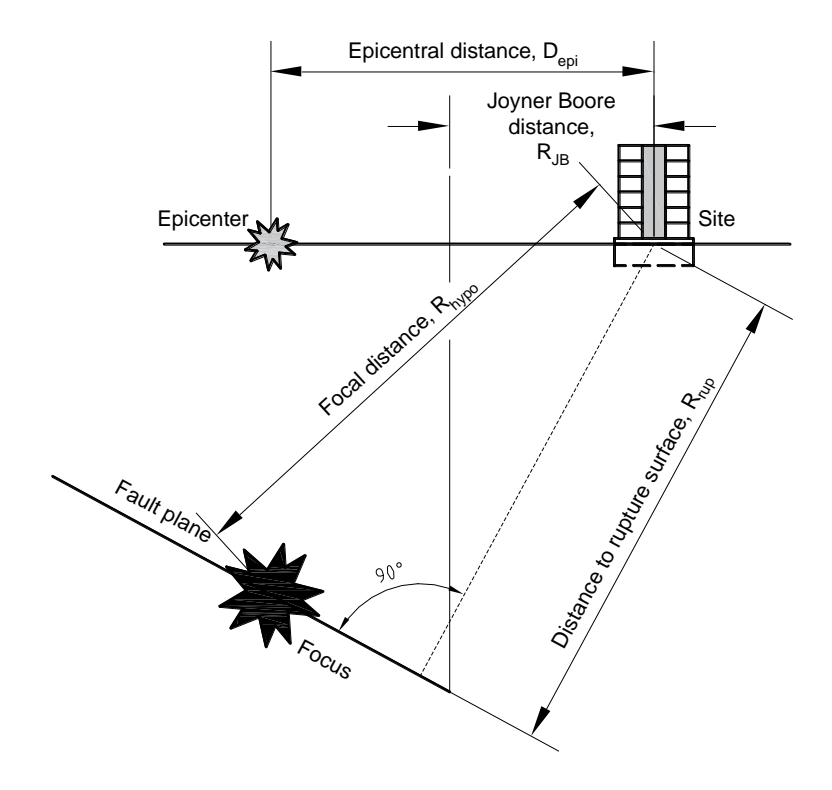


Fig. 2-3 Distance metrics for GMPE

Atenuation models by Văcăreanu et al 2015, (Văcăreanu, Pavel, Aldea, Arion & Neagu, 2015) use as distance metric hypocentral (focal) distance. For this study, epicentral distance proved to be better correlated with recorded spectral displacements than hypocentral distance. Moreover, formally, the significance of the epicentral distance is closer to the Joyner-Boore distance than the focal distance. Below are presented side by side the correlations of spectral displacements (for moderate - large earthquakes recorded in Romania) with D_{epi} şi R_{hypo} for T=1.0s.

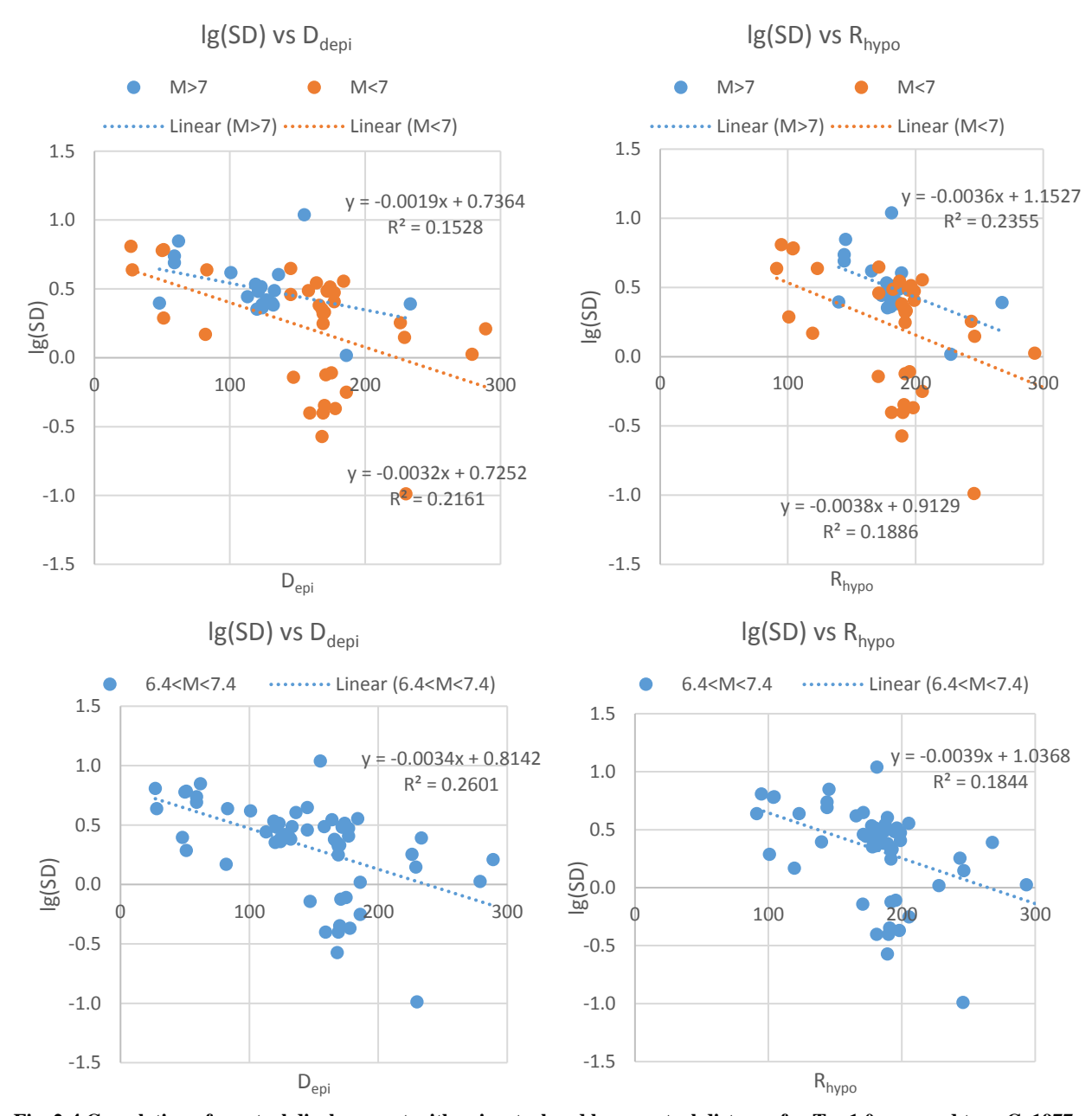


Fig. 2-4 Correlation of spectral displacement with epicentral and hypocentral distance for T=1.0s, ground type C, 1977, 1986, 1990 earthquakes recorded in Romania.

One can notice that for large earthquakes, focal distance correlates well with the logarithm of the spectral ordinate, while for $M_w < 7.0$ and for the set containing national records of moderate-large events (1977, 1986 and 1990) epicentral distance correlates better.

Moment magnitude scale was selected to express the size of the earthquakes used in the database, latest attenuation models developed in US, New Zeeland and Europe using it as a predictor. The functional form used in this study considers a magnitude independent term for the contribution of path/distance attenuation.

The first two terms of the GMPE take into account the quasilinear variation of the logarithm of amplitude with magnitude. The third term corresponds to the geometric attenuation of the seismic waves, which decreases proportionally with the inverse of the distance. The fourth term corresponds to the inelastic attenuation, due to the media traversed by the seismic waves.

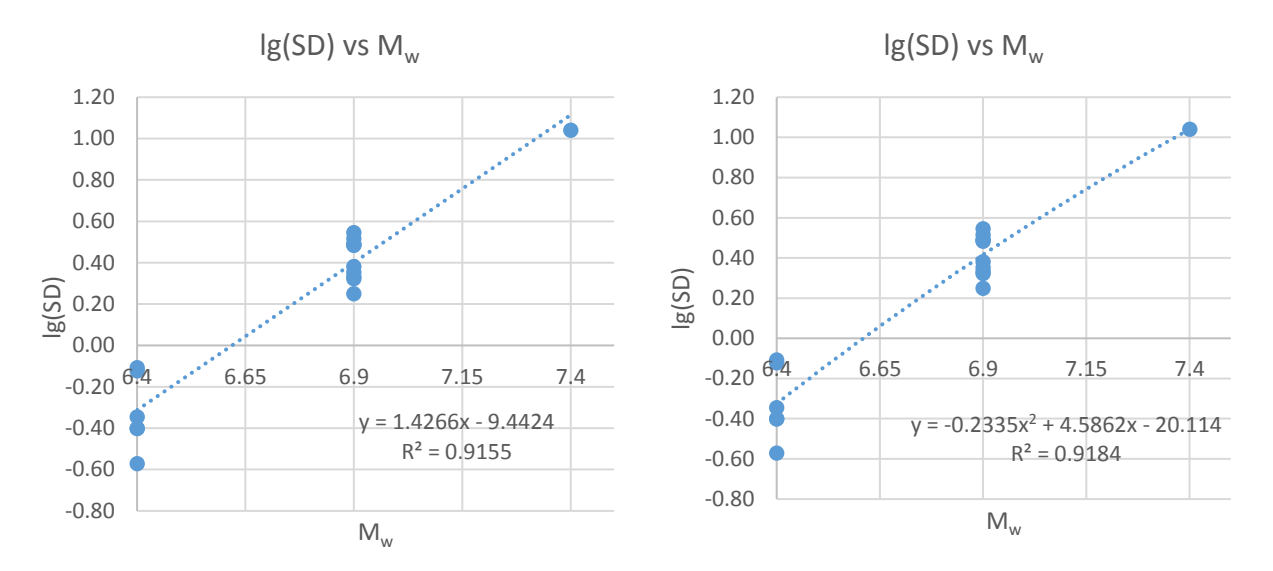


Fig. 2-5 Spectral displacement as a function of moment magnitude for T=1.0s, $150km < d_{epi} < 175km$, ground type C, moderate-large national records 1977, 1986, 1990. Linear (left) and quadratic shape (right).

The above figure shows good correlation for both types of magnitude variation with spectral displacements. A slightly better correlation is observed for a quadratic expression of the log variation (SD), which would include an additional term in the functional form.

In this study, the relative displacement spectrum ordinates are expressed as the geometric mean of two perpendicular horizontal components. It is preferred to perform the regression analysis based on geometric mean for it is regarded as statistically representative for any random direction. Most attenuation models use the geometric mean instead of the maximum value as the expected parameter. The logarithm of the geometric mean (the result of the attenuation relationship) can be regarded as the arithmetic mean of the logarithms of the two components:

$$GM(SD_{1}, SD_{2}) = \sqrt{SD_{1} \times SD_{2}} = (SD_{1} \times SD_{2})^{1/2}$$

$$\lg[(SD_{1} \times SD_{2})^{1/2}] = \frac{1}{2}\lg(SD_{1} \times SD_{2}) = \frac{\lg(SD_{1}) + \lg(SD_{2})}{2}$$
Ec. 2-5

An exception to this is the study performed by (Akkar & Bommer, 2007) in which regressions were made for both the maximum values of the two components of peak ground velocity (PGV) and for their geometric mean (which, according to authors of the study, did not significantly reduce the random variability of residuals).

Variability between seismic stations (intra-event), expressed through variance σ^2_r can be computed, adapted after (Boore, Joyner & Fumal, 1997), as:

$$\sigma_r^2 = \frac{1}{no.rec} \sum_{j=1}^{no.rec} \frac{\left(|gY_{1j} - |gY_{2j}| \right)^2}{4}$$
 Ec. 2-6

where indexes 1 and 2 are the horizontal perpendicular components of the record j. The original expression has natural logarithms instead decimal logarithms at the right side of the equation, and the GMPE was also expressed in terms of natural logarithms.

The coefficients of the attenuation model were determined separately for ground type B and ground type C, due to much smaller ordinates and different spectral shapes of displacement spectra computed on ground type B. Moreover, convergence problems have been encountered, especially for ground type B. In this case, coefficients were determined by single stage regression, for some of the periods.

Aiming a better prediction of the response for large earthquakes (M_w >7.1) it was explored the opportunity of adding a quadratic term to the basic attenuation model, leading to the following equation:

$$\lg(SD) = a + b(M_W - 6) + d(M_W - 6)^2 - \lg\sqrt{D_{epi}^2 + h^2} + c\sqrt{D_{epi}^2 + h^2} + \varepsilon_r + \varepsilon_e$$
 Ec. 2-7

which has indeed led to the improvement of predictions for the earthquake recorded on 4th of March 1977 and has, to some extent, reduced the residual values.

Due to the fact that all the moderate and major earthquakes recorded in Romania are analogical, the calculated values of the displacement spectra can be considered valid up to periods of maximum 4s. Efforts have been made to predict spectral values up to 8s. National records post 2004 are digital and high quality, but were produced by earthquakes with $M_w \le 6.0$. This was one of the reasons why Japanese intermediate depth earthquakes, with magnitudes close to the major events in Romania, were added to the database. Recordings from Japan are quality digital records that can be considered reliable until periods of over 10s.

To investigate database dependence of the attenuation model, the regression was performed on three sets of data, one which contains national records of moderate-large earthquakes of 1977, 1986 and 1990, the second set of data was made up of digital records only (national, with $5.2 \le M_w \le 6.0$ and Japanese, from Kik-Net and K-NET networks, with $6.0 \le M_w \le 7.1$) with coefficients calculated up to periods of 8s and, finally, a set which contains the entire database and coefficients calculated for periods in the range 0.1 - 4.0s.

Due to the scarcity of firm ground records (rock and rocky lands, type A according to Eurocode 8) and the lack of records of strong seismic movements behind the Carpathian arch, these were not selected in the data. The GMPE is valid in the area in front of the Carpathian arch: Moldova, Muntenia and Dobrogea on land types B and C.

2.2.1 Moderate - strong national set of records

The first data set includes records from 4^{th} of March 1977 earthquake ($M_w = 7.4$), 31^{th} of August 1986 ($M_w = 7.1$), 30^{th} and 31^{th} of May 1990 ($M_w = 6.9$ and $M_w = 6.4$). These are distinguished by the large displacement demands imposed on high rise structures (T > 1.0s) located on ground type C, this feature being common amongst historical earthquakes (1940 earthquake that inflicted heavy damage on tall buildings in Bucharest, and, probably, the devastating earthquake of 1802 that caused the collapse of Coltei Tower and the large majority of bell towers in Bucharest).

Due to the fact that the set of accelerograms from these earthquakes had already been processed (Borcia, 2008), no further adjustments were made. The records were then sorted by the ground type and then the computation of elastic displacement spectra for a 5% damping was performed. The software used for spectra calculation was Seismosignal (Seismosoft, 2016) for a range of periods between 0.025 and 4.000s, with 0.025s increment. Geometrical mean and intra-event variance for every period and records in the set was then computed.

To illustrate the difference between soil type categories and then between magnitudes, some graphs are shown below.

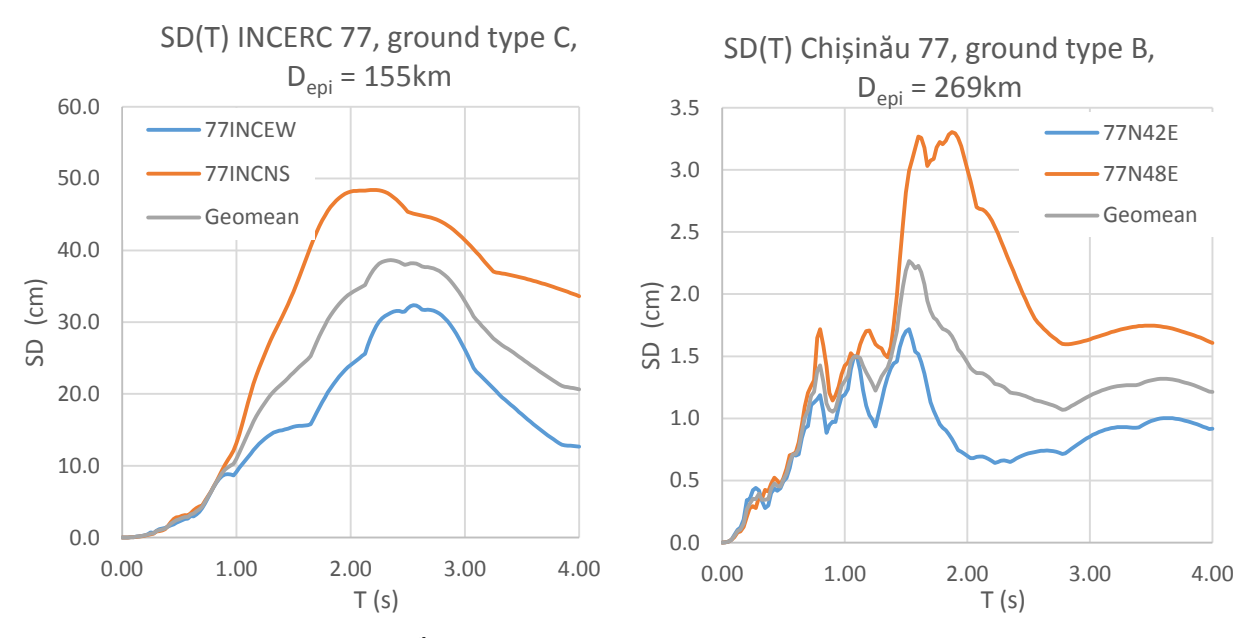


Fig. 2-6 Displacement spectra from 4th of March 1977 earthquake for two sites: INCERC Bucharest and Chişinău.

One can observe the large difference between the maximum displacements values (48.5cm at INCERC, compared to 3.3 cm in Chisinau) and between the spectral forms, although the maximum values of the displacements are located within the same period interval: 1.5 - 2.0 s.

Displacement spectra for INCERC Bucharest site 1977, 1986, 1990 earthquakes

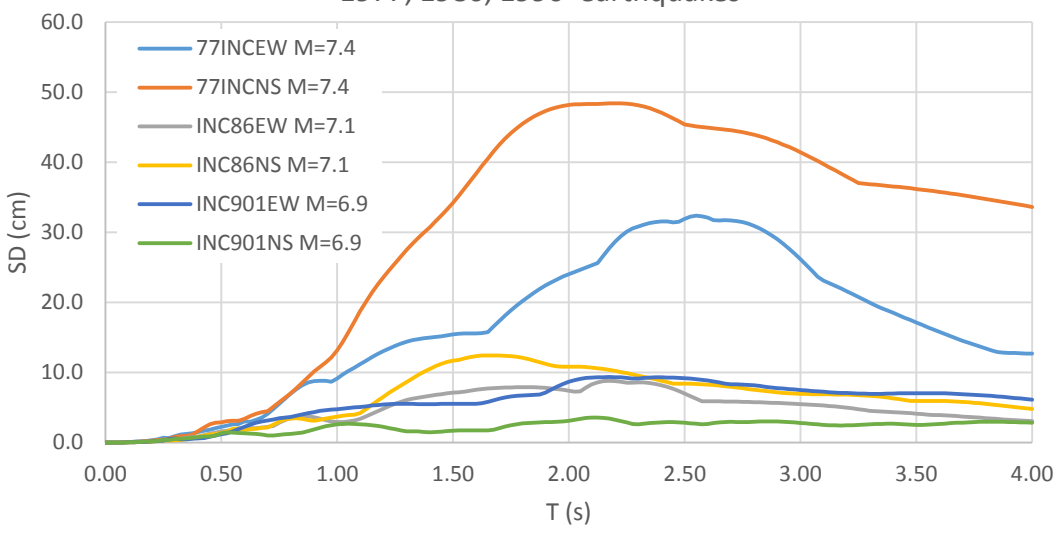


Fig. 2-7 Displacement spectra for 4.03.1977, 31.081986. 30.05.1990 earthquakes recorded at INCERC Bucharest

The important increase in the displacement demand with increasing moment magnitude is highlighted. Summarizing in a table the spectral maximum values for INCERC recordings for the earthquakes mentioned above, along with magnitude information and the peak ground acceleration (PGA) we obtain:

Event	$M_{\rm w}$	PGA, cm/s ²		SD _{max} , cm		
Event		EW	NS	EW	NS	
04.03.1977	7.4	188	207	32.4	48.4	
31.08.1986	7.1	109	96	8.8	12.4	
30.05.1990	6.9	99	66	9.3	3.4	

Table 2-3 Magnitude scaling of displacement spectra, INCERC site

From the table above, for an increase in magnitude from 7.1 to 7.4, the PGA increases two-fold, while the maximum spectral range increases four times, and for a magnitude increase from 6.9 to 7.1, PGA increases by 25% and displacements double (the geometric mean of the two components). Starting from the moment magnitude definition, we can estimate the ratio of energies released by two earthquakes.

$$M_{w1} = \frac{2}{3} \lg M_{01} - 10.7$$

$$M_{w2} = \frac{2}{3} \lg M_{02} - 10.7$$

$$M_{w2} - M_{w1} = \frac{2}{3} (\lg M_{02} - \lg M_{01}) = \frac{2}{3} \lg \frac{M_{02}}{M_{01}} \Rightarrow \frac{M_{02}}{M_{01}} = 10^{\frac{3}{2}(M_{w2} - M_{w1})}$$
Ec. 2-8

where M_{w1} and M_{w2} are the moment magnitudes and M_{01} and M_{02} are the seismic moments of the earthquakes. Seismic moment is considered as a measure of the energy released by the earthquake.

Applying the equation for the three earthquakes, it can be said that the earthquake in 1977 was about 2.8 times more energetic than the one in 1986, which in turn was about twice as energetic as that of 1990. It is a good correlation between the ratio of energies released by the three earthquakes and the ratio between maximum spectral displacements for the INCERC station.

After calculating geometric mean and intra-event variance, the two-step regression was performed following the procedure described in (Joyner & Boore, 1993), the coefficients of the attenuation model being determined by maximizing likelihood. Coefficients were determined for periods ranging from 0.10s to 4.00s with an increment of 0.1s and are presented in Appendix.

Below are some simulations of recorded seismic ground motions found in the database.

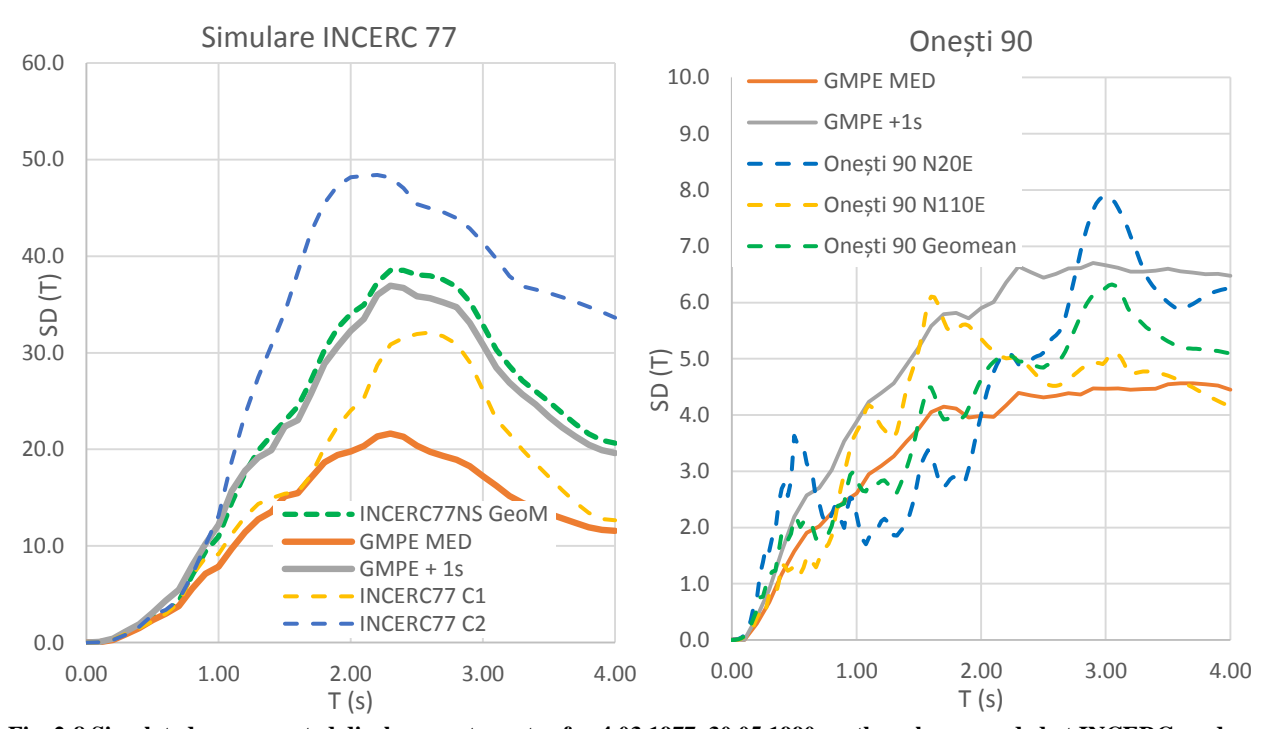


Fig. 2-8 Simulated vs. computed displacement spectra for 4.03.1977, 30.05.1990 earthquakes recorded at INCERC, and Onești sites, attenuation model without quadratic term

Using the attenuation relationship (median values) the change in displacement spectra with changing magnitude, ground type and epicentral distance was analysed. There is a narrowing of the area of large amplifications of the displacement spectrum with increasing magnitude of the earthquake, especially for soil type C. Smaller earthquakes tend to have quasi-flat areas over an extended range of periods, as confirmed by the displacement spectra calculated for the 1986 and 1990 earthquakes. Regarding the soil conditions, there are very high values of the relative amplification between the expected spectral values on soil C with respect to soil B. However, for moderate magnitudes ($M_w \approx 7.0$), these are reduced to values found in literature, (Cauzzi & Faccioli, 2008).

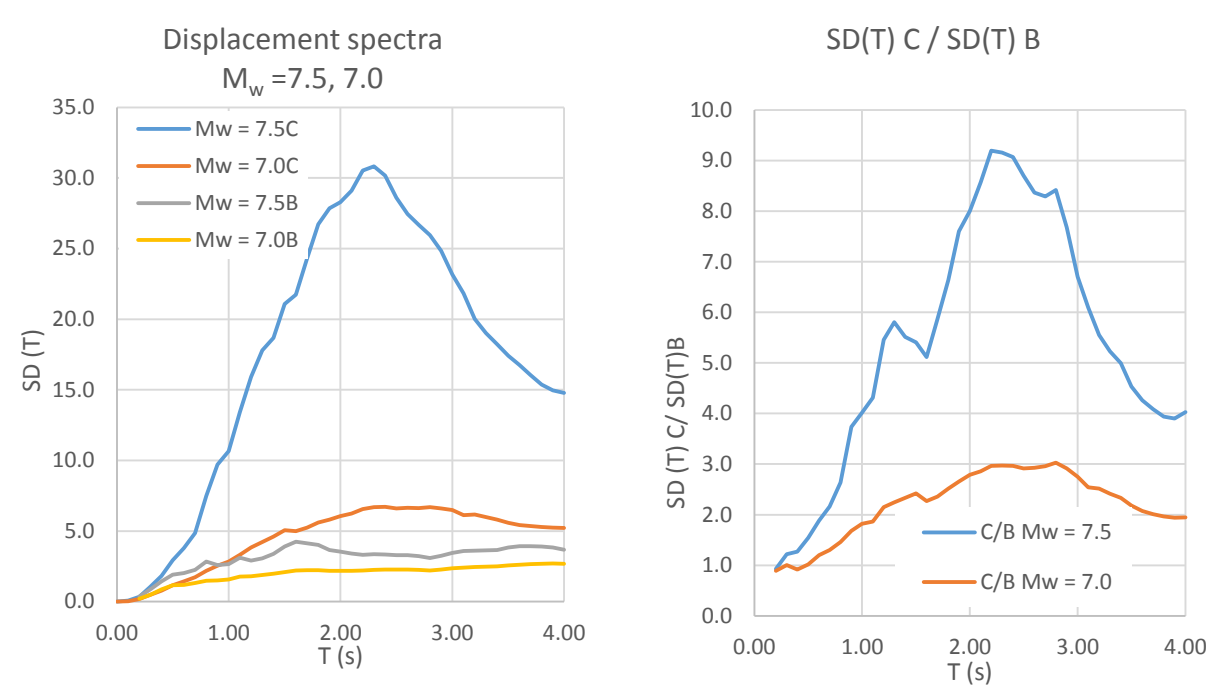


Fig. 2-9 Displacement demand as a function of magnitude and ground type C, type B respectively

The epicentral distance variation is analysed in the following figures. For soil type C, the pronounced peak is near 2.20s and has a slight tendency to migrate to longer periods with increasing epicentral distance. Soil type B is characterized by much lower spectral displacements, with a pronounced peak around 1.80s followed by a relatively flat area.

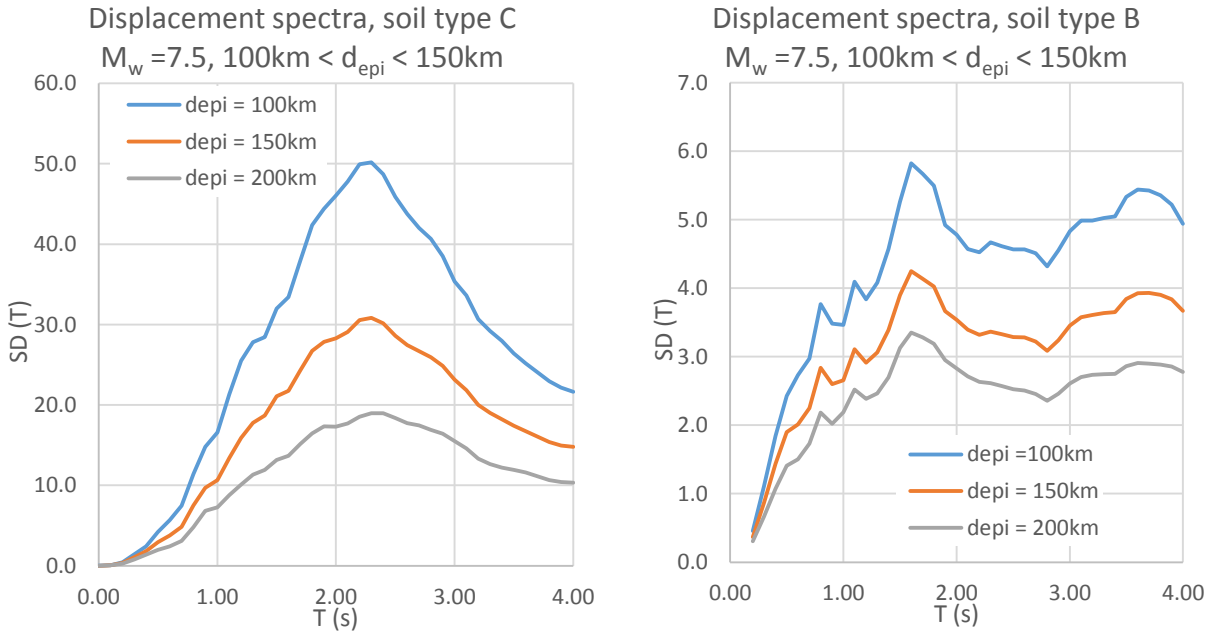


Fig. 2-10 Displacement spectra for three epicentral distances, ground type C and B

Aiming to bring the GMPE outcomes closer to the data collected during strong earthquakes ($M_w \ge 7.1$), it was attempted to introduce a quadratic term in the attenuation model.

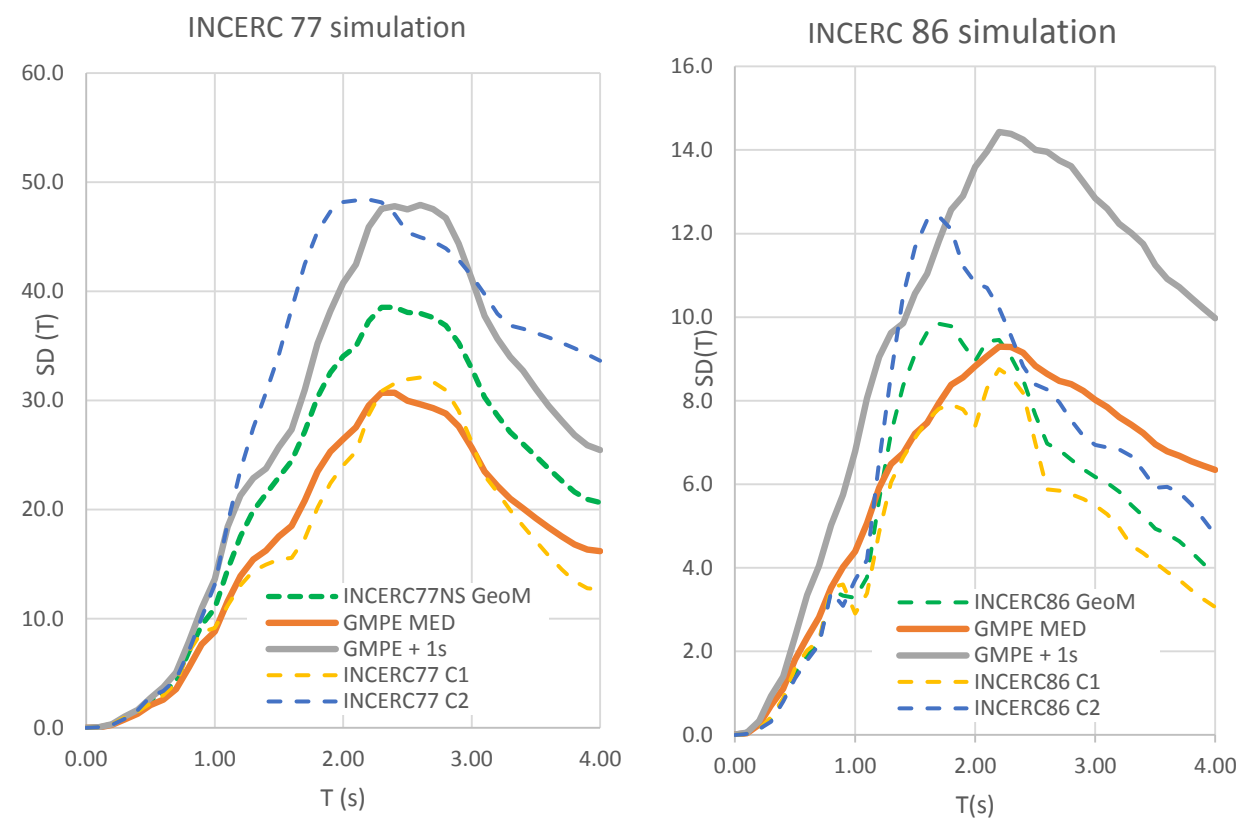


Fig. 2-11 Simulated displacement spectra for 4.03.1977, 31.08.1986 earthquakes, INCERC site, with quadratic term

It is noted that, in general, the median value $\pm 1\sigma$ envelopes the two components of each record.

Due to the quadratic term, the attenuation model reaches an extremum point. Its numerical value is obtained by deriving the expression of the GMPE in relation to the magnitude, zeroing and solving the equation (Văcăreanu, Pavel, Aldea, Arion & Neagu, 2015):

$$\frac{\partial (\lg(SD(T)))}{\partial M_w} = \frac{\partial}{\partial M_w} \left(b(M_w - 6) + d(M_w - 6)^2 \right) = b + 2d(M_w - 6) = 0$$

$$M^{sat}_{w} = 6 - \frac{b}{2d}$$
Ec. 2-9

where M_w^{sat} is the magnitude of the extremum point. Saturation magnitude, M_w^{sat} must be calculated at each period where SD(T) it is evaluated.

If d < 0, M_w^{sat} is a maximum point and the model will provide uncoservative results for SD(T) if $M_w > M_w^{sat}$. The relationship must be capped at an upper limit magnitude if M_w^{sat} is within its range.

If d > 0, M_w^{sat} is a minimum point and the model will provide uncoservative results for SD(T) if $M_w < M_w^{sat}$. The relationship must be capped at a lower limit magnitude if M_w^{sat} is within its range.

For ground type B, d <0 for the whole range of periods, so an upper limit magnitude must be set. Unfortunately, M_w^{sat} is in the magnitude range of the data set analysed. So the square-attenuation law for soil type B is:

$$\lg(SD) = a + b(M_W - 6) + d(M_W - 6)^2 - \lg\sqrt{D_{epi}^2 + h^2} + c\sqrt{D_{epi}^2 + h^2} + \varepsilon_r + \varepsilon_e,$$

$$M_W = 7.00 \text{ for } M_W > 7.00, \ 0.0 \le T \le 4.0s$$
Ec. 2-10

For ground type C, d < 0 for $T \le 0.2s$ and M_w^{sat} is larger than 7.60, and for T > 0.2s d > 0 and M_w^{sat} is lower than 6.40. So, the GMPE with quadratic term, for soil type C is:

$$\begin{split} \lg(SD) &= a + b(M_W - 6) + d(M_W - 6)^2 - \lg\sqrt{D_{epi}^2 + h^2} + c\sqrt{D_{epi}^2 + h^2} + \varepsilon_r + \varepsilon_e, \\ M_W &= 7.60 \text{ for } M_W > 7.60, \ T \le 0.20s, \\ M_W &= 6.40 \text{ for } M_W < 6.40, \ T > 0.20s \end{split}$$
 Ec. 2-11

2.2.2 The set of digital records

This set includes only high quality digital records from earthquakes with magnitudes in the range $5.2 \le M_w \le 7.1$, which had occurred at depth between 66 and 135km in Romania and Japan. After filtering the records according to the procedure described above, the shift spectra were calculated to 8.0s using Seismosignal (Seismosoft, 2016) and ViewWave (Kashima, 2016) software. The purpose for which the investigation was pushed to large values of period was to "map" the area for periods exceeding 4s, where reliable information from the large and moderately analogous earthquakes is not reliable. There is information that spectral peaks have higher ordinates than those present in the relative displacement spectrum at 2.0s for large earthquakes and locations in the Romanian Plain. Both seismological (Brune model) and geotechnical considerations lead to the conclusion that such peaks would be around 5-6s. Unfortunately, this study could only highlight this to a small extent.

Up to 4.00s the increment was 0.10s, then it was set to 0.20s for periods between 4.0 and 6.0s and finally, for periods up to 8.00s the regression coefficients were determined at a 0.40s increment.

There have been convergence issues for ground type C within 0.20-0.60s and then between 4.40 and 8.00s. For the second interval, however, the regression algorithm (and the values of the coefficients) was run in a single stage.

Simulation EREN86, $M_w = 7.10$, $d_{eni} = 120$ km

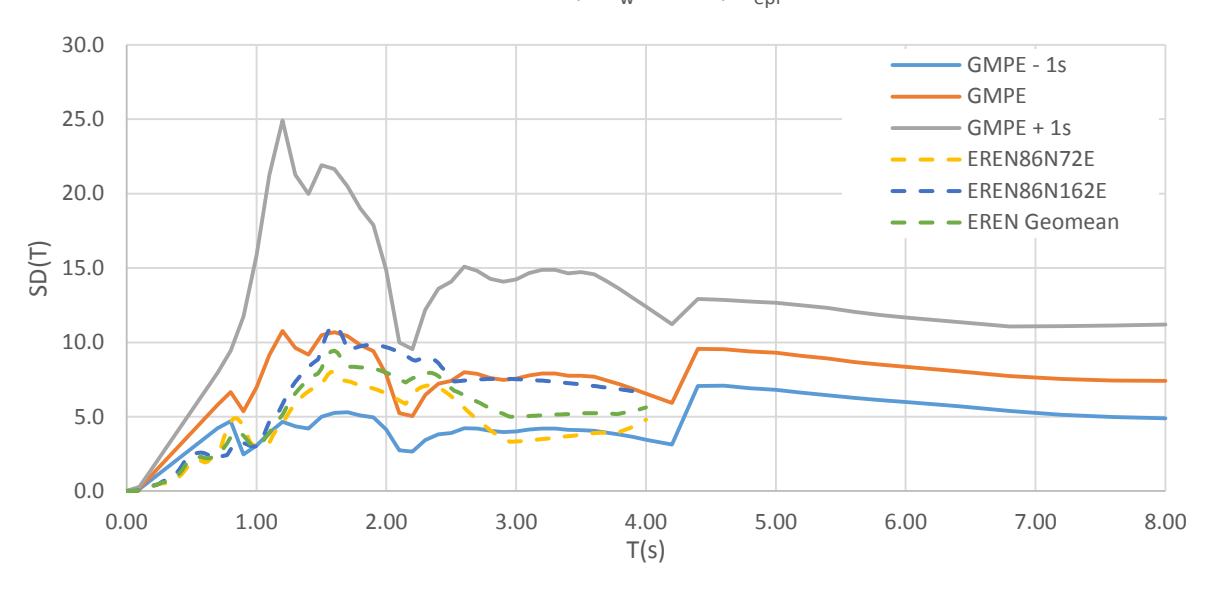


Fig. 2-12 Simulation EREN site, 1986 earthquake

They are highlighted peaks and flat zones after 4.00s, probably because the database did not contained earthquakes strong enough to excite the layers of sediment that have fundamental periods between 4.0 and 8.0s. Spectral values are lower than those corresponding to the first peak, which is around 1.20s for ground type C (instead of about 2.00-2.30s for the first set of records). However, the model manages to reasonably predict the spectrum of a record that was not included in the regression data set, EREN 1986.

2.2.3 Data set containing whole database

The set includes all records in the database, 272 pairs of perpendicular horizontal components. Again, problems with convergence occur in the interval between 0.30 and 0.70s for soil type C. Numerical problems may have propagated with the introduction of the digital record group (who also suffered from this problem in the same range of periods). With the increase in the number of records (especially those of small magnitude earthquakes, $M_w = 5.2 - 6.0$) the variability increases. The ground motions of March 4, 1977 earthquake, which imposes the highest displacement demands, loses its share in the first set (containing only 116 pairs of components), which is reflected in the shape and spectral values generated by this model.

Below is a simulation of the median displacement spectra corresponding to a seismic event having $M_w = 7.50$, which occurred at an epicentral distance of 150km, all three sets of regression coefficients for both C and B soils are analysed. For ground type C, the similarity between the shapes and values of the set one and three to 1.50s is observed, after which they evolve separately, having both peaks at approximately 2.30s. The second set, containing only small and moderate earthquakes, has a very different spectral shape, with peaks between 1.20 and 1.50s. Dependence on database results is more evident in type B soil, where, although spectrum shapes are similar and reach their maximum between 1.30s and 1.50s, the plateaus which occur after the peak are at completely different levels.

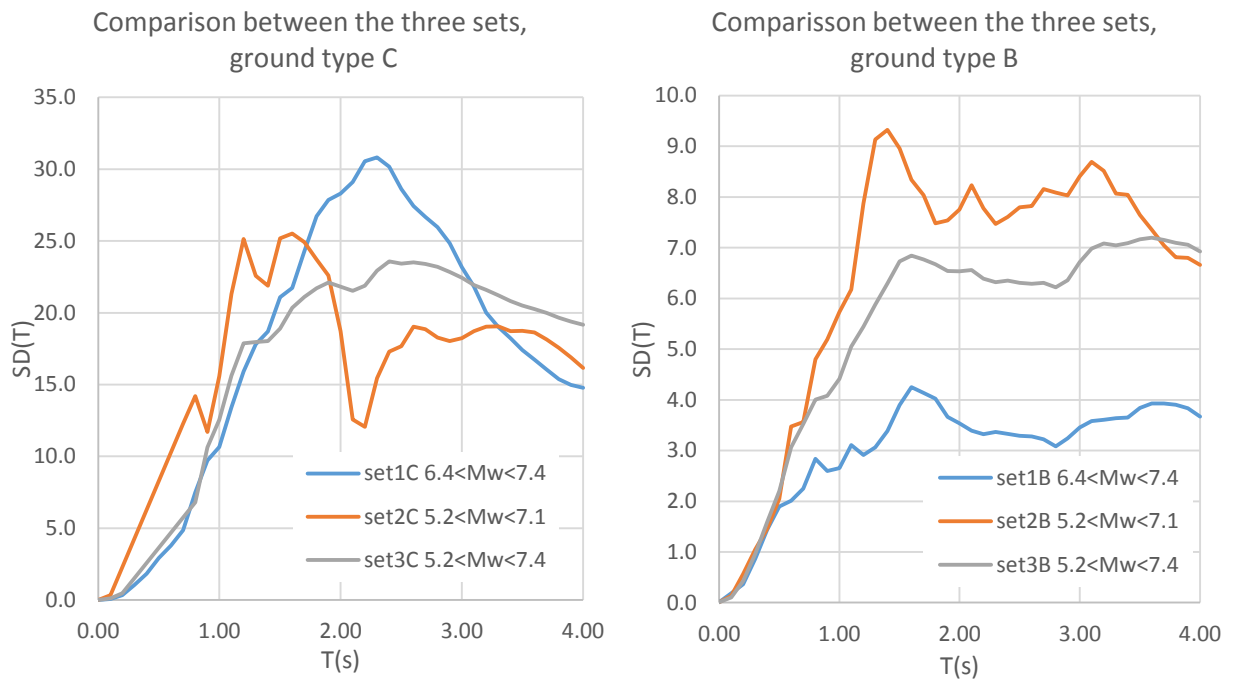


Fig. 2-13 Simulation of a seismic event with $M_w = 7.50$, $d_{epi} = 150$ km, median values, three sets

After examining the above figure, the following conclusions can be drawn:

- For explanation / simulation of very strong earthquakes M_w≥7.40, the GMPE with the coefficients resulting from the regression of the first set is closer to the observed data for type C soils;
- For Type B soils, the coefficients of the attenuation model corresponding to the complete set seem to be a reasonable compromise with respect to the values for the other two groups of records.

2.3 Testing the attenuation model

Once regression coefficients have been calculated, one has to check that the data provided by the attenuation law is reliable and whether the attenuation model can generate useful information from a data set other than that used for regression. An important role in model testing is played by residuals, quantities resulting from the differences between the recorded values and the values predicted by the attenuation model. Positive values of residual indicate underestimation of the seismic motion amplitudes, negative ones indicating overestimation. Normalized residues are defined (Văcăreanu, Pavel, Aldea, Arion & Neagu, 2015) as:

$$\varepsilon = \frac{Y_{es} - \mu_{es}}{\sigma}$$
 Ec. 2-12

 ϵ being the normalized residual, Y_{es} is the logarithm of the amplitude of ground motion recorded during the earthquake e at station s, μ_{es} is the logarithm of the median value provided by the GMPE, and σ is the standard deviation of the attenuation model. Below are the distributions of normalized

residuals and the distribution of normal normalized residuals compared to those produced by a standard normal distribution for three periods: 0.10s, 0.70s and 1.40s.

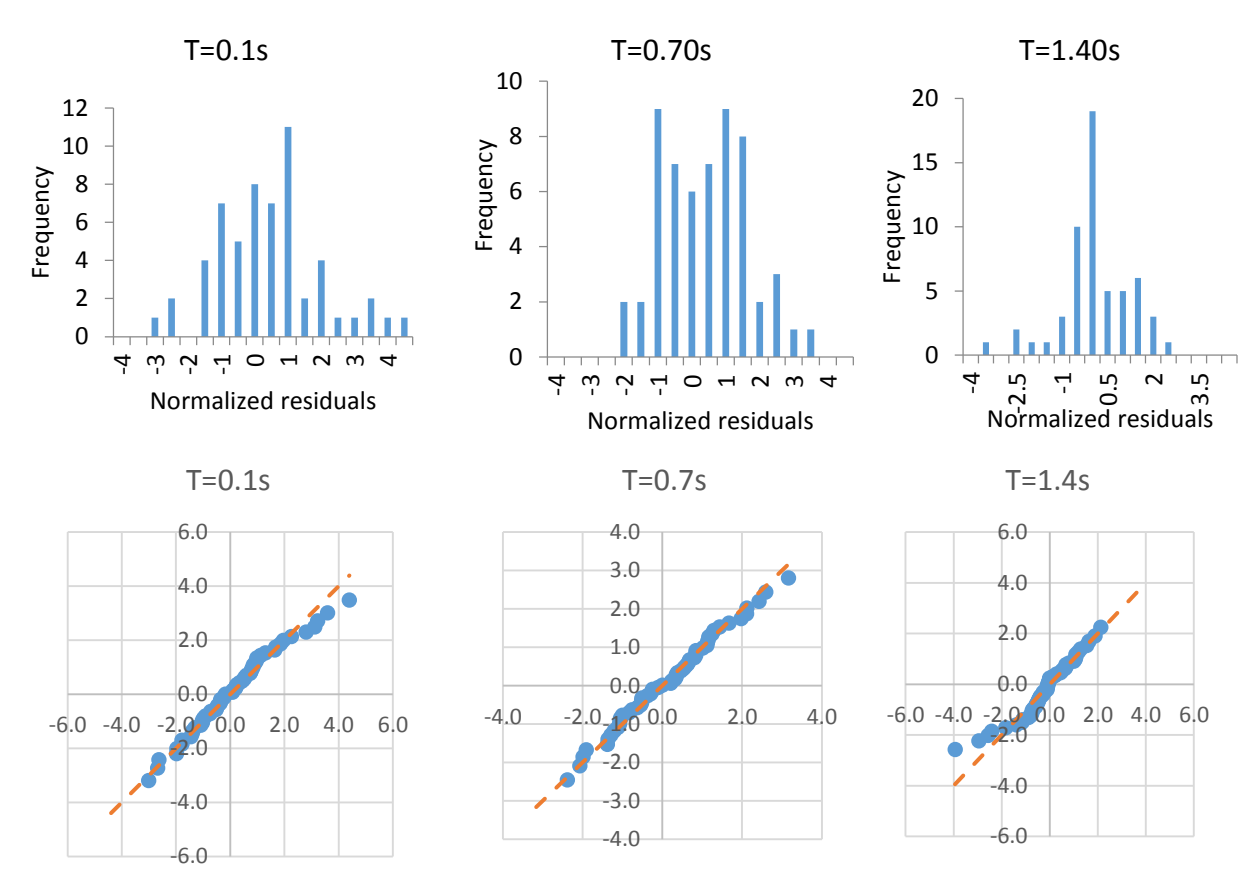


Fig. 2-14 Normalized residuals (up), QQ plot (down)

The more normalized residuals are approaching by the dashed line that passes through the origin, the better the normal distribution describes the residual distribution. We see a distribution close to the normal one, both in histograms and in the alignment of residuals with the line that passes through origin.

With the values of the residuals, it is possible to calculate some statistical parameters by which the quality of the attenuation relation can be assessed. Those where proposed in (Scherbaum, Delavaud & Riggelsen, 2009) and they are: median of the normalized residuals (MEDNR), mean of the normalized residuals (MEANNR) and standard deviation of the normalized residuals (STDNR). Depending on these indicators and limit values, the attenuation models are grouped into four categories of confidence, rated from A (best) to D (those not recommended to apply). The three statistical indicators are calculated for each period, for each set of data, and are reported in the regression coefficients tables. At the bottom of the table are given the mean and median values of these three indicators for the entire range of periods where the regression coefficients were calculated.

Inter-event residues are calculated (Văcăreanu, Pavel, Aldea, Arion & Neagu, 2015) using the following equation:

$$\delta B_e = \frac{1}{N_c} \sum_{s=1}^{N_s} (Y_{es} - \mu_{es})$$
 Ec. 2-13

where N_s is the number of stations, and Y_{es} and μ_{es} are previously defined. Intra-event residuals are given by:

$$\delta W_{\rho_S} = Y_{\rho_S} - (\mu_{\rho_S} + \delta B_{\rho})$$
 Ec. 2-14

The evaluation of these parameters allows verification of the distribution of inter-event residues with magnitude and distribution of intra-event residues with distance. Below are presented for two periods of 0.80s and 1.60s for the whole set of data and soil type C.

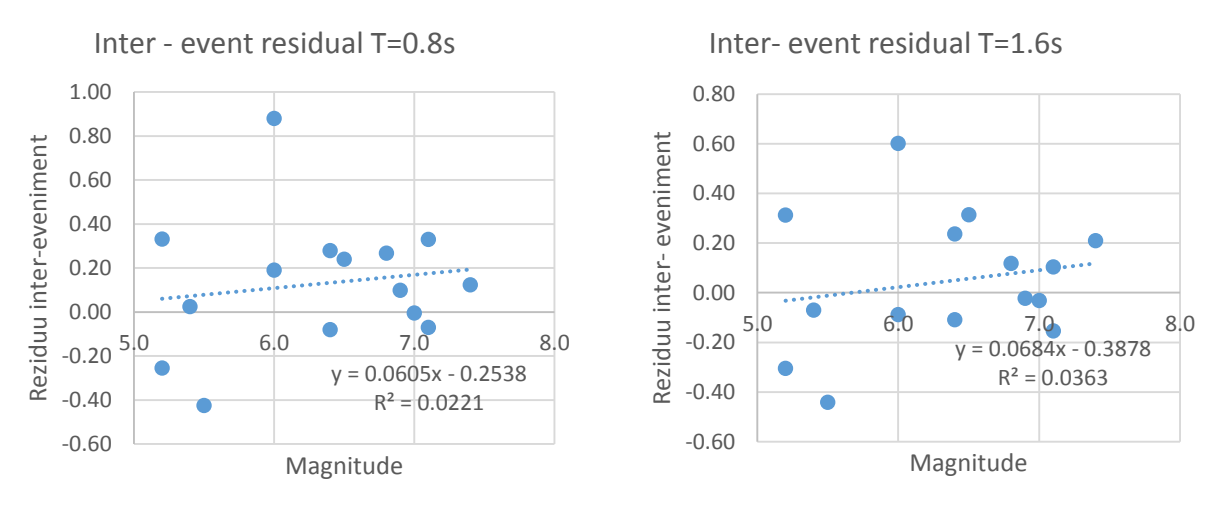


Fig. 2-15 Inter-event residuals dependence on magnitude, whole database

There is a slight correlation between the magnitude of the moment and the value of the inter-event residues for both periods. Considering the data presented in the literature, for example in (Văcăreanu, Pavel, Aldea, Arion, & Neagu 2015), the results shown above can be considered satisfactory.

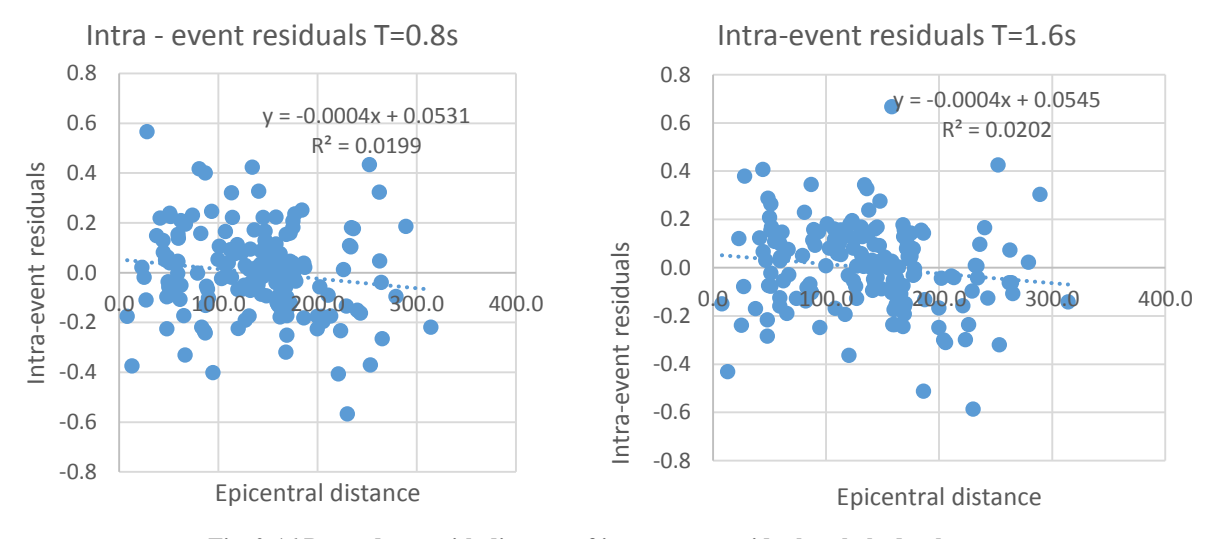


Fig. 2-16 Dependence with distance of intra-event residuals, whole database

From the above figures we can see a very low correlation between residues and distance. The above figures are representative of the entire range of periods covered by the GMPE. The weaker correlations (better attenuation models) are obtained on smaller and more homogeneous datasets (e.g. the earthquake record group from 1977, 1986, 1990).

3 Nonlinear displacement spectra

Since the 1960s, scientists have realized that the relative displacements (drifts) imposed during the earthquake for structurally inelastic structures are greater than those corresponding to systems with elastic behaviour, for certain intervals of vibration periods. For periods greater than a certain value, which takes into account the frequency content of the seismic motion, the response of the two systems, with inelastic or elastic behaviour, is approximately equal. The term used by researchers for this phenomenon was "equal displacement rule". One of the first articles that tackle this topic (Veletsos, Newmark & Chelapati, 1965), has practically led the way in which the displacements of structures with inelastic behaviour subjected to strong seismic motions are evaluated.

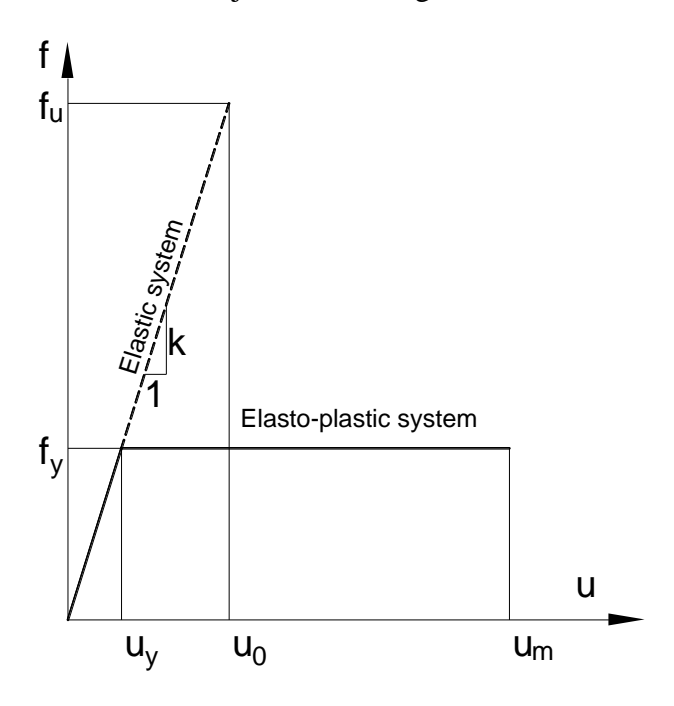


Fig. 3-1 Elasto-plastic system and corresponding elastic system, after (Chopra, 2012)

In (Chopra, 2012) is described extensively the behaviour of inelastic single degree of freedom (SDOF) systems to earthquake excitation. Given two systems with the same elastic stiffness, one with elasto-plastic behaviour and an associated one, with ideal elastic behaviour, the maximum displacements recorded during a strong earthquake will be u_m for elasto-plastic system, and u_0 respectively for the elastic system. In the elasto-plastic system, the yielding takes place at f_y , which is the yielding force. f_0 is the minimum necessary strength of the associated system to remain in the elastic range of behaviour. Between these forces the following relationship takes place, due to the fact that the systems have the same elastic stiffness:

$$f_{y} = ku_{y}$$

$$f_{0} = ku_{0}$$
Ec. 3-1

where k is the elastic stiffness of the associated system.

An important feature of the elasto plastic-system is μ , the displacement ductility, the ratio between maximum displacement of the elasto-plastic system and the yielding displacement, u_y .

$$\mu = \frac{u_m}{u_v}$$
 Ec. 3-2

The normalized yield strength, $\overline{f_y}$ and the reduction factor (related to yield strength), R_y are defined as:

$$\overline{f}_{y} = \frac{f_{y}}{f_{0}} = \frac{u_{y}}{u_{0}} = \frac{1}{R_{y}}$$

$$R_{y} = \frac{f_{0}}{f_{y}} = \frac{u_{0}}{u_{y}} = \frac{1}{\overline{f}_{y}}$$
Ec. 3-3

These two factors are linked (Chopra, 2012) by the following equation:

$$\frac{u_m}{u_0} = \mu \overline{f}_y = \frac{\mu}{R_y}$$
 Ec. 3-4

The equation of motion which describes the inelastic system response is:

$$m\ddot{u} + c\dot{u} + f_s(u) = -m\ddot{u}_a(t)$$
 Ec. 3-5

where $f_S(u)$ is the constitutive force-displacement law of the system. Using the following notation:

$$\omega_n = \sqrt{\frac{k}{m}}, \quad \xi = \frac{c}{2m\omega_n}, \quad \overline{f}_{\varsigma}(u) = \frac{f_{\varsigma}(u)}{f_{\varsigma}}$$
 Ec. 3-6

we get (Chopra, 2012):

$$\ddot{u} + 2\xi \omega_n \dot{u} + \omega_n^2 u_y \overline{f}_s(u) = -\ddot{u}_q(t)$$
 Ec. 3-7

The equation indicates a complex connection between system response u(t) on one hand and the natural circular frequency $\omega_n = 2\pi/T_n$, damping ξ , force - deformation constitutive law $f_S(u)$ and yielding deformation u_y on the other hand. These parameters govern the non-linear response of the SDOF. For this reason, it is very important to precisely determine the vibration periods of structures, both in the design phase and after the completion of the building. By solving the above equation using numerical methods, it is possible to determine the time histories of the displacements, velocities, accelerations and other nonlinear system response parameters.

By solving the equation for several values of vibration periods, non-linear spectra of accelerations, velocities, and displacements can be obtained. They can be expressed according to one of the parameters described above $(R_y, \mu \text{ sau } \overline{f_y})$.

Seismic design codes, (CEN, 2004), (MDRAP, 2013), generally use for estimation of inelastic displacement methods based on increasing by a factor (which depends on vibration period of the

structure) greater than one the displacement of the elastic system - "coefficient method". Some seismic evaluation codes (ATC-40, 1996), FEMA440 use the concept of equivalent hysteretic damping to reduce the displacement demand of the structure. The displacement and ductility requirements of the real structure with non-linear behaviour can be evaluated using an equivalent structure (Priestley, Calvi & Kowalsky, 2007), with linear behaviour and increased damping, due to yielding.

Extensive studies on inelastic spectra and displacement demands were conducted in (Miranda & Ruiz-Garcia, 2007), (Goda & Atkinson, 2009) şi (Michel, Lestuzzi & Lacave, 2014).

A comprehensive study on elastic and inelastic response spectra is performed in (Craifăleanu, 2005) using a database of national earthquake records from 1977, 1986 and 1990. The influence of a multitude of factors on the response of SDOF was considered.

Studies on the displacement demands for Vrancea intermediate depth earthquakes were made in order to calibrate the elastic movement coefficients adopted in code P100-1/2013. In (Gutunoi & Zamfirescu, 2013) a coefficient expression is proposed, depending on the behaviour factor q, the vibration period of the structure and the corner period. The database comprises 40 artificial accelerograms and the coefficients are calculated using bilinear and Takeda models.

In (Crăciun, Văcăreanu & Pavel, 2016) a relationship is proposed for the calculation of the coefficient, depending on the behaviour factor, the period of the system and the corner period. The database contains earthquake records from 1986 and 1990, and the hysteretic model is Takeda modified.

The aim of this study is to evaluate the displacement demands of inelastic SDOF systems using coefficient's method, as a function of system's displacement ductility, μ . Using a database of strong motion records, one can obtain the coefficient of amplification of the elastic deformation, corresponding to a given hysteretic material / model. The study focuses on new reinforced concrete structures, the hysteretic model used being modified Takeda, with stiffness degradation.

In the displacement based design framework, using displacement spectra expressed in terms of ductility, one of the intermediate steps is eliminated, resulting in a slightly simplified calculation procedure. The biggest advantage is that there is no need to use the equivalent hysteretic damping concept, challenged by some researchers for being uncoservative and not appropriate to model the hysteretic behaviour of structures subjected to earthquakes.

By combining the attenuation law presented in Chapter 2 with the results of this study, it is possible to create inelastic displacement spectra for a given seismic scenario.

3.1 Database

The database for this study was constructed starting from a databank used for creating the attenuation model of the relative displacement spectrum. A minimum value for PGA was imposed for this new set of records because some features of weaker motions differ significantly from strong motion records. In literature there are studies that use different values for this threshold. The limit varies from 40cm/s^2 (Miranda & Ruiz Garcia, 2003) to $50-100 \text{cm/s}^2$, values sometimes

referring to the minimum value of a component, sometimes to the average value of the two components. For this study, the PGA limit value was selected at 75cm/s², corresponding to the geometric mean of the two horizontal components, according to the best practice recommendations given in (Goda & Atkinson, 2009).

The database includes 107 horizontal component pairs (214 records) generated by intermediary depth earthquakes with $6.0 \le M_w \le 7.4$ from Romania and Japan. There were also two earthquake records of magnitude 5.2 (6.10.2013), which satisfy the imposed PGA threshold. Following the PGA selection, the records were grouped according to the type of ground on which the site is located, according to Eurocode 8. Below are some features of the new dataset. Of the total of 214 records, 140 being recorded on type C soil, while the remaining 74 are from soil type B.

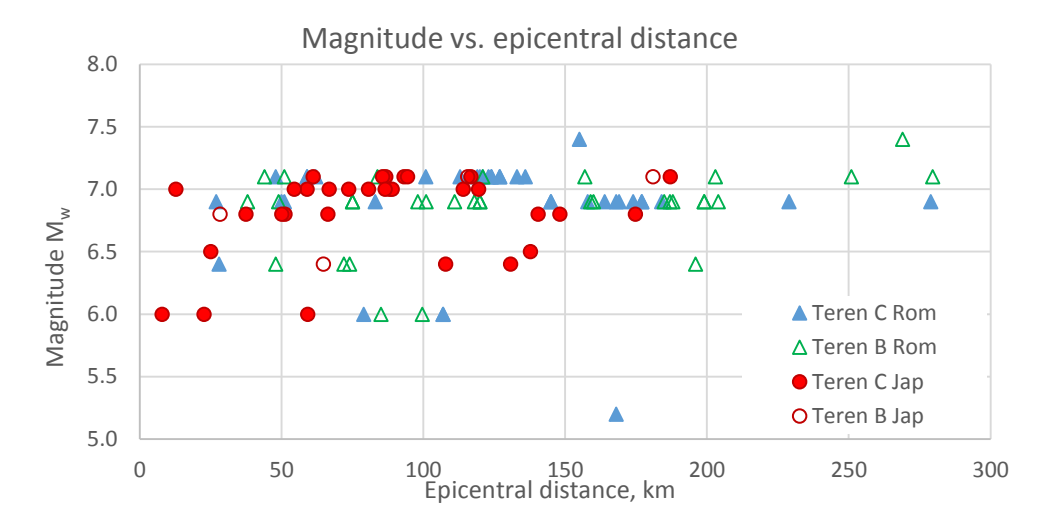


Fig. 3-2 Distribution by origin, ground type, magnitude and distance of records in the database

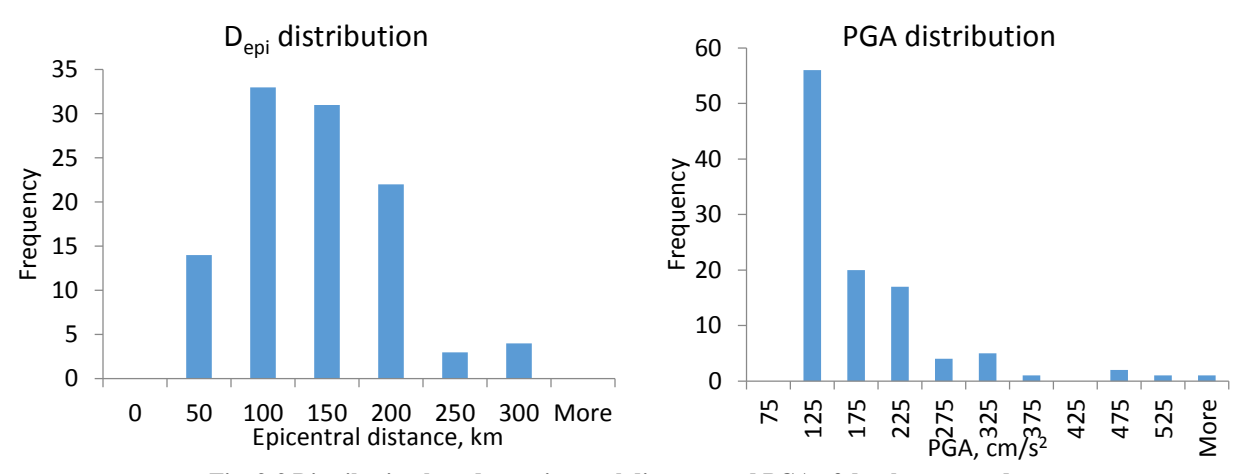


Fig. 3-3 Distribution based on epicentral distance and PGA of database records

3.2 Hysteretic model

The hysteretic model used to obtain amplification coefficients is the modified Takeda, which is part of the "peak-oriented" family models that include the Clough model. The main characteristic feature of this type of hysteretic models is that the reloading path is given by the maximum displacement point of the previous cycle. The modified Takeda model has advantages over the Clough model for changing stiffness after cracking, yield and degradation of rigidity at unloading; it can reproduce with sufficient precision the behaviour of reinforced concrete elements under cyclic loading.

Hysteretic models can be classified according to the surface of the loops in two categories: "fat" and "thin". In (Craifăleanu, 2005) is presented a criterion for delimitation between the two types of hysteretic loops. The index is defined as:

$$E_h = \frac{dW}{2\pi F_{\nu} D_m}$$
 Ec. 3-8

dW being the hysterical energy dissipated in a cycle, F_y yield strength and D_m maximum displacement. If E_h index is smaller than 0.2, the loop is thin, otherwise the loop is fat.

In USDP software, defining modified Takeda model with degrading stiffness requires the following parameters:

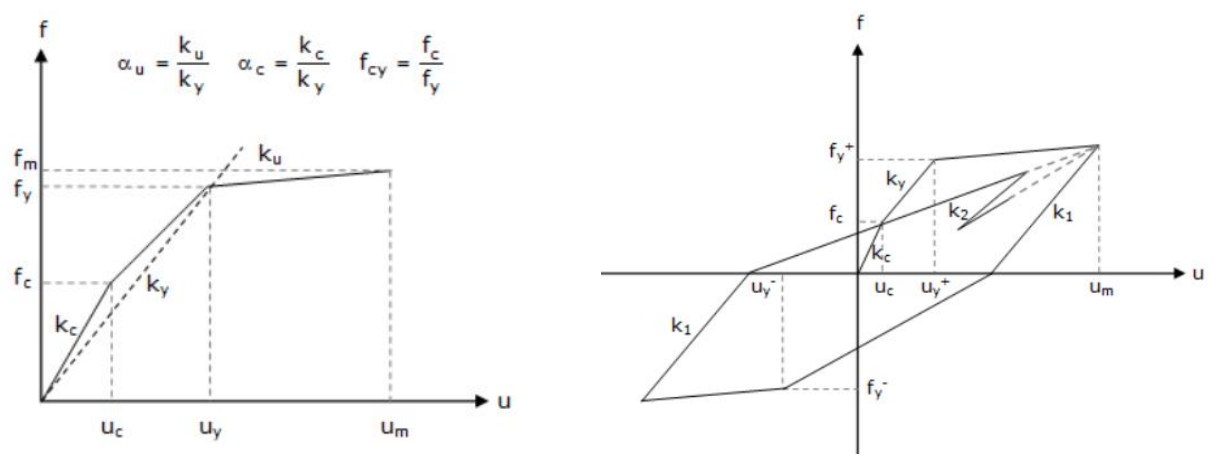


Fig. 3-4 Modified Takeda with stiffness degradation, (Utility Software for Data Processing, 2016)

 α_u – controls post yielding stiffness, α_c – post cracking stiffness, f_{cy} – is the ratio between the cracking and the yielding strength.

Unloading stiffness, k_1 , it is defined as:

$$k_1 = \left(\frac{u_y}{u_m}\right)^{\beta_0} \cdot \left(\frac{f_c + f_y}{u_c + u_y}\right)$$
 Ec. 3-9

 f_c and u_c are the cracking strength and displacement , f_y şi u_y are the yielding strength and displacement, u_m maximum displacement and β_0 unloading degrading stiffness factor.

For unloading on a inner loop, the k₂ stiffness is:

$$k_2 = k_1 \cdot \beta_1$$
 Ec. 3-10

 β_1 is reloading degrading stiffness factor, $\beta_1 = 0.6$.

The numerical values of the parameters used in the nonlinear dynamic analyses were:

$$\alpha_u = 0.02^{\dagger}$$
, $\alpha_c = 1.00$, $f_{cv} = 0.0001$;

 $\beta_0 = 0.3$, (as recommended in (Priestley, Calvi & Kowalsky, 2007) for well conformed reinforced concrete beams – fat loop). These values are representative for new reinforced concrete buildings.

The damping was introduced as 5% of critical, mass proportional viscous damping.

3.3 Results

Dynamic nonlinear analyses carried out on SDOF systems were performed with the USDP software (Akkar, Utility Software for Data Processing, 2016). The amplification coefficient was computed as:

$$C(T) = \frac{SD_{inel}(T)}{SD_{el}(T)}$$
Ec. 3-11

for all 214 strong motion records, for periods between 0.05s and 4.00s with a 0.05s increment, for six displacement ductility values: 1.5, 2.0, 3.0, 4.0, 5.0 and 6.0.

3.3.1 Amplification coefficient values

For the entire range of records, periods and ductility, the c(T) coefficients were calculated with USDP software. The distribution of the obtained values was considered lognormal, literature studies (Goda & Atkinson, 2009) confirming this. The mean, median, the upper and lower fractiles corresponding to $\pm 1\sigma$ were determined. Below are the median values considering all ground types (B, C).

[†] The value was selected following a number of sectional analyses for beams, columns and walls, reinforced with BST500C steel. Literature typically provides values between 0.00 and 0.05.

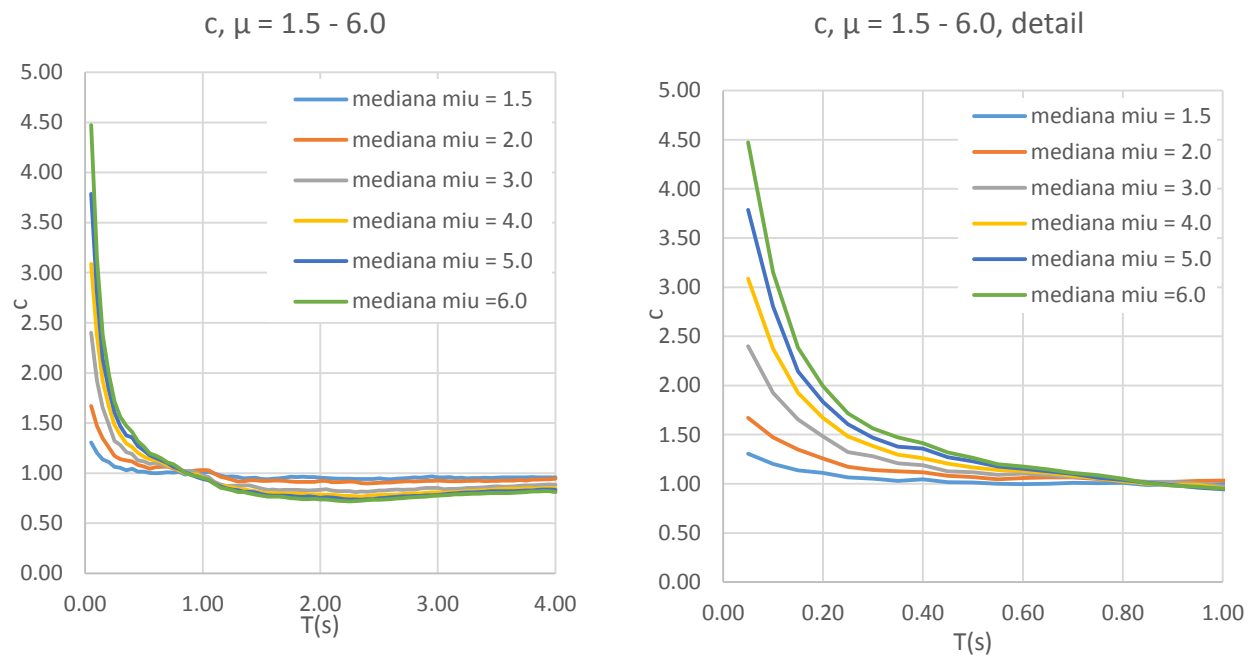


Fig. 3-5 Inelastic amplification coefficients, median values, ground type B and C (left), detail (right)

From the above figures it is observed that the equal displacement rule applies from 0.80s - 0.90s, considering the median values and data on both types of soil. As expected, higher coefficients are associated with high ductility.

Below are the median c values for each ground type. Different periods mark the starting point for the equal displacements rule (median values). For soil type B, this period is between 0.60s - 0.70s, while for soil type C it is approximately 1.00s.

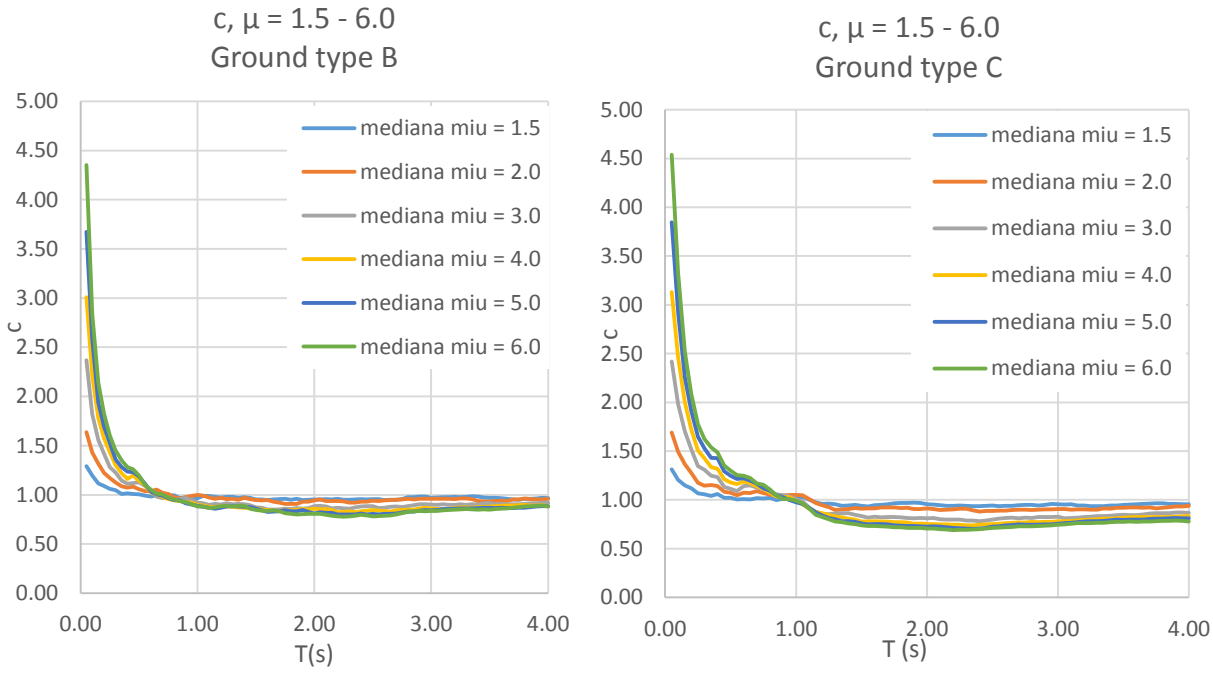


Fig. 3-6 Inelastic amplification coefficients, median values, ground type B (Left) and C (Right)

For displacement ductility $\mu = 3$ and ground type B and C, the median and 15.9% and 84.1% fractile values are shown below, these being representative for the entire range of displacement ductility.

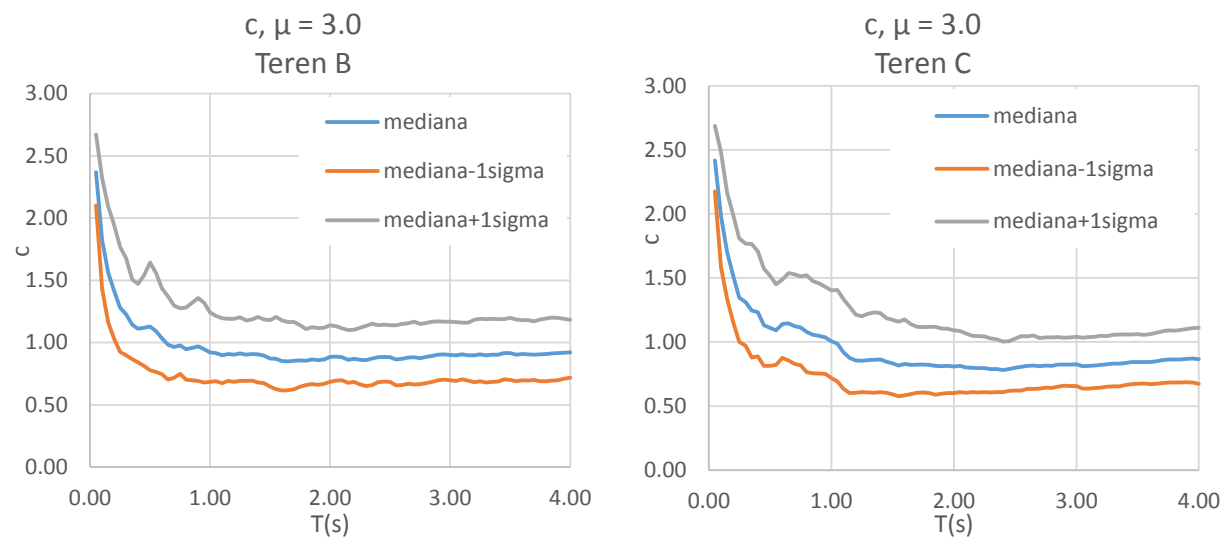


Fig. 3-7 Amplification coefficients, median values \pm 1 σ , soil B (left) and C (right)

From the above figures, one can see a more pronounced variability for periods up to 0.80s for soil type B and 1.10s for type C soil. It is also observed that the equal displacement rule is only valid for median values (at least for the modified Takeda model), values corresponding to higher fractiles (e.g. 84%) may not reach coefficients equal to 1.00.

For $\mu = 3$ and C type soil, the standard deviation as a function of the period is shown below.

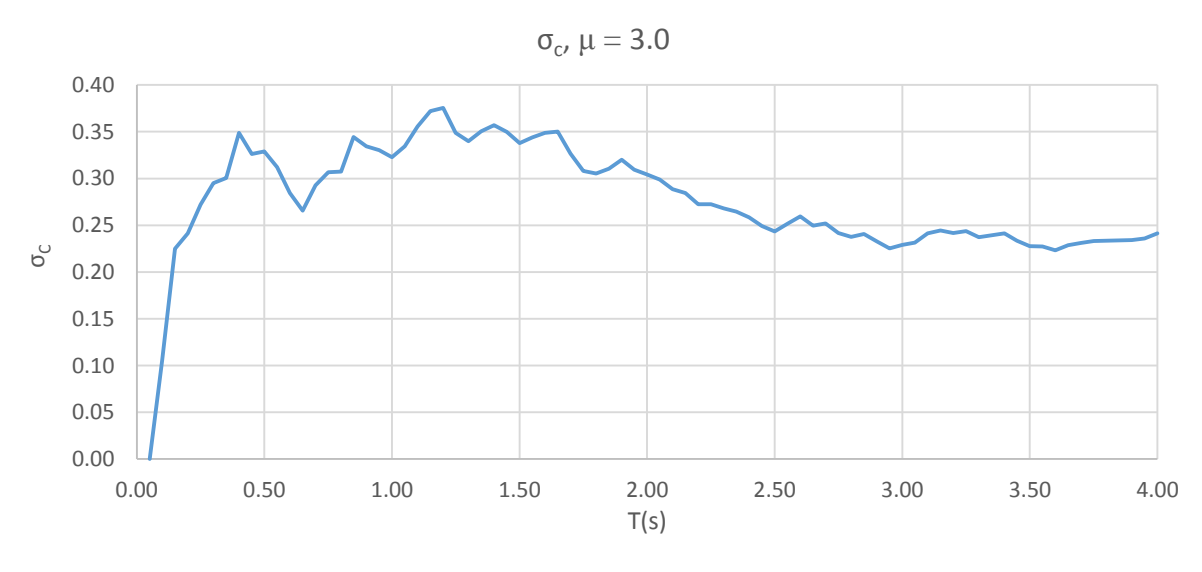


Fig. 3-8 σ_c variation with period, $\mu = 3$. Ground type C

For a wide range of periods, the σ_c value remains quasi-constant, yet reaching local peaks in the range of 0.30s - 1.50s.

3.3.2 Influence of soil type

Soil type influences the displacement response of the structural system. In order to highlight the displacement demand differences for structures located on ground type B and C, the ratio between the c(T) values for ground type B and C (considered separately) and the corresponding mean values for ground type B and C (whole database) were computed (Miranda & Ruiz Garcia, 2003).

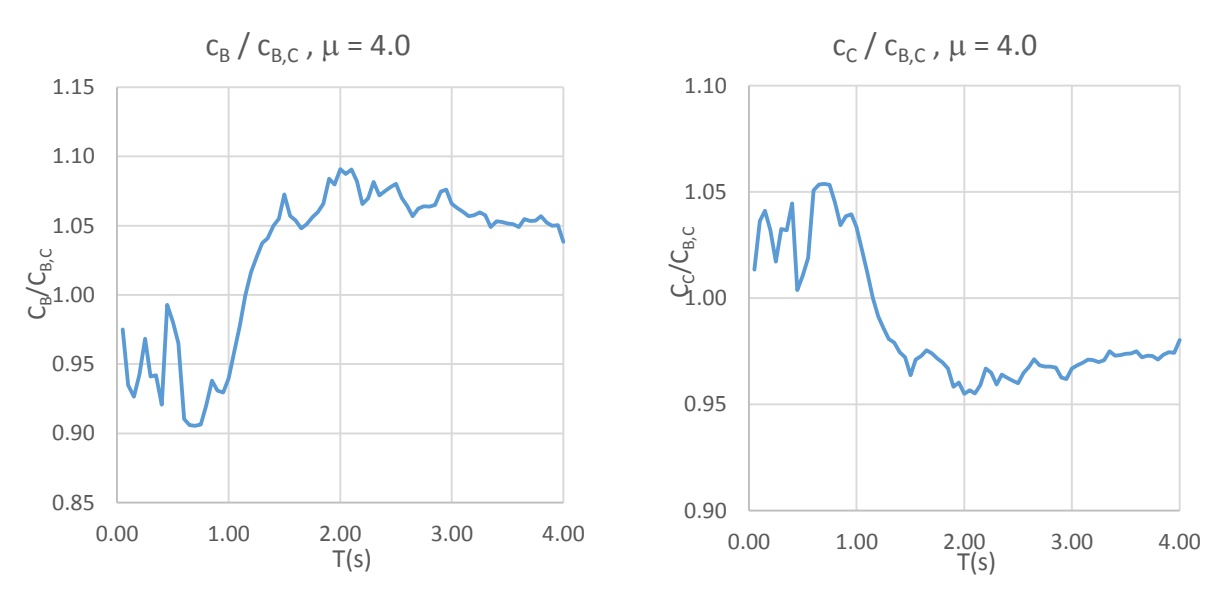


Fig. 3-9 Soil influence, $\mu = 4$. Soil type B, left; type C right

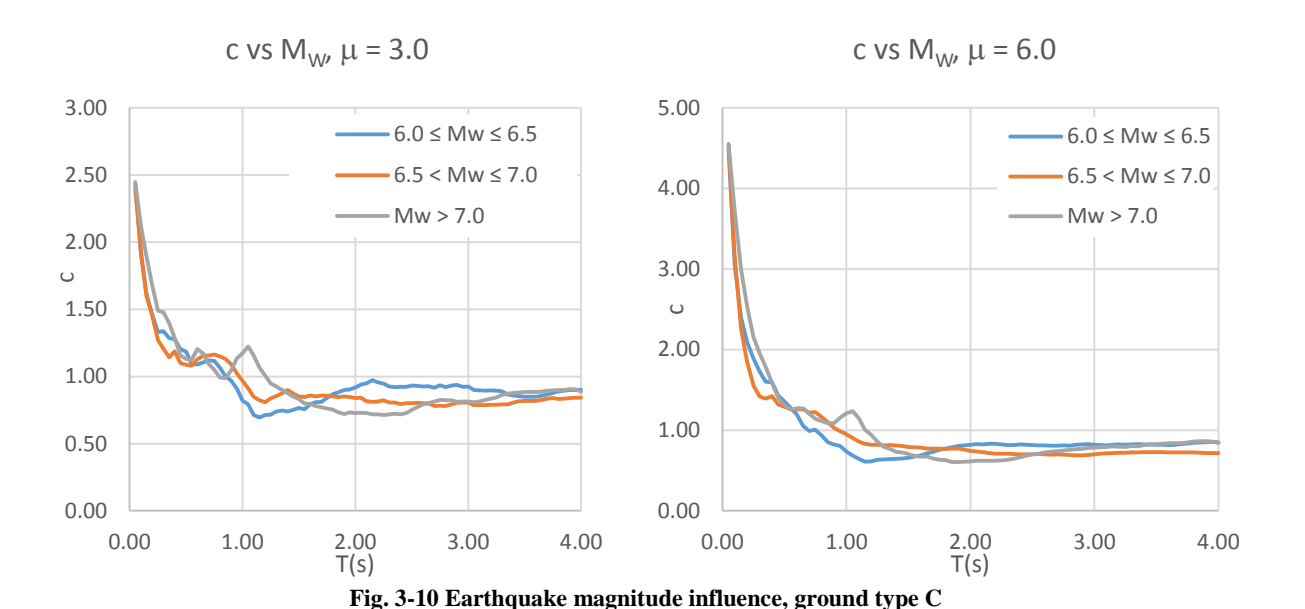
Not considering soil conditions is conservative for type B soils for periods up to 1.20s. For type C soil, the situation is reversed. The differences are accentuated by the increase in displacement ductility, yet not exceeding 10%. The values are in agreement with the ones presented in (Miranda & Ruiz Garcia, 2003), which report differences of 10-15% for type B soil and maximum 20% for type C soil. In the database of the above study there were an equal number of motions recorded on ground type A, B and C.

3.3.3 Influence of earthquake magnitude

In (Crăciun, Văcăreanu & Pavel, 2016) is highlighted the increase of the value c(T) with the increase of the earthquake magnitude, especially for periods below 0.40s. In this study the influence of magnitude was investigated for ground type C, which contains the largest number of records. Records were ordered in three sets, depending on magnitude. The results for two displacement ductility, $\mu = 3$ and $\mu = 6$, are presented below.

The increase of the coefficient is indeed present for systems with significant yielding (i.e. for $\mu \ge$ 4), while for $\mu = 3$ being recorded only over a limited range of periods.

For all six calculated ductility values, a zone centred on 1.10s is where the influence of magnitude increase is more severe, earthquakes with magnitudes above 7.00 produce amplifications more than 30% greater than those with $6.5 \le M_w \le 7.00$.



3.3.4 Epicentral distance influence

In order to highlight the effect of distance on the c(T), a sorting according to the epicentral distance has been made, for motions recorded on type C soil. These were grouped in three sets. The first includes earthquakes produced less than 70km, the next set contains 70-140km records, and the last has records of earthquakes produced at 140 - 210 km from the site.

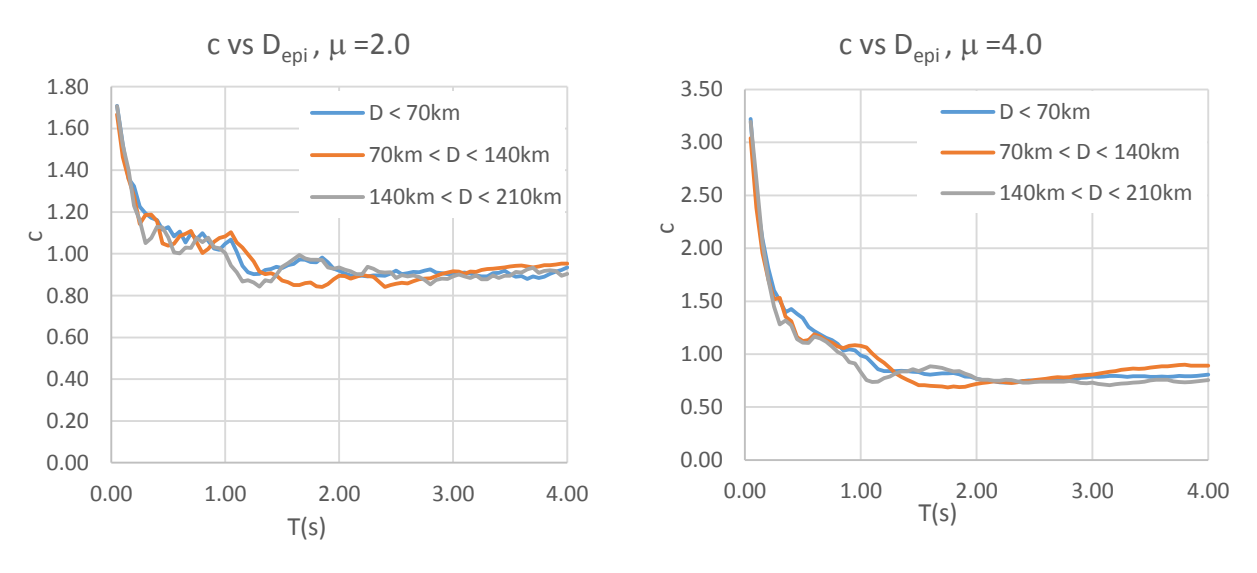


Fig. 3-11 Epicentral distance influence, ground type C, $\mu = 2.0$ and $\mu = 4.0$

Analysing the above figures, it can be concluded that the epicentral distance does not significantly affect the values of the displacement amplification coefficient. The same conclusion was reached by (Miranda & Ruiz Garcia, 2003), but is pointed out that it is possible that motions recorded near the fault would have a stronger influence on the coefficient. This only influences the systems with reduced ductility, $\mu \le 2$, while for ductile systems the influence of epicentral distance is reduced by increasing ductility.

Examining the influence of all the factors listed above, it can be concluded that on the global level, the ground conditions have the greatest influence. These are influencing the form of the c(T) variation and the period values to which it can be considered as equal to one.

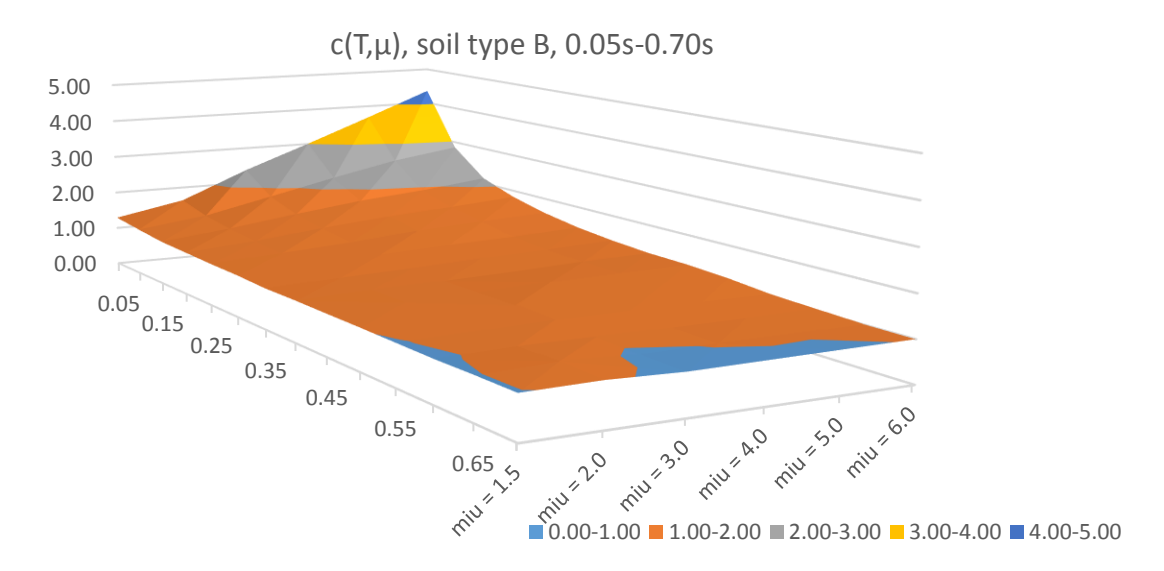


Fig. 3-12 $c(T, \mu)$ surface, soil type B

An overview of the coefficient as a function of ductility, for periods between 0.0 and 1.0s, can be provided by the picture above. Coefficient's values generate a surface in T, μ space, the values obtained by calculation acting as generating curves.

3.3.5 Functional form for median values

To facilitate the use of amplification coefficient data, a functional form has been found to provide its median values. The function has the following form:

$$c(T) = a_1 \sqrt{T} + \frac{a_2}{T} + a_3 \ln(T), \ T \le T_1$$

 $c(T) = 1.00, \ T > T_1$

where a_1 , a_2 , a_3 are coefficients obtained by regression, for each ground category and each level of displacement ductility, and T_1 is the period after which the median amplification coefficient becomes equal to one (this period is determined by the ground category). The following coefficient values were obtained for a_1 , a_2 , a_3 şi T_1 :

Ground type B	a ₁	a_2	a ₃	$T_1(s)$
$\mu = 1.5$	1.028	-0.001	-0.421	
$\mu = 2.0$	1.015	-0.003	-0.489	
$\mu = 3.0$	0.913	0.029	-0.532	0.70
$\mu = 4.0$	0.842	0.056	-0.576	0.70
$\mu = 5.0$	0.791	0.093	-0.560	
$\mu = 6.0$	0.743	0.131	-0.531	

Table 3-1 Functional form's coefficients, ground type B

Ground type C	a_1	a_2	a ₃	$T_1(s)$
$\mu = 1.5$	1.033	-0.013	-0.444	
$\mu = 2.0$	1.047	-0.003	-0.506	
$\mu = 3.0$	1.002	0.023	-0.587	1.00
$\mu = 4.0$	0.948	0.051	-0.654	1.00
$\mu = 5.0$	0.903	0.081	-0.699	
$\mu = 6.0$	0.864	0.113	-0.723	

Table 3-2 Functional form's coefficients, ground type C

They have a correlation coefficient of at least 0.99 with the original data and provide coefficient's values in a \pm 5% interval over the values obtained by the nonlinear calculation.

By setting the value of the standard deviation σ_c to the mean value throughout the period considered, the value of the coefficient c (T) can be obtained, just using the functional form and the above tables. For ground type C and $\mu = 3$, a comparison is made between the calculated values and the values obtained from the functional form.

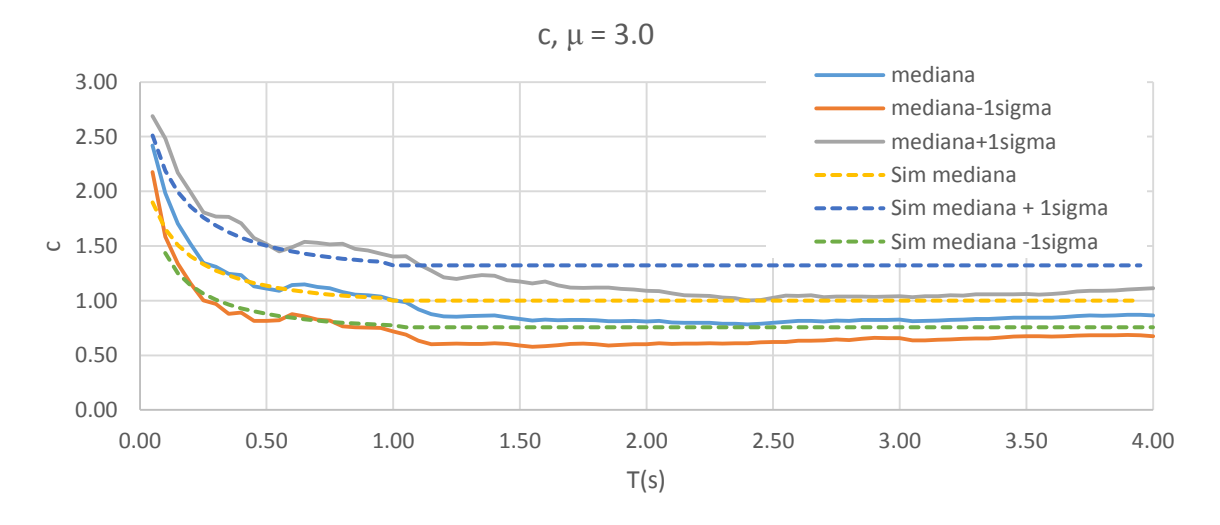


Fig. 3-13 Amplification coefficient – prediction vs. observed – soil type C and $\mu=3.0$

There is a good agreement to the median, the curve is slightly below the observed upper fractile. This situation arises from the simplified approach to consider standard deviation. Simple expression for σ_c was preferred, leading to underestimations of the higher fractile. For greater precision a more accurate expression of σ_c can be developed.

3.3.6 Inelastic displacement spectra for a given seismic scenario

Having determined the attenuation model, it can be used together with the amplification coefficients to obtain inelastic displacement spectra. In turn, they can be used as input for displacement-based design.

The procedure for constructing the inelastic spectrum is simple:

- Following seismic hazard disaggregation, a number of events which generates the larger values of seismic amplitude on the considered site can be found. These events are described through (M_w, d_{epi}) pairs;
- Using the attenuation model shown above, it can be generated the elastic displacement spectrum, SD_{el}(T), with the associated variability;
- Determine the coefficient of amplification, c(T), depending on the structural material, the hysteretic model, the soil conditions, etc., together with the associated variability;
- Considering $SD_{el}(T)$ and c(T) as independent variables (their numerical values are not statistically correlated), knowing the distributions of each variable (both lognormal), the inelastic displacement spectrum can be obtained as:

$$SD_{inel}(T) = SD_{el}(T) \cdot c(T)$$
 Ec. 3-13

- Accordingly, the product of two lognormal distributed independent variables, is also lognormal distributed with the mean and the variance (Lungu & Ghiocel, 1982):

$$m_{\ln SDinel(T)} = m_{\ln SDel(T)} + m_{\ln c(T)}$$

$$\sigma^{2}_{\ln SDinel(T)} = \sigma^{2}_{\ln SDel(T)} + \sigma^{2}_{\ln c(T)}$$
Ec. 3-14

Taking into account that the attenuation model is expressed in base 10 logarithms and natural logarithms were used to determine the amplification coefficient c(T), we can convert the attenuation model from lg to ln units. Then, using the equations above, SD_{inel}(T) can be obtained.

Analysing the correlation between numerical values $SD_{el}(T)$ and c(T) for a number of periods (and only the national database with moderate-large events of 1977, 1986 and 1990) it has been concluded that there is a weak correlation (<0.15), for some periods, or not correlated, for other periods. Therefore, the expression of $SD_{inel}(T)$ should be written as:

$$SD_{inel}(T) \approx SD_{el}(T) \cdot c(T)$$
 Ec. 3-15

Below are some results for two seismic events, INCERC1977 and EREN1986. The quadratic ground motion model was used and the amplification coefficients resulting from the nonlinear analysis.

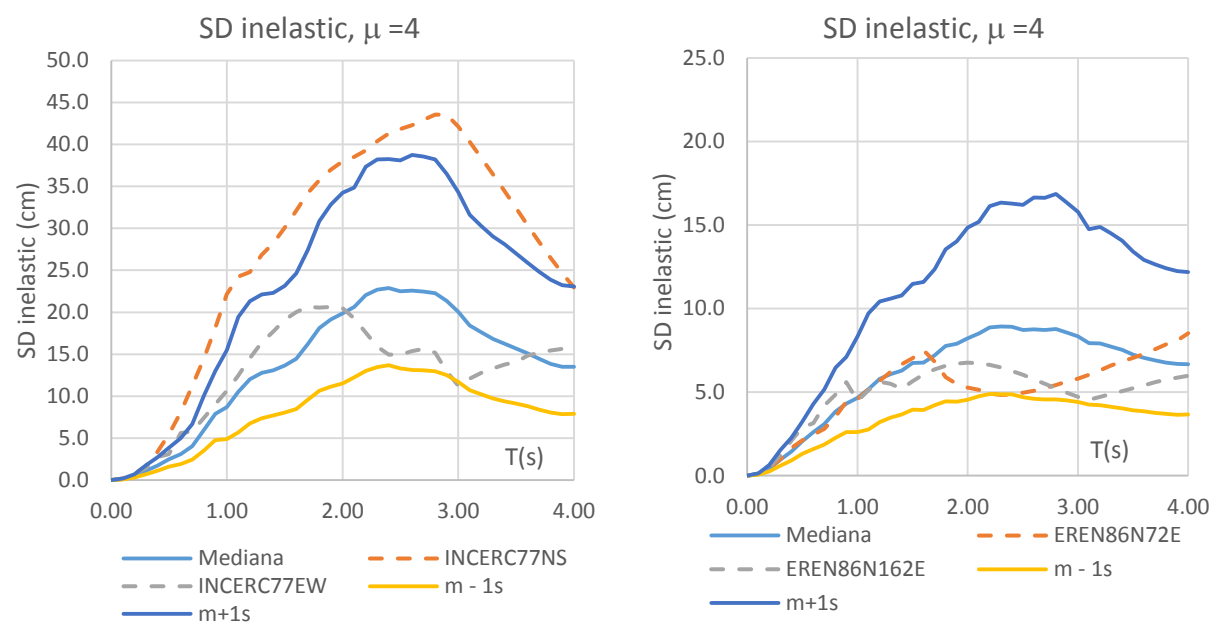


Fig. 3-14 Simulated nonlinear spectra (full line) for INCER1977 and EREN1986, μ = 4, ground type C

We can see the match between the generated inelastic spectra and those calculated from the records of the two events. For the 1977 event it is found that the calculated inelastic spectrum is relatively close to the one simulated (median + 1σ) over a large range of periods. For the 1986 earthquake, the median value generated is very close to the values for the two components.

Conclusions

An attenuation model for the relative displacement spectrum, corresponding to 5% damping, was obtained for intermediate-depth earthquakes of magnitude $5.2 \le M_w \le 7.4$, representative of the Vrancea subcrustal source. The ground motion prediction equations are applicable to sites located on ground types B and C, in front of the Carpathian arch (Moldova, Muntenia, and Dobrogea). The attenuation model was tested according to available literature. The coefficients of the model were obtained on three sets of data, with the best results being obtained for ground type C for the set of moderate-high national magnitude records and the set comprising the whole database. The best fit between the recorded data set and the one predicted by the attenuation model is given by the attenuation model containing a quadratic term, with coefficients determined for the first set of data (1977, 1986, and 1990 earthquakes). Generally, the observed spectra of the two horizontal perpendicular motion components are bounded by the median values \pm one standard deviation for soil type C. For soil type B, a larger number of standard deviations (about 2.0-2.5) are needed to envelope the values of the displacement spectra of the horizontal component pairs.

The database dependence of the attenuation model has been identified, expanding the database resulting in increased variability. Since the INCERC77 record produces the highest spectral values, the inclusion of a large number of moderate and small earthquakes (the complete set of records) leads to a reduction of the maximum spectral ordinates and to a lower capacity to simulate very strong seismic events.

A study was conducted on the inelastic displacement demands of SDOF systems, with characteristics representative for new reinforced concrete structures, subjected to earthquakes generated by the intermediate-depth Vrancea source. The terrain conditions, the magnitude of the earthquake and the epicentral distance influence on the amplification coefficient of the elastic displacements was examined. Of these, the soil conditions have the greatest effect on how the coefficient changes with the period. A pronounced local influence has the magnitude of the earthquake, for all analysed ductility values, around the period of 1.10s (for type C soil). The median values and the main statistical indicators for the amplification coefficient were calculated. A functional form was determined to represent the inelastic amplification coefficient as a function of system ductility, soil conditions and earthquake magnitude.

Using the attenuation model developed in the first part of the paper, together with the study on the displacement demands of the nonlinear systems, inelastic displacement spectra can be obtained for a given seismic scenario (given the magnitude, type of soil and epicentral distance). The variability of the attenuation model and of the inelastic displacement demand are included in the model of the estimated inelastic displacement spectrum. The inelastic displacement spectra may be a key element in displacement-based design, (Chopra & Goel, 2001), and the above approach provides useful information in this matter.

Acknowledgements

National Research Institute for Earth Science and Disaster Resilience (NIED) for granting the access to the Japanese network record database K-NET şi KiK-net.

Mr. Florin Pavel for the access to a great number of records and for USDP software without which the last part of the paper would have been almost impossible to finish.

Apendix Regression coefficients for the 1977 – 1990 earthquakes set

T [s]	a	b	С	h	σr ²	$\sigma_{e}{}^{2}$	σ^2	MEANNR	MEDNR	STDNR
0.00	0.00E+00	0.00E+00	0.00E+00	0.00E+00	0.00E+00	0.00E+00	0.00E+00	0.00	0.00	0.00
0.10	N/A	N/A	N/A	N/A	N/A	N/A	N/A	N/A	N/A	N/A
0.20	9.45E-01	5.05E-01	5.62E-04	85.17	8.94E-03	1.18E-02	2.07E-02	0.06	0.16	1.69
0.30	1.72E+00	5.07E-01	-1.07E-03	144.82	7.13E-03	9.33E-03	1.65E-02	0.09	0.24	1.73
0.40	2.42E+00	4.51E-01	-2.20E-03	197.99	8.04E-03	8.59E-03	1.66E-02	0.24	0.05	2.00
0.50	2.73E+00	4.34E-01	-2.59E-03	217.73	1.03E-02	1.01E-02	2.05E-02	0.39	0.65	2.16
0.60	2.03E+00	4.59E-01	-8.34E-04	105.74	1.01E-02	6.77E-03	1.69E-02	0.03	0.25	2.53
0.70	2.02E+00	4.66E-01	-5.42E-04	105.80	1.08E-02	5.35E-03	1.61E-02	0.04	0.07	2.52
0.80	1.96E+00	5.62E-01	-4.99E-04	102.04	1.07E-02	5.41E-03	1.61E-02	0.08	0.21	2.49
0.90	1.97E+00	4.75E-01	-1.77E-04	83.60	1.50E-02	1.00E-02	2.50E-02	0.03	0.10	1.99
1.00	1.84E+00	4.62E-01	5.82E-04	59.58	1.81E-02	1.16E-02	2.97E-02	0.06	0.19	1.81
1.10	1.91E+00	4.86E-01	3.88E-04	65.36	1.66E-02	8.15E-03	2.47E-02	0.03	0.07	1.89
1.20	1.95E+00	4.24E-01	5.40E-04	57.12	1.52E-02	7.83E-03	2.31E-02	0.03	0.04	1.92
1.30	2.01E+00	4.23E-01	3.41E-04	62.20	1.36E-02	7.38E-03	2.10E-02	0.03	0.15	2.04
1.40	1.99E+00	4.69E-01	2.76E-04	58.84	1.40E-02	6.09E-03	2.01E-02	0.03	0.22	2.03
1.50	1.92E+00	5.40E-01	3.90E-04	52.78	1.23E-02	7.57E-03	1.99E-02	0.07	0.17	2.03
1.60	1.94E+00	5.70E-01	2.39E-04	52.86	1.13E-02	8.20E-03	1.95E-02	0.08	0.10	2.02
1.70	1.96E+00	5.42E-01	2.99E-04	49.75	1.18E-02	9.16E-03	2.10E-02	0.08	0.18	1.91
1.80	1.99E+00	5.14E-01	2.80E-04	52.68	1.18E-02	1.08E-02	2.26E-02	0.10	0.10	1.82
1.90	2.03E+00	4.49E-01	4.08E-04	54.02	1.26E-02	1.31E-02	2.57E-02	0.11	0.10	1.72
2.00	2.06E+00	4.24E-01	3.39E-04	54.78	1.48E-02	1.44E-02	2.91E-02	0.10	0.23	1.60
2.10	2.11E+00	3.84E-01	3.18E-04	57.76	1.51E-02	1.74E-02	3.25E-02	0.12	0.10	1.53
2.20	2.15E+00	3.55E-01	2.55E-04	55.13	1.46E-02	1.88E-02	3.34E-02	0.13	0.06	1.50
2.30	2.20E+00	3.49E-01	6.29E-05	56.10	1.39E-02	1.82E-02	3.21E-02	0.13	0.02	1.49
2.40	2.23E+00	3.35E-01	-1.72E-05	60.57	1.28E-02	1.87E-02	3.15E-02	0.14	0.09	1.48
2.50	2.26E+00	3.24E-01	-1.02E-04	64.08	1.18E-02	1.85E-02	3.03E-02	0.14	0.15	1.49
2.60	2.27E+00	3.21E-01	-1.56E-04	64.85	1.13E-02	1.96E-02	3.09E-02	0.16	0.28	1.46
2.70	2.27E+00	3.14E-01	-1.55E-04	62.21	1.14E-02	2.02E-02	3.16E-02	0.16	0.28	1.43
2.80	2.29E+00	2.89E-01	-1.31E-04	61.24	1.09E-02	2.17E-02	3.26E-02	0.18	0.32	1.41
2.90	2.29E+00	3.09E-01	-1.86E-04	62.25	1.05E-02	2.04E-02	3.09E-02	0.17	0.32	1.43
3.00	2.31E+00	3.31E-01	-3.15E-04	70.13	1.02E-02	1.99E-02	3.01E-02	0.16	0.17	1.44
3.10	2.32E+00	3.42E-01	-3.57E-04	73.92	1.02E-02	1.87E-02	2.89E-02	0.15	0.10	1.47
3.20	2.34E+00	3.36E-01	-3.52E-04	76.97	1.03E-02	1.80E-02	2.83E-02	0.14	0.01	1.51
3.30	2.36E+00	3.33E-01	-4.27E-04	80.35	1.05E-02	1.74E-02	2.79E-02	0.13	0.05	1.57

3.40	2.37E+00	3.33E-01	-4.56E-04	81.44	1.09E-02	1.70E-02	2.79E-02	0.12	0.01	1.61
3.50	2.41E+00	3.52E-01	-6.34E-04	87.19	1.10E-02	1.52E-02	2.62E-02	0.09	0.04	1.66
3.60	2.45E+00	3.52E-01	-7.80E-04	94.13	1.10E-02	1.37E-02	2.48E-02	0.07	0.20	1.70
3.70	2.50E+00	3.41E-01	-8.87E-04	99.97	1.11E-02	1.31E-02	2.42E-02	0.05	0.14	1.72
3.80	2.54E+00	3.25E-01	-9.48E-04	105.06	1.13E-02	1.28E-02	2.42E-02	0.03	0.16	1.73
3.90	2.55E+00	3.05E-01	-8.64E-04	105.30	1.18E-02	1.31E-02	2.49E-02	0.02	0.29	1.71
4.00	2.54E+00	2.74E-01	-6.72E-04	102.90	1.17E-02	1.49E-02	2.66E-02	0.05	0.26	1.67
							mean	0.10	0.16	1.72
							median	0.09	0.15	1.70

Table A-1 Set 1, Ground type B, original GMPE (without quadratic term)

T [s]	a	b	С	h	σ_{r}^{2}	$\sigma_e{}^2$	σ^2	MEANNR	MEDNR	STDNR
0.00	0.00E+00	0.00E+00	0.00E+00	0.00	0.00E+00	0.00E+00	0.00E+00	0.00	0.00	0.00
0.10	2.04E-01	5.86E-01	-1.89E-04	103.88	5.58E-03	1.11E-02	1.66E-02	0.14	0.10	1.58
0.20	1.05E+00	5.43E-01	-3.94E-04	102.82	5.12E-03	1.21E-02	1.73E-02	0.19	0.03	1.69
0.30	1.45E+00	6.76E-01	-9.06E-04	112.61	3.59E-03	1.21E-02	1.57E-02	0.18	0.01	1.74
0.40	1.57E+00	7.37E-01	-7.56E-04	112.63	7.17E-03	3.83E-03	1.10E-02	0.30	0.18	1.90
0.50	2.10E+00	7.98E-01	-2.47E-03	142.49	8.77E-03	5.67E-03	1.44E-02	0.31	0.36	1.61
0.60	2.21E+00	8.51E-01	-2.93E-03	137.18	1.22E-02	1.52E-02	2.74E-02	0.24	0.34	1.29
0.70	2.12E+00	9.04E-01	-2.65E-03	118.35	1.20E-02	1.38E-02	2.57E-02	0.17	0.31	1.25
0.80	2.10E+00	1.08E+00	-2.79E-03	126.15	1.44E-02	9.45E-03	2.39E-02	0.14	0.16	1.25
0.90	1.57E+00	1.17E+00	-8.27E-04	55.58	1.19E-02	1.22E-02	2.41E-02	0.02	0.04	1.27
1.00	1.71E+00	1.15E+00	-1.18E-03	62.46	1.16E-02	2.50E-02	3.66E-02	0.07	0.20	1.14
1.10	1.82E+00	1.22E+00	-1.74E-03	76.03	1.16E-02	3.19E-02	4.35E-02	0.14	0.02	1.09
1.20	1.98E+00	1.23E+00	-2.22E-03	89.12	1.45E-02	2.25E-02	3.71E-02	0.13	0.09	1.06
1.30	2.10E+00	1.25E+00	-2.49E-03	107.31	1.70E-02	1.41E-02	3.11E-02	0.11	0.02	1.10
1.40	2.31E+00	1.22E+00	-2.85E-03	128.98	1.84E-02	9.89E-03	2.83E-02	0.17	0.12	1.14
1.50	2.59E+00	1.24E+00	-3.63E-03	155.56	1.87E-02	1.01E-02	2.88E-02	0.28	0.24	1.16
1.60	2.33E+00	1.28E+00	-3.06E-03	131.89	1.91E-02	1.08E-02	2.98E-02	0.16	0.07	1.19
1.70	2.25E+00	1.33E+00	-2.98E-03	122.53	1.83E-02	1.39E-02	3.21E-02	0.17	0.08	1.18
1.80	2.25E+00	1.36E+00	-3.03E-03	118.88	1.74E-02	1.86E-02	3.60E-02	0.22	0.23	1.15
1.90	2.16E+00	1.36E+00	-2.69E-03	106.19	1.70E-02	2.24E-02	3.94E-02	0.23	0.20	1.11
2.00	2.22E+00	1.34E+00	-2.83E-03	103.36	1.73E-02	2.78E-02	4.52E-02	0.25	0.25	1.05
2.10	2.23E+00	1.34E+00	-2.83E-03	100.13	1.54E-02	3.16E-02	4.70E-02	0.26	0.24	1.03
2.20	2.28E+00	1.34E+00	-2.93E-03	104.51	1.44E-02	3.70E-02	5.14E-02	0.29	0.29	1.00
2.30	2.24E+00	1.33E+00	-2.69E-03	98.81	1.36E-02	4.04E-02	5.40E-02	0.31	0.29	1.00
2.40	2.17E+00	1.31E+00	-2.34E-03	90.38	1.34E-02	4.26E-02	5.60E-02	0.31	0.25	1.01
2.50	2.12E+00	1.27E+00	-2.00E-03	81.68	1.50E-02	4.51E-02	6.01E-02	0.30	0.27	0.99
2.60	2.15E+00	1.23E+00	-1.92E-03	80.76	1.59E-02	5.00E-02	6.58E-02	0.31	0.29	0.98

.70	2.15E+00	+00 1.21E+00	-1.79E-03	80.66	1.60E-02	5.18E-02	6.78E-02	0.31	0.30	0.98
.80	2.23E+00	+00 1.18E+00	-1.95E-03	88.15	1.57E-02	5.36E-02	6.93E-02	0.32	0.28	0.99
.90	2.22E+00	+00 1.15E+00	-1.79E-03	86.74	1.56E-02	5.11E-02	6.66E-02	0.32	0.30	1.02
.00	2.24E+00	+00 1.11E+00	-1.70E-03	88.92	1.65E-02	4.76E-02	6.40E-02	0.31	0.30	1.04
.10	2.20E+00	+00 1.10E+00	-1.64E-03	83.46	1.74E-02	4.22E-02	5.96E-02	0.28	0.21	1.11
.20	2.32E+00	+00 1.02E+00	-1.79E-03	90.86	1.75E-02	4.45E-02	6.20E-02	0.29	0.26	1.06
.30	2.33E+00	+00 1.00E+00	-1.78E-03	89.79	1.73E-02	4.47E-02	6.20E-02	0.28	0.22	1.07
.40	2.29E+00	+00 9.95E-01	-1.63E-03	84.87	1.75E-02	4.43E-02	6.17E-02	0.27	0.19	1.08
.50	2.21E+00	+00 9.89E-01	-1.33E-03	77.94	1.80E-02	4.13E-02	5.93E-02	0.26	0.21	1.10
.60	2.18E+00	+00 9.79E-01	-1.17E-03	75.45	1.80E-02	3.88E-02	5.68E-02	0.25	0.26	1.13
.70	2.20E+00	+00 9.55E-01	-1.19E-03	77.27	1.76E-02	3.82E-02	5.57E-02	0.25	0.26	1.15
.80	2.24E+00	+00 9.29E-01	-1.25E-03	81.50	1.70E-02	3.78E-02	5.48E-02	0.25	0.30	1.17
.90	2.27E+00	+00 9.11E-01	-1.30E-03	86.76	1.64E-02	3.71E-02	5.35E-02	0.26	0.34	1.19
.00	2.29E+00	+00 9.04E-01	-1.30E-03	90.69	1.58E-02	3.70E-02	5.28E-02	0.27	0.38	1.21
•					•		mean	0.23	0.21	1.15
							median	0.25	0.24	1.11
						-	5.28E-02 mean	0.27	0.38	

Table A-2 Set 1, Ground type C, original GMPE (without quadratic term)

T [s]	a	b	С	d	h	σ_{r}^{2}	σ_{e}^{2}	σ^2	MEANNR	MEDNR	STDNR
0.00	0.00	0.00	0.00	0.00	0.00	0.00	0.00	0.00	0.00	0.00	0.00
0.10	N/A	N/A	N/A	N/A	N/A	N/A	N/A	N/A	N/A	N/A	N/A
0.20	9.41E-01	5.15E-01	5.39E-04	-0.01	85.21	8.94E-03	1.18E-02	2.07E-02	0.09	0.19	1.69
0.30	1.48E+00	1.14E+00	-1.07E-03	-0.37	144.91	7.13E-03	1.18E-02	1.89E-02	0.12	0.39	1.56
0.40	1.82E+00	1.80E+00	-2.20E-03	-0.82	198.15	8.04E-03	1.42E-03	9.46E-03	0.96	1.17	2.53
0.50	1.96E+00	2.00E+00	-2.59E-03	-0.96	218.04	1.03E-02	1.08E-03	1.14E-02	1.50	1.36	2.77
0.60	1.55E+00	1.72E+00	-8.33E-04	-0.78	105.81	1.01E-02	1.16E-03	1.13E-02	0.31	0.07	3.02
0.70	1.77E+00	1.11E+00	-5.42E-04	-0.40	105.86	1.08E-02	3.19E-03	1.40E-02	0.21	0.33	2.68
0.80	1.79E+00	1.00E+00	-4.99E-04	-0.27	102.11	1.07E-02	4.10E-03	1.48E-02	0.18	0.25	2.58
0.90	1.48E+00	1.80E+00	-1.76E-04	-0.82	83.66	1.50E-02	3.19E-03	1.81E-02	0.17	0.13	2.26
1.00	1.37E+00	1.79E+00	5.82E-04	-0.82	59.62	1.81E-02	4.64E-03	2.27E-02	0.11	0.00	1.99
1.10	1.50E+00	1.64E+00	3.88E-04	-0.72	65.40	1.66E-02	2.99E-03	1.96E-02	0.13	0.41	2.06
1.20	1.42E+00	1.91E+00	5.40E-04	-0.93	57.16	1.52E-02	1.06E-03	1.63E-02	0.15	0.01	2.21
1.30	1.49E+00	1.86E+00	3.42E-04	-0.90	62.24	1.36E-02	9.49E-04	1.46E-02	0.16	0.11	2.37
1.40	1.61E+00	1.54E+00	2.77E-04	-0.67	58.88	1.40E-02	1.87E-03	1.59E-02	0.13	0.07	2.23
1.50	1.71E+00	1.14E+00	3.91E-04	-0.37	52.81	1.23E-02	5.57E-03	1.79E-02	0.08	0.11	2.11
1.60	1.70E+00	1.23E+00	2.39E-04	-0.40	52.89	1.13E-02	5.91E-03	1.72E-02	0.08	0.02	2.10
1.70	1.53E+00	1.73E+00	2.99E-04	-0.73	49.78	1.18E-02	3.61E-03	1.55E-02	0.09	0.20	2.13
1.80	1.49E+00	1.93E+00	2.81E-04	-0.86	52.71	1.18E-02	3.21E-03	1.50E-02	0.10	0.28	2.11
1.90	1.47E+00	2.00E+00	4.07E-04	-0.93	54.05	1.26E-02	3.94E-03	1.65E-02	0.09	0.48	2.00

2.00	1.43E+00	2.20E+00	3.39E-04	-1.08	54.81	1.48E-02	3.01E-03	1.78E-02	0.11	0.24	1.89
2.10	1.42E+00	2.32E+00	3.19E-04	-1.17	57.79	1.51E-02	3.54E-03	1.87E-02	0.11	0.19	1.83
2.20	1.43E+00	2.36E+00	2.56E-04	-1.21	55.16	1.46E-02	3.74E-03	1.84E-02	0.10	0.13	1.81
2.30	1.47E+00	2.37E+00	6.32E-05	-1.22	56.14	1.39E-02	3.09E-03	1.70E-02	0.11	0.22	1.83
2.40	1.47E+00	2.45E+00	-1.68E-05	-1.26	60.61	1.28E-02	2.36E-03	1.51E-02	0.12	0.28	1.89
2.50	1.50E+00	2.44E+00	-1.02E-04	-1.27	64.12	1.18E-02	1.96E-03	1.38E-02	0.13	0.13	1.95
2.60	1.48E+00	2.53E+00	-1.56E-04	-1.32	64.90	1.13E-02	1.63E-03	1.29E-02	0.14	0.04	1.97
2.70	1.46E+00	2.57E+00	-1.55E-04	-1.34	62.25	1.14E-02	1.63E-03	1.31E-02	0.14	0.02	1.93
2.80	1.46E+00	2.57E+00	-1.30E-04	-1.35	61.28	1.09E-02	2.05E-03	1.30E-02	0.12	0.05	1.92
2.90	1.50E+00	2.48E+00	-1.86E-04	-1.29	62.29	1.05E-02	2.32E-03	1.29E-02	0.12	0.20	1.91
3.00	1.55E+00	2.45E+00	-3.15E-04	-1.26	70.18	1.02E-02	2.37E-03	1.26E-02	0.13	0.07	1.93
3.10	1.58E+00	2.40E+00	-3.57E-04	-1.22	73.97	1.02E-02	2.24E-03	1.24E-02	0.15	0.03	1.96
3.20	1.61E+00	2.34E+00	-3.51E-04	-1.20	77.02	1.03E-02	2.31E-03	1.26E-02	0.15	0.14	2.01
3.30	1.66E+00	2.26E+00	-4.26E-04	-1.15	80.41	1.05E-02	2.71E-03	1.32E-02	0.15	0.16	2.05
3.40	1.68E+00	2.23E+00	-4.56E-04	-1.13	81.49	1.09E-02	2.86E-03	1.37E-02	0.15	0.12	2.08
3.50	1.75E+00	2.13E+00	-6.34E-04	-1.06	87.25	1.10E-02	2.72E-03	1.37E-02	0.17	0.10	2.10
3.60	1.83E+00	2.05E+00	-7.79E-04	-1.02	94.20	1.10E-02	2.50E-03	1.35E-02	0.20	0.00	2.13
3.70	1.88E+00	2.00E+00	-8.86E-04	-1.00	100.04	1.11E-02	2.36E-03	1.35E-02	0.23	0.03	2.14
3.80	1.91E+00	2.01E+00	-9.47E-04	-1.02	105.14	1.13E-02	2.00E-03	1.33E-02	0.26	0.02	2.17
3.90	1.86E+00	2.13E+00	-8.63E-04	-1.11	105.37	1.18E-02	1.19E-03	1.29E-02	0.32	0.06	2.20
4.00	1.78E+00	2.31E+00	-6.72E-04	-1.24	102.97	1.17E-02	6.44E-04	1.23E-02	0.36	0.02	2.25
								mean	0.20	0.20	2.06
								median	0.14	0.12	2.07

TableA-3 Set 1, Ground type B, with quadratic term

T [s]	a	b	С	d	h	σ_{r}^{2}	$\sigma_{\text{e}}{}^2$	σ^2	MEANNR	MEDNR	STDNR
0.00	0.00	0.00	0.00	0.00	0.00	0.00	0.00	0.00	0.00	0.00	0.00
0.10	7.00E-02	9.68E-01	-1.89E-04	-0.223	103.88	5.58E-03	1.02E-02	1.57E-02	0.04	0.01	1.59
0.20	8.31E-01	1.16E+00	-3.94E-04	-0.356	102.82	5.12E-03	1.01E-02	1.52E-02	0.04	0.10	1.75
0.30	1.24E+00	1.28E+00	-9.06E-04	-0.350	112.61	3.59E-03	1.01E-02	1.37E-02	0.02	0.02	1.80
0.40	1.42E+00	1.18E+00	-7.56E-04	-0.271	112.63	7.17E-03	2.70E-03	9.86E-03	0.19	0.07	1.98
0.50	1.95E+00	1.24E+00	-2.47E-03	-0.271	142.49	8.77E-03	4.40E-03	1.32E-02	0.14	0.28	1.65
0.60	1.99E+00	1.49E+00	-2.93E-03	-0.375	137.18	1.22E-02	1.27E-02	2.49E-02	0.08	0.25	1.30
0.70	2.00E+00	1.26E+00	-2.61E-03	-0.210	118.46	1.20E-02	1.28E-02	2.47E-02	0.04	0.14	1.24
0.80	2.09E+00	1.12E+00	-2.79E-03	-0.024	126.15	1.44E-02	9.37E-03	2.38E-02	0.13	0.14	1.25
0.90	1.67E+00	8.83E-01	-8.27E-04	0.168	55.58	1.19E-02	1.23E-02	2.41E-02	0.08	0.07	1.28
1.00	1.90E+00	5.91E-01	-1.18E-03	0.324	62.46	1.16E-02	2.42E-02	3.58E-02	0.03	0.42	1.18
1.10	2.15E+00	3.08E-01	-1.74E-03	0.523	76.12	1.16E-02	2.90E-02	4.06E-02	0.02	0.29	1.15
1.20	2.31E+00	2.73E-01	-2.22E-03	0.560	89.12	1.45E-02	1.96E-02	3.41E-02	0.07	0.14	1.13

1.30	2.39E+00	3.68E-01	-2.49E-03	0.522	107.31	1.70E-02	1.24E-02	2.95E-02	0.12	0.28	1.15
1.40	2.58E+00	3.13E-01	-2.85E-03	0.544	128.98	1.84E-02	8.67E-03	2.71E-02	0.17	0.26	1.18
1.50	2.85E+00	3.39E-01	-3.63E-03	0.542	155.56	1.87E-02	8.88E-03	2.76E-02	0.14	0.31	1.20
1.60	2.61E+00	3.86E-01	-3.06E-03	0.535	131.89	1.91E-02	9.59E-03	2.86E-02	0.16	0.27	1.23
1.70	2.57E+00	3.37E-01	-2.98E-03	0.593	122.53	1.83E-02	1.15E-02	2.98E-02	0.14	0.17	1.24
1.80	2.66E+00	1.31E-01	-3.03E-03	0.719	118.88	1.74E-02	1.36E-02	3.10E-02	0.12	0.31	1.25
1.90	2.64E+00	-5.09E-02	-2.69E-03	0.824	106.19	1.70E-02	1.48E-02	3.18E-02	0.11	0.25	1.24
2.00	2.76E+00	-2.25E-01	-2.83E-03	0.908	103.36	1.73E-02	1.80E-02	3.53E-02	0.09	0.30	1.19
2.10	2.80E+00	-3.19E-01	-2.83E-03	0.957	100.13	1.54E-02	1.99E-02	3.53E-02	0.07	0.29	1.18
2.20	2.91E+00	-4.84E-01	-2.93E-03	1.048	104.51	1.44E-02	2.22E-02	3.66E-02	0.06	0.24	1.18
2.30	2.93E+00	-6.49E-01	-2.69E-03	1.134	98.81	1.36E-02	2.26E-02	3.62E-02	0.05	0.12	1.20
2.40	2.90E+00	-7.42E-01	-2.34E-03	1.175	90.38	1.34E-02	2.36E-02	3.70E-02	0.05	0.14	1.21
2.50	2.87E+00	-8.53E-01	-2.00E-03	1.221	81.68	1.50E-02	2.51E-02	4.00E-02	0.05	0.26	1.19
2.60	2.94E+00	-1.02E+00	-1.92E-03	1.292	80.76	1.59E-02	2.75E-02	4.33E-02	0.05	0.36	1.18
2.70	2.97E+00	-1.10E+00	-1.79E-03	1.323	80.66	1.60E-02	2.81E-02	4.41E-02	0.05	0.32	1.18
2.80	3.06E+00	-1.18E+00	-1.95E-03	1.350	88.15	1.57E-02	2.84E-02	4.40E-02	0.05	0.20	1.20
2.90	3.04E+00	-1.16E+00	-1.79E-03	1.327	86.74	1.56E-02	2.68E-02	4.24E-02	0.05	0.03	1.24
3.00	3.03E+00	-1.11E+00	-1.70E-03	1.275	88.92	1.65E-02	2.54E-02	4.19E-02	0.06	0.03	1.26
3.10	2.90E+00	-8.99E-01	-1.64E-03	1.153	83.46	1.74E-02	2.50E-02	4.23E-02	0.06	0.03	1.31
3.20	3.06E+00	-1.07E+00	-1.79E-03	1.205	90.86	1.75E-02	2.51E-02	4.26E-02	0.06	0.01	1.26
3.30	3.05E+00	-1.04E+00	-1.78E-03	1.177	89.79	1.73E-02	2.64E-02	4.37E-02	0.06	0.01	1.26
3.40	2.99E+00	-1.01E+00	-1.63E-03	1.152	84.87	1.75E-02	2.70E-02	4.45E-02	0.06	0.15	1.26
3.50	2.89E+00	-9.57E-01	-1.33E-03	1.122	77.94	1.80E-02	2.54E-02	4.35E-02	0.06	0.14	1.28
3.60	2.83E+00	-8.88E-01	-1.17E-03	1.077	75.45	1.80E-02	2.45E-02	4.25E-02	0.06	0.12	1.30
3.70	2.84E+00	-8.67E-01	-1.19E-03	1.052	77.27	1.76E-02	2.46E-02	4.21E-02	0.06	0.06	1.32
3.80	2.87E+00	-8.72E-01	-1.25E-03	1.039	81.50	1.70E-02	2.44E-02	4.14E-02	0.06	0.04	1.34
3.90	2.90E+00	-8.83E-01	-1.30E-03	1.035	86.76	1.64E-02	2.35E-02	4.00E-02	0.06	0.06	1.38
4.00	2.92E+00	-9.16E-01	-1.30E-03	1.049	90.69	1.58E-02	2.28E-02	3.86E-02	0.06	0.01	1.41
								mean	0.07	0.16	1.27
								median	0.06	0.14	1.24
											_

Table A-4 Set 1, Ground type C, with quadratic term

Regression coefficients for the digital set of records

T [s]	a	b	С	h	σr ²	σ_{e}^{2}	σ^2	MEANNR	MEDNR	STDNR
0.00	0.00E+00	0.00E+00	0.00E+00	0.00	0.00E+00	0.00E+00	0.00E+00	0.00	0.00	0.00
0.10	4.71E-01	6.31E-01	-5.34E-04	47.96	9.76E-03	2.93E-03	1.27E-02	0.30	0.21	3.03
0.20	1.50E+00	5.87E-01	-1.97E-03	107.90	1.29E-02	0.00E+00	1.29E-02	0.44	0.30	2.75
0.30	1.39E+00	6.29E-01	-5.46E-04	74.55	1.33E-02	0.00E+00	1.33E-02	0.23	0.13	2.92
0.40	1.26E+00	6.83E-01	4.08E-04	37.18	1.38E-02	2.04E-02	3.42E-02	0.29	0.07	2.03
0.50	1.46E+00	6.84E-01	1.16E-04	41.20	1.24E-02	3.98E-03	1.64E-02	0.17	0.08	2.87
0.60	1.69E+00	7.24E-01	-2.26E-04	45.08	1.43E-02	0.00E+00	1.43E-02	0.86	0.89	2.88
0.70	1.67E+00	7.29E-01	-9.36E-05	45.39	1.48E-02	0.00E+00	1.48E-02	0.44	0.52	2.82
0.80	1.74E+00	7.78E-01	-1.83E-04	44.31	1.39E-02	1.76E-03	1.57E-02	0.28	0.27	2.65
0.90	1.73E+00	8.03E-01	-1.84E-04	43.40	1.28E-02	2.13E-03	1.49E-02	0.00	0.37	2.68
1.00	1.70E+00	8.26E-01	2.20E-05	34.94	1.37E-02	2.60E-03	1.63E-02	0.01	0.11	2.50
1.10	1.72E+00	8.35E-01	4.32E-05	34.87	1.30E-02	1.75E-03	1.48E-02	0.05	0.04	2.54
1.20	1.81E+00	8.91E-01	-3.78E-04	43.10	1.23E-02	4.14E-03	1.65E-02	0.06	0.08	2.38
1.30	1.85E+00	9.24E-01	-5.37E-04	43.66	1.08E-02	7.27E-03	1.81E-02	0.08	0.04	2.22
1.40	1.87E+00	9.28E-01	-5.99E-04	46.08	1.23E-02	1.14E-02	2.37E-02	0.13	0.12	1.91
1.50	1.89E+00	9.25E-01	-7.60E-04	51.27	1.07E-02	1.13E-02	2.19E-02	0.06	0.27	1.92
1.60	1.88E+00	9.09E-01	-7.80E-04	51.21	1.09E-02	1.06E-02	2.14E-02	0.05	0.19	1.92
1.70	1.86E+00	9.09E-01	-7.73E-04	50.62	1.21E-02	1.39E-02	2.59E-02	0.01	0.20	1.73
1.80	1.86E+00	8.92E-01	-8.12E-04	49.81	1.28E-02	1.14E-02	2.42E-02	0.05	0.07	1.79
1.90	1.85E+00	9.00E-01	-7.88E-04	49.81	1.24E-02	1.70E-02	2.95E-02	0.01	0.19	1.65
2.00	1.85E+00	9.06E-01	-7.94E-04	49.35	1.19E-02	1.79E-02	2.98E-02	0.00	0.16	1.65
2.10	1.92E+00	8.99E-01	-9.29E-04	59.48	1.13E-02	7.43E-03	1.87E-02	0.28	0.11	2.05
2.20	1.89E+00	8.90E-01	-8.21E-04	56.39	9.96E-03	6.13E-03	1.61E-02	0.31	0.20	2.16
2.30	1.88E+00	8.82E-01	-7.89E-04	55.10	9.23E-03	5.04E-03	1.43E-02	0.37	0.17	2.27
2.40	1.92E+00	8.84E-01	-9.66E-04	60.93	8.71E-03	4.52E-03	1.32E-02	0.45	0.12	2.36
2.50	1.93E+00	8.86E-01	-9.62E-04	63.47	8.33E-03	4.04E-03	1.24E-02	0.53	0.05	2.44
2.60	1.91E+00	8.96E-01	-9.01E-04	63.20	7.79E-03	7.41E-03	1.52E-02	0.35	0.03	2.21
2.70	1.92E+00	9.11E-01	-9.92E-04	67.54	8.08E-03	9.94E-03	1.80E-02	0.26	0.06	2.05
2.80	1.93E+00	9.15E-01	-1.06E-03	68.76	8.10E-03	9.94E-03	1.80E-02	0.22	0.00	2.06
2.90	1.94E+00	9.11E-01	-1.09E-03	69.97	8.61E-03	6.63E-03	1.52E-02	0.33	0.11	2.23
3.00	1.91E+00	9.26E-01	-9.31E-04	68.23	8.62E-03	6.56E-03	1.52E-02	0.29	0.13	2.22
3.10	1.90E+00	9.38E-01	-9.07E-04	67.81	8.82E-03	6.65E-03	1.55E-02	0.26	0.07	2.20
3.20	1.89E+00	9.37E-01	-9.10E-04	66.58	9.23E-03	5.36E-03	1.46E-02	0.28	0.00	2.27
3.30	1.85E+00	9.31E-01	-8.06E-04	62.63	9.20E-03	4.90E-03	1.41E-02	0.22	0.12	2.31
3.40	1.86E+00	9.33E-01	-8.42E-04	63.76	9.56E-03	5.43E-03	1.50E-02	0.20	0.23	2.25
3.50	1.82E+00	9.26E-01	-7.04E-04	59.26	9.94E-03	4.88E-03	1.48E-02	0.18	0.24	2.26
3.60	1.79E+00	9.20E-01	-6.45E-04	55.65	1.03E-02	4.45E-03	1.47E-02	0.18	0.25	2.26

3.70	1.79E+00	9.10E-01	-6.41E-04	54.92	1.04E-02	3.71E-03	1.41E-02	0.20	0.30	2.29
3.80	1.78E+00	9.06E-01	-6.19E-04	54.11	1.03E-02	3.70E-03	1.40E-02	0.17	0.35	2.30
3.90	1.76E+00	9.09E-01	-5.75E-04	54.83	1.03E-02	4.00E-03	1.43E-02	0.13	0.38	2.28
4.00	1.74E+00	9.09E-01	-4.75E-04	51.15	1.03E-02	4.44E-03	1.48E-02	0.07	0.39	2.23
4.20	1.71E+00	9.04E-01	-4.30E-04	46.10	1.11E-02	3.59E-03	1.47E-02	0.05	0.44	2.20
4.40	1.71E+00	8.96E-01	-4.84E-04	45.95	1.11E-02	2.14E-03	1.33E-02	0.05	0.47	2.25
4.60	1.68E+00	9.01E-01	-3.70E-04	43.72	1.06E-02	2.60E-03	1.32E-02	0.04	0.29	2.24
4.80	1.67E+00	9.04E-01	-3.57E-04	43.50	1.10E-02	3.54E-03	1.45E-02	0.02	0.38	2.13
5.00	1.63E+00	9.06E-01	-2.26E-04	39.52	1.19E-02	3.89E-03	1.58E-02	0.02	0.39	2.07
5.20	1.62E+00	8.99E-01	-2.41E-04	39.82	1.20E-02	3.72E-03	1.57E-02	0.04	0.43	2.10
5.40	1.61E+00	9.05E-01	-1.89E-04	39.68	1.13E-02	4.58E-03	1.59E-02	0.07	0.43	2.11
5.60	1.60E+00	9.17E-01	-1.57E-04	39.81	1.08E-02	6.59E-03	1.74E-02	0.11	0.45	2.04
5.80	1.61E+00	9.15E-01	-2.41E-04	41.50	1.07E-02	7.17E-03	1.79E-02	0.12	0.48	2.00
6.00	1.58E+00	9.05E-01	-1.21E-04	37.28	1.02E-02	6.55E-03	1.68E-02	0.14	0.45	2.05
6.40	1.58E+00	9.05E-01	-1.26E-04	37.27	1.03E-02	5.80E-03	1.61E-02	0.08	0.29	2.09
6.80	1.61E+00	9.05E-01	-2.82E-04	41.43	1.09E-02	5.91E-03	1.68E-02	0.05	0.27	2.02
7.20	1.62E+00	9.06E-01	-3.94E-04	42.91	1.05E-02	9.09E-03	1.96E-02	0.09	0.28	1.88
7.60	1.62E+00	9.13E-01	-4.92E-04	42.02	1.09E-02	1.28E-02	2.37E-02	0.11	0.17	1.73
8.00	1.62E+00	9.13E-01	-5.09E-04	41.43	1.04E-02	1.35E-02	2.39E-02	0.11	0.24	1.72
							mean	0.18	0.23	2.18
							median	0.20	0.13	2.26

Table A-5 Set 2, Ground type B

T [s]	a	b	С	h	σ _r ²	${\sigma_{\text{e}}}^2$	σ^2	MEANNR	MEDNR	STDNR
0.00	0.00E+00	0.00E+00	0.00E+00	0.00	0.00E+00	0.00E+00	0.00E+00	0.00	0.00	0.00
0.10	3.16E+00	7.73E-01	-6.64E-03	306.12	5.98E-03	1.99E-02	2.58E-02	0.76	0.78	1.57
0.20	N/A	N/A	N/A	N/A	N/A	N/A	N/A	N/A	N/A	N/A
0.30	N/A	N/A	N/A	N/A	N/A	N/A	N/A	N/A	N/A	N/A
0.40	N/A	N/A	N/A	N/A	N/A	N/A	N/A	N/A	N/A	N/A
0.50	N/A	N/A	N/A	N/A	N/A	N/A	N/A	N/A	N/A	N/A
0.60	N/A	N/A	N/A	N/A	N/A	N/A	N/A	N/A	N/A	N/A
0.70	1.37E+01	1.05E+00	-1.59E-02	697.86	1.24E-02	6.41E-03	1.88E-02	0.37	0.41	2.33
0.80	4.68E+00	1.07E+00	-7.27E-03	322.52	1.49E-02	8.10E-03	2.30E-02	0.27	0.47	2.10
0.90	4.44E+00	1.11E+00	-7.29E-03	307.35	1.51E-02	1.01E-01	1.16E-01	0.60	0.55	0.94
1.00	4.75E+00	1.14E+00	-7.76E-03	316.86	1.45E-02	1.13E-01	1.28E-01	0.42	0.28	0.92
1.10	4.57E+00	1.19E+00	-7.42E-03	301.08	1.47E-02	1.20E-01	1.34E-01	0.30	0.12	0.93
1.20	3.86E+00	1.20E+00	-6.25E-03	246.70	1.52E-02	1.18E-01	1.33E-01	0.18	0.04	0.95
1.30	4.01E+00	1.21E+00	-6.65E-03	258.78	1.59E-02	1.03E-01	1.19E-01	0.36	0.04	0.99

1.50 3.806+00 1.23E+00 -6.19E+03 246.75 1.37E+02 8.90E+02 1.03E+01 0.36 0.12 1.02 1.60 3.58E+00 1.23E+00 5.58E+03 228.03 1.36E+02 8.09E+02 9.45E+02 0.33 0.11 1.05 1.70 3.40E+00 1.23E+00 5.58E+03 226.92 1.23E+02 6.98E+02 8.21E+02 0.39 0.27 1.08 1.80 3.45E+00 1.22E+00 5.54E+03 226.34 1.22E+02 6.56E+02 7.78E+02 0.43 0.28 1.10 2.00 4.02E+00 1.22E+00 -5.7EE+03 271.61 1.24E+02 6.48E+02 7.78E+02 0.48 0.57 1.09 2.10 4.98E+00 1.22E+00 -8.66E+03 347.03 1.23E+02 6.45E+02 7.57E+02 0.68 0.57 1.06 2.20 5.09E+00 1.21E+00 -7.66E+03 38.22 1.13E+02 6.47E+02 7.56E+02 0.58 0.81 1.07 2.40	1 1										
160 3.58E+00 1.23E+00 5.78E+03 228.03 1.36E+02 8.09E+02 9.45E+02 0.33 0.11 1.05 1.70 3.40E+00 1.23E+00 5.53E+03 217.41 1.27E+02 7.36E+02 8.63E+02 0.33 0.12 1.07 1.80 3.45E+00 1.23E+00 5.54E+03 226.92 1.23E+02 6.98E+02 8.1E+02 0.43 0.28 1.10 1.90 3.45E+00 1.22E+00 5.45E+03 226.34 1.22E+02 6.56E+02 7.78E+02 0.43 0.28 1.10 2.10 4.98E+00 1.22E+00 -6.72E+03 271.61 1.24E+02 6.48E+02 7.73E+02 0.68 0.57 1.00 2.20 5.09E+00 1.21E+00 -8.60E+03 347.03 1.23E+02 6.47E+02 7.59E+02 0.95 0.81 1.07 2.40 4.23E+00 1.21E+00 -6.79E+03 272.58 1.13E+02 6.69E+02 7.59E+02 0.95 0.81 1.07 2.50	1.40	4.26E+00	1.22E+00	-7.06E-03	280.99	1.45E-02	1.00E-01	1.14E-01	0.47	0.21	0.99
1.70 3.40E+00 1.23E+00 -5.39E+03 217.41 1.27E+02 7.36E+02 8.63E+02 0.33 0.12 1.07 1.80 3.45E+00 1.23E+00 5.44E+03 226.92 1.23E+02 6.98E+02 8.21E+02 0.39 0.27 1.08 1.90 3.43E+00 1.22E+00 5.45E+03 27.63 1.22E+02 6.56E+02 7.78E+02 0.43 0.28 1.10 2.00 4.02E+00 1.22E+00 2.67E+03 27.16E+03 340.88 1.23E+02 6.48E+02 7.78E+02 0.68 0.57 1.09 2.20 5.09E+00 1.22E+00 -8.42E+03 340.88 1.33E+02 6.56E+02 7.59E+02 0.95 0.81 1.07 2.40 4.23E+00 1.21E+00 -7.11E+03 288.33 1.07E+02 6.54E+02 7.59E+02 0.95 0.81 1.07 2.50 4.02E+00 1.22E+00 -6.05E+03 241.22 1.21E+02 6.29E+02 7.59E+02 0.95 0.81 1.08 <	1.50	3.80E+00	1.23E+00	-6.19E-03	246.75	1.37E-02	8.90E-02	1.03E-01	0.36	0.12	1.02
1.80 3.45E+00 1.23E+00 -5.44E+03 226 92 1.23E+02 6.98E+02 8.21E+02 0.39 0.27 1.08 1.90 3.43E+00 1.22E+00 5.45E+03 226.34 1.22E+02 6.56E+02 7.78E+02 0.43 0.28 1.10 2.00 4.02E+00 1.22E+03 226.34 1.22E+02 6.56E+02 7.78E+02 0.68 0.57 1.09 2.10 4.98E+00 1.22E+00 8.42E+03 340.38 1.33E+02 6.55E+02 7.87E+02 1.30 1.17 1.06 2.20 5.09E+00 1.21E+00 -6.60E+03 347.03 1.23E+02 7.59E+02 1.34 1.18 1.06 2.40 4.23E+00 1.22E+00 -7.64E+03 308.32 1.13E+02 6.47E+02 7.61E+02 0.78 0.61 1.08 2.50 4.02E+00 1.22E+00 -6.0E+03 227.58 1.13E+02 6.66E+02 7.79E+02 0.70 0.49 1.08 2.50 3.53E+00 1.22E+00	1.60	3.58E+00	1.23E+00	-5.78E-03	228.03	1.36E-02	8.09E-02	9.45E-02	0.33	0.11	1.05
1.90	1.70	3.40E+00	1.23E+00	-5.39E-03	217.41	1.27E-02	7.36E-02	8.63E-02	0.33	0.12	1.07
2.00 4.02E+00 1.22E+00 -6.72E-03 271.61 1.24E-02 6.48E-02 7.73E-02 0.68 0.57 1.09 2.10 4.98E+00 1.22E+00 -8.42E-03 340.88 1.33E-02 6.55E-02 7.87E-02 1.30 1.17 1.06 2.20 5.09E+00 1.21E+00 -8.60E-03 347.03 1.23E-02 6.43E-02 7.66E-02 1.34 1.18 1.06 2.30 4.52E+00 1.21E+00 -7.64E-03 308.32 1.13E-02 6.47E-02 7.59E-02 0.95 0.81 1.07 2.40 4.23E+00 1.22E+00 -6.79E-03 272.58 1.13E-02 6.66E-02 7.79E-02 0.70 0.49 1.08 2.50 3.64E+00 1.22E+00 -6.05E-03 241.22 1.21E-02 6.49E-02 7.63E-02 0.57 0.30 1.09 2.00 3.53E+00 1.22E+00 -5.93E-03 242.33 1.29E-02 7.49E-02 0.58 0.34 1.11 3.00 3.43E+00 <td>1.80</td> <td>3.45E+00</td> <td>1.23E+00</td> <td>-5.44E-03</td> <td>226.92</td> <td>1.23E-02</td> <td>6.98E-02</td> <td>8.21E-02</td> <td>0.39</td> <td>0.27</td> <td>1.08</td>	1.80	3.45E+00	1.23E+00	-5.44E-03	226.92	1.23E-02	6.98E-02	8.21E-02	0.39	0.27	1.08
2.10 4.98E+00 1.22E+00 -8.42E-03 340.88 1.33E-02 6.55E-02 7.87E-02 1.30 1.17 1.06 2.20 5.09E+00 1.21E+00 -8.60E-03 347.03 1.23E-02 6.43E-02 7.66E-02 1.34 1.18 1.06 2.30 4.52E+00 1.21E+00 -7.64E-03 308.32 1.13E-02 6.47E-02 7.59E-02 0.95 0.81 1.07 2.40 4.23E+00 1.22E+00 -6.79E-03 272.58 1.31E-02 6.65E-02 7.61E-02 0.78 0.61 1.08 2.50 4.02E+00 1.22E+00 -6.05E-03 244.17 1.14E-02 6.49E-02 7.63E-02 0.57 0.30 1.09 2.70 3.58E+00 1.22E+00 -5.93E-03 241.22 1.21E-02 6.29E-02 7.49E-02 0.58 0.34 1.11 2.80 3.63E+00 1.22E+00 -5.80E-03 242.31 1.29E-02 7.55E-02 0.62 0.42 1.11 3.00 3.43E+00 <td>1.90</td> <td>3.43E+00</td> <td>1.22E+00</td> <td>-5.45E-03</td> <td>226.34</td> <td>1.22E-02</td> <td>6.56E-02</td> <td>7.78E-02</td> <td>0.43</td> <td>0.28</td> <td>1.10</td>	1.90	3.43E+00	1.22E+00	-5.45E-03	226.34	1.22E-02	6.56E-02	7.78E-02	0.43	0.28	1.10
2.20 5.99E+00 1.21E+00 -8.60E+03 347.03 1.23E+02 6.43E+02 7.66E+02 1.34 1.18 1.06 2.30 4.52E+00 1.21E+00 -7.64E+03 308.32 1.13E+02 6.47E+02 7.59E+02 0.95 0.81 1.07 2.40 4.23E+00 1.22E+00 -7.1E+03 288.33 1.07E+02 6.54E+02 7.59E+02 0.078 0.61 1.08 2.50 4.02E+00 1.22E+00 -6.05E+03 244.17 1.14E+02 6.66E+02 7.79E+02 0.70 0.49 1.08 2.60 3.64E+00 1.22E+00 -6.05E+03 244.17 1.14E+02 6.9E+02 7.63E+02 0.58 0.34 1.11 2.80 3.65E+00 1.22E+00 -5.96E+03 242.33 1.29E+02 6.27E+02 7.48E+02 0.62 0.42 1.11 2.90 3.53E+00 1.22E+00 -5.61E-03 234.96 1.33E+02 6.21E-02 7.55E-02 0.58 0.40 1.11 3.10 <td>2.00</td> <td>4.02E+00</td> <td>1.22E+00</td> <td>-6.72E-03</td> <td>271.61</td> <td>1.24E-02</td> <td>6.48E-02</td> <td>7.73E-02</td> <td>0.68</td> <td>0.57</td> <td>1.09</td>	2.00	4.02E+00	1.22E+00	-6.72E-03	271.61	1.24E-02	6.48E-02	7.73E-02	0.68	0.57	1.09
2.30 4.52E+00 1.21E+00 -7.64E-03 308.32 1.13E-02 6.47E-02 7.59E-02 0.95 0.81 1.07 2.40 4.23E+00 1.22E+00 -7.11E-03 288.33 1.07E-02 6.54E-02 7.61E-02 0.78 0.61 1.08 2.50 4.02E+00 1.22E+00 -6.79E-03 272.58 1.13E-02 6.66E-02 7.79E-02 0.70 0.49 1.08 2.60 3.64E+00 1.22E+00 -6.05E-03 244.17 1.14E-02 6.49E-02 7.63E-02 0.58 0.34 1.11 2.80 3.63E+00 1.22E+00 -5.93E-03 242.33 1.29E-02 7.58E-02 0.62 0.42 1.11 2.90 3.53E+00 1.22E+00 -5.61E-03 234.96 1.33E-02 6.27E-02 7.55E-02 0.62 0.42 1.11 3.00 3.24E+00 1.23E+00 -5.25E-03 217.41 1.36E-02 6.20E-02 7.5Ee-02 0.58 0.40 1.11 3.10 3.30E+00 <td>2.10</td> <td>4.98E+00</td> <td>1.22E+00</td> <td>-8.42E-03</td> <td>340.88</td> <td>1.33E-02</td> <td>6.55E-02</td> <td>7.87E-02</td> <td>1.30</td> <td>1.17</td> <td>1.06</td>	2.10	4.98E+00	1.22E+00	-8.42E-03	340.88	1.33E-02	6.55E-02	7.87E-02	1.30	1.17	1.06
2.40 4.23E+00 1.22E+00 -7.11E-03 288.33 1.07E-02 6.54E-02 7.61E-02 0.78 0.61 1.08 2.50 4.02E+00 1.22E+00 -6.79E-03 272.58 1.13E-02 6.66E-02 7.79E-02 0.70 0.49 1.08 2.60 3.64E+00 1.22E+00 -6.05E-03 244.17 1.14E-02 6.69E-02 7.69E-02 0.57 0.30 1.09 2.70 3.58E+00 1.22E+00 -5.93E-03 241.22 1.21E-02 6.29E-02 7.49E-02 0.58 0.34 1.11 2.80 3.63E+00 1.22E+00 -6.02E-03 246.86 1.24E-02 6.24E-02 7.48E-02 0.62 0.42 1.11 3.00 3.43E+00 1.23E+00 -5.61E-03 234.96 1.33E-02 6.20E-02 7.57E-02 0.52 0.39 1.12 3.20 3.24E+00 1.23E+00 -5.25E-03 217.41 1.36E-02 6.20E-02 7.56E-02 0.50 0.38 1.13 3.40 <td>2.20</td> <td>5.09E+00</td> <td>1.21E+00</td> <td>-8.60E-03</td> <td>347.03</td> <td>1.23E-02</td> <td>6.43E-02</td> <td>7.66E-02</td> <td>1.34</td> <td>1.18</td> <td>1.06</td>	2.20	5.09E+00	1.21E+00	-8.60E-03	347.03	1.23E-02	6.43E-02	7.66E-02	1.34	1.18	1.06
2.50 4.02E+00 1.22E+00 -6.79E-03 272.58 1.13E-02 6.66E-02 7.79E-02 0.70 0.49 1.08 2.60 3.64E+00 1.22E+00 -6.05E-03 244.17 1.14E-02 6.69E-02 7.63E-02 0.57 0.30 1.09 2.70 3.58E+00 1.22E+00 -5.93E-03 241.22 1.21E-02 6.29E-02 7.49E-02 0.58 0.34 1.11 2.80 3.63E+00 1.22E+00 -6.02E-03 246.86 1.24E-02 6.24E-02 7.48E-02 0.62 0.37 1.11 2.90 3.53E+00 1.22E+00 -5.61E-03 234.96 1.33E-02 6.21E-02 7.54E-02 0.58 0.40 1.11 3.00 3.49E+00 1.23E+00 -5.36E-03 222.50 1.37E-02 6.20E-02 7.57E-02 0.52 0.39 1.13 3.30 3.26E+00 1.23E+00 -5.25E-03 217.41 1.36E-02 6.20E-02 7.56E-02 0.50 0.38 1.13 3.40 <td>2.30</td> <td>4.52E+00</td> <td>1.21E+00</td> <td>-7.64E-03</td> <td>308.32</td> <td>1.13E-02</td> <td>6.47E-02</td> <td>7.59E-02</td> <td>0.95</td> <td>0.81</td> <td>1.07</td>	2.30	4.52E+00	1.21E+00	-7.64E-03	308.32	1.13E-02	6.47E-02	7.59E-02	0.95	0.81	1.07
2.60 3.64E+00 1.22E+00 -6.05E-03 244.17 1.14E-02 6.49E-02 7.63E-02 0.57 0.30 1.09 2.70 3.58E+00 1.22E+00 -5.93E-03 241.22 1.21E-02 6.29E-02 7.49E-02 0.58 0.34 1.11 2.80 3.63E+00 1.22E+00 -6.02E-03 246.86 1.24E-02 6.24E-02 7.48E-02 0.62 0.37 1.11 3.00 3.43E+00 1.22E+00 -5.61E-03 234.96 1.33E-02 6.21E-02 7.54E-02 0.58 0.40 1.11 3.10 3.30E+00 1.23E+00 -5.52E-03 227.41 1.36E-02 6.0E-02 7.57E-02 0.52 0.39 1.12 3.20 3.24E+00 1.23E+00 -5.52E-03 221.81 1.33E-02 6.2E-02 7.56E-02 0.50 0.38 1.13 3.40 3.33E+00 1.23E+00 -5.54E-03 227.79 1.26E-02 6.46E-02 7.72E-02 0.52 0.38 1.12 3.50	2.40	4.23E+00	1.22E+00	-7.11E-03	288.33	1.07E-02	6.54E-02	7.61E-02	0.78	0.61	1.08
2.70 3.58E+00 1.22E+00 -5.93E-03 241.22 1.21E-02 6.29E-02 7.49E-02 0.58 0.34 1.11 2.80 3.63E+00 1.22E+00 -6.02E-03 246.86 1.24E-02 6.24E-02 7.48E-02 0.62 0.37 1.11 2.90 3.53E+00 1.22E+00 -5.86E-03 242.33 1.29E-02 6.27E-02 7.55E-02 0.62 0.42 1.11 3.00 3.43E+00 1.22E+00 -5.66E-03 224.33 1.39E-02 6.20E-02 7.57E-02 0.52 0.39 1.12 3.10 3.30E+00 1.23E+00 -5.25E-03 217.41 1.36E-02 6.0E-02 7.56E-02 0.50 0.38 1.13 3.40 3.33E+00 1.23E+00 -5.45E-03 225.15 1.29E-02 6.31E-02 7.61E-02 0.52 0.38 1.13 3.50 3.37E+00 1.23E+00 -5.54E-03 227.79 1.26E-02 6.46E-02 7.72E-02 0.52 0.36 1.12 3.60 <td>2.50</td> <td>4.02E+00</td> <td>1.22E+00</td> <td>-6.79E-03</td> <td>272.58</td> <td>1.13E-02</td> <td>6.66E-02</td> <td>7.79E-02</td> <td>0.70</td> <td>0.49</td> <td>1.08</td>	2.50	4.02E+00	1.22E+00	-6.79E-03	272.58	1.13E-02	6.66E-02	7.79E-02	0.70	0.49	1.08
2.80 3.63E+00 1.22E+00 -6.02E+03 246.86 1.24E+02 6.24E+02 7.48E+02 0.62 0.37 1.11 2.90 3.53E+00 1.22E+00 -5.80E+03 242.33 1.29E+02 6.27E+02 7.55E+02 0.62 0.42 1.11 3.00 3.43E+00 1.22E+00 -5.61E+03 234.96 1.33E+02 6.21E+02 7.54E+02 0.58 0.40 1.11 3.10 3.30E+00 1.23E+00 -5.36E+03 242.50 1.37E+02 6.21E+02 7.54E+02 0.52 0.39 1.12 3.20 3.24E+00 1.23E+00 -5.25E+03 217.41 1.36E+02 6.20E+02 7.56E+02 0.50 0.38 1.13 3.30 3.26E+00 1.23E+00 -5.29E+03 218.81 1.33E+02 6.21E+02 7.54E+02 0.50 0.39 1.13 3.40 3.33E+00 1.23E+00 -5.45E+03 225.15 1.29E+02 6.31E+02 7.54E+02 0.52 0.38 1.13 3.50 3.37E+00 1.23E+00 -5.54E+03 225.15 1.29E+02 6.31E+02 7.72E+02 0.52 0.38 1.13 3.50 3.41E+00 1.23E+00 -5.54E+03 225.15 1.29E+02 6.46E+02 7.74E+02 0.54 0.35 1.12 3.70 3.49E+00 1.24E+00 -5.61E+03 241.07 1.27E+02 6.44E+02 7.74E+02 0.54 0.35 1.12 3.80 3.62E+00 1.24E+00 -6.03E+03 240.70 1.27E+02 6.44E+02 7.76E+02 0.60 0.45 1.12 3.90 3.81E+00 1.24E+00 -6.03E+03 267.09 1.23E+02 6.48E+02 7.76E+02 0.67 0.57 1.12 4.00 3.96E+00 1.24E+00 -6.06-03 278.97 1.23E+02 6.48E+02 7.76E+02 0.76 1.12 1.12 4.00 4.10E+00 1.23E+00 -6.08E+03 278.97 1.23E+02 6.48E+02 7.71E+02 0.99 0.80 1.10 4.40 4.02E+00 1.23E+00 -6.46E+03 284.67 1.28E+02 4.27E+03 1.71E+02 0.27 0.10 2.26 4.60 4.30E+00 1.23E+00 -6.47E+03 316.46 1.29E+02 4.27E+03 1.71E+02 0.29 0.14 2.24 4.80 4.98E+00 1.23E+00 -6.48E+03 383.70 1.39E+02 5.73E+03 1.90E+02 0.29 0.10 2.06 5.40 5.56E+00 1.21E+00 -8.8E+03 383.70 1.39E+02 6.35E+03 2.02E+02 0.27 0.19 2.00 5.60 5.56E+00 1.21E+00 -8.0E+03 383.70 1.39E+02 6.35E+03 2.02E+02 0.27 0.14 1.98 5.80 5.76E+00 1.21E+00 -8.0	2.60	3.64E+00	1.22E+00	-6.05E-03	244.17	1.14E-02	6.49E-02	7.63E-02	0.57	0.30	1.09
2.90 3.53E+00 1.22E+00 -5.80E-03 242.33 1.29E+02 6.27E-02 7.55E-02 0.62 0.42 1.11 3.00 3.43E+00 1.22E+00 -5.61E-03 234.96 1.33E-02 6.21E-02 7.54E-02 0.58 0.40 1.11 3.10 3.30E+00 1.23E+00 -5.36E-03 222.50 1.37E-02 6.20E-02 7.57E-02 0.52 0.39 1.12 3.20 3.24E+00 1.23E+00 -5.25E-03 217.41 1.36E-02 6.20E-02 7.56E-02 0.50 0.38 1.13 3.40 3.33E+00 1.23E+00 -5.45E-03 225.15 1.29E-02 6.31E-02 7.51E-02 0.52 0.38 1.13 3.60 3.34E+00 1.23E+00 -5.54E-03 227.79 1.26E-02 6.48E-02 7.72E-02 0.52 0.38 1.12 3.70 3.49E+00 1.24E+00 -5.76E-03 240.70 1.27E-02 6.48E-02 7.71E-02 0.60 0.45 1.12 3.80 <td>2.70</td> <td>3.58E+00</td> <td>1.22E+00</td> <td>-5.93E-03</td> <td>241.22</td> <td>1.21E-02</td> <td>6.29E-02</td> <td>7.49E-02</td> <td>0.58</td> <td>0.34</td> <td>1.11</td>	2.70	3.58E+00	1.22E+00	-5.93E-03	241.22	1.21E-02	6.29E-02	7.49E-02	0.58	0.34	1.11
3.00 3.43E+00 1.22E+00 -5.61E-03 234.96 1.33E-02 6.21E-02 7.54E-02 0.58 0.40 1.11 3.10 3.30E+00 1.23E+00 -5.36E-03 222.50 1.37E-02 6.20E-02 7.57E-02 0.52 0.39 1.12 3.20 3.24E+00 1.23E+00 -5.25E-03 217.41 1.36E-02 6.20E-02 7.56E-02 0.50 0.38 1.13 3.30 3.26E+00 1.23E+00 -5.45E-03 225.15 1.29E-02 6.31E-02 7.54E-02 0.50 0.39 1.13 3.40 3.33E+00 1.23E+00 -5.45E-03 227.79 1.26E-02 6.31E-02 7.61E-02 0.52 0.38 1.13 3.50 3.37E+00 1.23E+03 -5.61E-03 231.62 1.26E-02 6.48E-02 7.72E-02 0.52 0.36 1.12 3.60 3.41E+00 1.24E+00 -5.61E-03 231.62 1.26E-02 6.48E-02 7.74E-02 0.60 0.45 1.12 3.80 <td>2.80</td> <td>3.63E+00</td> <td>1.22E+00</td> <td>-6.02E-03</td> <td>246.86</td> <td>1.24E-02</td> <td>6.24E-02</td> <td>7.48E-02</td> <td>0.62</td> <td>0.37</td> <td>1.11</td>	2.80	3.63E+00	1.22E+00	-6.02E-03	246.86	1.24E-02	6.24E-02	7.48E-02	0.62	0.37	1.11
3.10 3.30E+00 1.23E+00 -5.36E-03 222.50 1.37E-02 6.20E-02 7.57E-02 0.52 0.39 1.12 3.20 3.24E+00 1.23E+00 -5.25E-03 217.41 1.36E-02 6.20E-02 7.56E-02 0.50 0.38 1.13 3.30 3.26E+00 1.23E+00 -5.29E-03 218.81 1.33E-02 6.21E-02 7.54E-02 0.50 0.39 1.13 3.40 3.33E+00 1.23E+00 -5.45E-03 225.15 1.29E-02 6.31E-02 7.61E-02 0.52 0.38 1.13 3.50 3.37E+00 1.23E+00 -5.54E-03 227.79 1.26E-02 6.46E-02 7.72E-02 0.52 0.36 1.12 3.60 3.41E+00 1.23E+00 -5.61E-03 231.62 1.26E-02 6.48E-02 7.74E-02 0.54 0.35 1.12 3.70 3.49E+00 1.24E+00 -6.03E-03 251.91 1.25E-02 6.37E-02 7.62E-02 0.67 0.54 1.12 3.80 <td>2.90</td> <td>3.53E+00</td> <td>1.22E+00</td> <td>-5.80E-03</td> <td>242.33</td> <td>1.29E-02</td> <td>6.27E-02</td> <td>7.55E-02</td> <td>0.62</td> <td>0.42</td> <td>1.11</td>	2.90	3.53E+00	1.22E+00	-5.80E-03	242.33	1.29E-02	6.27E-02	7.55E-02	0.62	0.42	1.11
3.20 3.24E+00 1.23E+00 -5.25E-03 217.41 1.36E-02 6.20E-02 7.56E-02 0.50 0.38 1.13 3.30 3.26E+00 1.23E+00 -5.29E-03 218.81 1.33E-02 6.21E-02 7.54E-02 0.50 0.39 1.13 3.40 3.33E+00 1.23E+00 -5.45E-03 225.15 1.29E-02 6.31E-02 7.61E-02 0.52 0.38 1.13 3.50 3.37E+00 1.23E+00 -5.54E-03 227.79 1.26E-02 6.46E-02 7.72E-02 0.52 0.36 1.12 3.60 3.41E+00 1.23E+00 -5.61E-03 231.62 1.26E-02 6.48E-02 7.74E-02 0.54 0.35 1.12 3.70 3.49E+00 1.24E+00 -5.76E-03 240.70 1.27E-02 6.44E-02 7.71E-02 0.60 0.45 1.12 3.80 3.62E+00 1.24E+00 -6.08E-03 257.91 1.23E-02 6.47E-02 7.64E-02 0.67 0.54 1.12 4.00 <td>3.00</td> <td>3.43E+00</td> <td>1.22E+00</td> <td>-5.61E-03</td> <td>234.96</td> <td>1.33E-02</td> <td>6.21E-02</td> <td>7.54E-02</td> <td>0.58</td> <td>0.40</td> <td>1.11</td>	3.00	3.43E+00	1.22E+00	-5.61E-03	234.96	1.33E-02	6.21E-02	7.54E-02	0.58	0.40	1.11
3.30 3.26E+00 1.23E+00 -5.29E-03 218.81 1.33E-02 6.21E-02 7.54E-02 0.50 0.39 1.13 3.40 3.33E+00 1.23E+00 -5.45E-03 225.15 1.29E-02 6.31E-02 7.61E-02 0.52 0.38 1.13 3.50 3.37E+00 1.23E+00 -5.54E-03 227.79 1.26E-02 6.46E-02 7.72E-02 0.52 0.36 1.12 3.60 3.41E+00 1.23E+00 -5.61E-03 231.62 1.26E-02 6.48E-02 7.74E-02 0.54 0.35 1.12 3.70 3.49E+00 1.24E+00 -5.76E-03 240.70 1.27E-02 6.44E-02 7.71E-02 0.60 0.45 1.12 3.80 3.62E+00 1.24E+00 -6.03E-03 251.91 1.25E-02 6.37E-02 7.62E-02 0.67 0.54 1.12 4.00 3.96E+00 1.24E+00 -6.70E-03 278.97 1.23E-02 6.49E-02 7.68E-02 0.84 0.67 1.12 4.20 <td>3.10</td> <td>3.30E+00</td> <td>1.23E+00</td> <td>-5.36E-03</td> <td>222.50</td> <td>1.37E-02</td> <td>6.20E-02</td> <td>7.57E-02</td> <td>0.52</td> <td>0.39</td> <td>1.12</td>	3.10	3.30E+00	1.23E+00	-5.36E-03	222.50	1.37E-02	6.20E-02	7.57E-02	0.52	0.39	1.12
3.40 3.33E+00 1.23E+00 -5.45E-03 225.15 1.29E-02 6.31E-02 7.61E-02 0.52 0.38 1.13 3.50 3.37E+00 1.23E+00 -5.54E-03 227.79 1.26E-02 6.46E-02 7.72E-02 0.52 0.36 1.12 3.60 3.41E+00 1.23E+00 -5.61E-03 231.62 1.26E-02 6.48E-02 7.74E-02 0.54 0.35 1.12 3.70 3.49E+00 1.24E+00 -5.76E-03 240.70 1.27E-02 6.44E-02 7.71E-02 0.60 0.45 1.12 3.80 3.62E+00 1.24E+00 -6.03E-03 251.91 1.25E-02 6.37E-02 7.62E-02 0.67 0.54 1.12 3.90 3.81E+00 1.24E+00 -6.40E-03 267.09 1.23E-02 6.45E-02 7.64E-02 0.76 1.12 1.12 4.00 3.96E+00 1.24E+00 -6.70E-03 278.97 1.23E-02 6.45E-02 7.68E-02 0.84 0.67 1.12 4.20 <td>3.20</td> <td>3.24E+00</td> <td>1.23E+00</td> <td>-5.25E-03</td> <td>217.41</td> <td>1.36E-02</td> <td>6.20E-02</td> <td>7.56E-02</td> <td>0.50</td> <td>0.38</td> <td>1.13</td>	3.20	3.24E+00	1.23E+00	-5.25E-03	217.41	1.36E-02	6.20E-02	7.56E-02	0.50	0.38	1.13
3.50 3.37E+00 1.23E+00 -5.54E-03 227.79 1.26E-02 6.46E-02 7.72E-02 0.52 0.36 1.12 3.60 3.41E+00 1.23E+00 -5.61E-03 231.62 1.26E-02 6.48E-02 7.74E-02 0.54 0.35 1.12 3.70 3.49E+00 1.24E+00 -5.76E-03 240.70 1.27E-02 6.44E-02 7.71E-02 0.60 0.45 1.12 3.80 3.62E+00 1.24E+00 -6.03E-03 251.91 1.25E-02 6.37E-02 7.62E-02 0.67 0.54 1.12 3.90 3.81E+00 1.24E+00 -6.40E-03 267.09 1.23E-02 6.41E-02 7.64E-02 0.76 1.12 1.12 4.00 3.96E+00 1.24E+00 -6.70E-03 278.97 1.23E-02 6.45E-02 7.68E-02 0.84 0.67 1.12 4.20 4.10E+00 1.25E+00 -6.89E-03 295.32 1.28E-02 6.43E-02 7.71E-02 0.99 0.80 1.10 4.40 <td>3.30</td> <td>3.26E+00</td> <td>1.23E+00</td> <td>-5.29E-03</td> <td>218.81</td> <td>1.33E-02</td> <td>6.21E-02</td> <td>7.54E-02</td> <td>0.50</td> <td>0.39</td> <td>1.13</td>	3.30	3.26E+00	1.23E+00	-5.29E-03	218.81	1.33E-02	6.21E-02	7.54E-02	0.50	0.39	1.13
3.60 3.41E+00 1.23E+00 -5.61E-03 231.62 1.26E-02 6.48E-02 7.74E-02 0.54 0.35 1.12 3.70 3.49E+00 1.24E+00 -5.76E-03 240.70 1.27E-02 6.44E-02 7.71E-02 0.60 0.45 1.12 3.80 3.62E+00 1.24E+00 -6.03E-03 251.91 1.25E-02 6.37E-02 7.62E-02 0.67 0.54 1.12 3.90 3.81E+00 1.24E+00 -6.40E-03 267.09 1.23E-02 6.41E-02 7.64E-02 0.76 1.12 1.12 4.00 3.96E+00 1.24E+00 -6.70E-03 278.97 1.23E-02 6.45E-02 7.68E-02 0.84 0.67 1.12 4.20 4.10E+00 1.25E+00 -6.89E-03 295.32 1.28E-02 4.27E-03 1.71E-02 0.99 0.80 1.10 4.40 4.02E+00 1.23E+00 -6.14E-03 284.67 1.28E-02 4.27E-03 1.71E-02 0.27 0.10 2.26 4.50 <td>3.40</td> <td>3.33E+00</td> <td>1.23E+00</td> <td>-5.45E-03</td> <td>225.15</td> <td>1.29E-02</td> <td>6.31E-02</td> <td>7.61E-02</td> <td>0.52</td> <td>0.38</td> <td>1.13</td>	3.40	3.33E+00	1.23E+00	-5.45E-03	225.15	1.29E-02	6.31E-02	7.61E-02	0.52	0.38	1.13
3.70 3.49E+00 1.24E+00 -5.76E-03 240.70 1.27E-02 6.44E-02 7.71E-02 0.60 0.45 1.12 3.80 3.62E+00 1.24E+00 -6.03E-03 251.91 1.25E-02 6.37E-02 7.62E-02 0.67 0.54 1.12 3.90 3.81E+00 1.24E+00 -6.40E-03 267.09 1.23E-02 6.41E-02 7.64E-02 0.76 1.12 1.12 4.00 3.96E+00 1.24E+00 -6.70E-03 278.97 1.23E-02 6.45E-02 7.68E-02 0.84 0.67 1.12 4.20 4.10E+00 1.25E+00 -6.89E-03 295.32 1.28E-02 6.43E-02 7.71E-02 0.99 0.80 1.10 4.40 4.02E+00 1.23E+00 -6.14E-03 284.67 1.28E-02 4.27E-03 1.71E-02 0.27 0.10 2.26 4.60 4.30E+00 1.23E+00 -6.47E-03 310.10 1.26E-02 4.17E-03 1.67E-02 0.29 0.14 2.24 4.80 <td>3.50</td> <td>3.37E+00</td> <td>1.23E+00</td> <td>-5.54E-03</td> <td>227.79</td> <td>1.26E-02</td> <td>6.46E-02</td> <td>7.72E-02</td> <td>0.52</td> <td>0.36</td> <td>1.12</td>	3.50	3.37E+00	1.23E+00	-5.54E-03	227.79	1.26E-02	6.46E-02	7.72E-02	0.52	0.36	1.12
3.80 3.62E+00 1.24E+00 -6.03E-03 251.91 1.25E-02 6.37E-02 7.62E-02 0.67 0.54 1.12 3.90 3.81E+00 1.24E+00 -6.40E-03 267.09 1.23E-02 6.41E-02 7.64E-02 0.76 1.12 1.12 4.00 3.96E+00 1.24E+00 -6.70E-03 278.97 1.23E-02 6.45E-02 7.68E-02 0.84 0.67 1.12 4.20 4.10E+00 1.25E+00 -6.89E-03 295.32 1.28E-02 6.43E-02 7.71E-02 0.99 0.80 1.10 4.40 4.02E+00 1.23E+00 -6.14E-03 284.67 1.28E-02 4.27E-03 1.71E-02 0.27 0.10 2.26 4.60 4.30E+00 1.23E+00 -6.47E-03 310.10 1.26E-02 4.17E-03 1.67E-02 0.29 0.14 2.24 4.80 4.98E+00 1.23E+00 -7.45E-03 354.64 1.29E-02 4.59E-03 1.75E-02 0.33 0.03 2.16 5.00 <td>3.60</td> <td>3.41E+00</td> <td>1.23E+00</td> <td>-5.61E-03</td> <td>231.62</td> <td>1.26E-02</td> <td>6.48E-02</td> <td>7.74E-02</td> <td>0.54</td> <td>0.35</td> <td>1.12</td>	3.60	3.41E+00	1.23E+00	-5.61E-03	231.62	1.26E-02	6.48E-02	7.74E-02	0.54	0.35	1.12
3.90 3.81E+00 1.24E+00 -6.40E-03 267.09 1.23E-02 6.41E-02 7.64E-02 0.76 1.12 1.12 4.00 3.96E+00 1.24E+00 -6.70E-03 278.97 1.23E-02 6.45E-02 7.68E-02 0.84 0.67 1.12 4.20 4.10E+00 1.25E+00 -6.89E-03 295.32 1.28E-02 6.43E-02 7.71E-02 0.99 0.80 1.10 4.40 4.02E+00 1.23E+00 -6.14E-03 284.67 1.28E-02 4.27E-03 1.71E-02 0.27 0.10 2.26 4.60 4.30E+00 1.23E+00 -6.47E-03 310.10 1.26E-02 4.17E-03 1.67E-02 0.29 0.14 2.24 4.80 4.98E+00 1.23E+00 -7.45E-03 354.64 1.29E-02 4.59E-03 1.75E-02 0.33 0.03 2.16 5.00 6.49E+00 1.22E+00 -9.42E-03 431.86 1.30E-02 5.13E-03 1.81E-02 0.29 0.12 2.11 5.20 <td>3.70</td> <td>3.49E+00</td> <td>1.24E+00</td> <td>-5.76E-03</td> <td>240.70</td> <td>1.27E-02</td> <td>6.44E-02</td> <td>7.71E-02</td> <td>0.60</td> <td>0.45</td> <td>1.12</td>	3.70	3.49E+00	1.24E+00	-5.76E-03	240.70	1.27E-02	6.44E-02	7.71E-02	0.60	0.45	1.12
4.00 3.96E+00 1.24E+00 -6.70E-03 278.97 1.23E-02 6.45E-02 7.68E-02 0.84 0.67 1.12 4.20 4.10E+00 1.25E+00 -6.89E-03 295.32 1.28E-02 6.43E-02 7.71E-02 0.99 0.80 1.10 4.40 4.02E+00 1.23E+00 -6.14E-03 284.67 1.28E-02 4.27E-03 1.71E-02 0.27 0.10 2.26 4.60 4.30E+00 1.23E+00 -6.47E-03 310.10 1.26E-02 4.17E-03 1.67E-02 0.29 0.14 2.24 4.80 4.98E+00 1.23E+00 -7.45E-03 354.64 1.29E-02 4.59E-03 1.75E-02 0.33 0.03 2.16 5.00 6.49E+00 1.22E+00 -9.42E-03 431.86 1.30E-02 5.13E-03 1.81E-02 0.29 0.12 2.11 5.20 6.84E+00 1.22E+00 -9.88E-03 445.73 1.32E-02 5.73E-03 1.90E-02 0.29 0.10 2.06 5.40 7.69E+00 1.21E+00 -8.34E-03 383.70 1.39E-02 6.35E-03	3.80	3.62E+00	1.24E+00	-6.03E-03	251.91	1.25E-02	6.37E-02	7.62E-02	0.67	0.54	1.12
4.20 4.10E+00 1.25E+00 -6.89E-03 295.32 1.28E-02 6.43E-02 7.71E-02 0.99 0.80 1.10 4.40 4.02E+00 1.23E+00 -6.14E-03 284.67 1.28E-02 4.27E-03 1.71E-02 0.27 0.10 2.26 4.60 4.30E+00 1.23E+00 -6.47E-03 310.10 1.26E-02 4.17E-03 1.67E-02 0.29 0.14 2.24 4.80 4.98E+00 1.23E+00 -7.45E-03 354.64 1.29E-02 4.59E-03 1.75E-02 0.33 0.03 2.16 5.00 6.49E+00 1.22E+00 -9.42E-03 431.86 1.30E-02 5.13E-03 1.81E-02 0.29 0.12 2.11 5.20 6.84E+00 1.22E+00 -9.88E-03 445.73 1.32E-02 5.73E-03 1.90E-02 0.29 0.10 2.06 5.40 7.69E+00 1.22E+00 -1.08E-02 484.78 1.36E-02 6.15E-03 1.97E-02 0.27 0.09 2.00 5.80 5.76E+00 1.21E+00 -8.62E-03 393.17 1.40E-02 6.56E-03	3.90	3.81E+00	1.24E+00	-6.40E-03	267.09	1.23E-02	6.41E-02	7.64E-02	0.76	1.12	1.12
4.40 4.02E+00 1.23E+00 -6.14E-03 284.67 1.28E-02 4.27E-03 1.71E-02 0.27 0.10 2.26 4.60 4.30E+00 1.23E+00 -6.47E-03 310.10 1.26E-02 4.17E-03 1.67E-02 0.29 0.14 2.24 4.80 4.98E+00 1.23E+00 -7.45E-03 354.64 1.29E-02 4.59E-03 1.75E-02 0.33 0.03 2.16 5.00 6.49E+00 1.22E+00 -9.42E-03 431.86 1.30E-02 5.13E-03 1.81E-02 0.29 0.12 2.11 5.20 6.84E+00 1.22E+00 -9.88E-03 445.73 1.32E-02 5.73E-03 1.90E-02 0.29 0.10 2.06 5.40 7.69E+00 1.22E+00 -1.08E-02 484.78 1.36E-02 6.15E-03 1.97E-02 0.27 0.09 2.00 5.60 5.56E+00 1.21E+00 -8.34E-03 383.70 1.39E-02 6.35E-03 2.02E-02 0.27 0.14 1.98 5.80 5.76E+00 1.21E+00 -8.62E-03 393.17 1.40E-02 6.56E-03	4.00	3.96E+00	1.24E+00	-6.70E-03	278.97	1.23E-02	6.45E-02	7.68E-02	0.84	0.67	1.12
4.60 4.30E+00 1.23E+00 -6.47E-03 310.10 1.26E-02 4.17E-03 1.67E-02 0.29 0.14 2.24 4.80 4.98E+00 1.23E+00 -7.45E-03 354.64 1.29E-02 4.59E-03 1.75E-02 0.33 0.03 2.16 5.00 6.49E+00 1.22E+00 -9.42E-03 431.86 1.30E-02 5.13E-03 1.81E-02 0.29 0.12 2.11 5.20 6.84E+00 1.22E+00 -9.88E-03 445.73 1.32E-02 5.73E-03 1.90E-02 0.29 0.10 2.06 5.40 7.69E+00 1.22E+00 -1.08E-02 484.78 1.36E-02 6.15E-03 1.97E-02 0.27 0.09 2.00 5.60 5.56E+00 1.21E+00 -8.34E-03 383.70 1.39E-02 6.35E-03 2.02E-02 0.27 0.14 1.98 5.80 5.76E+00 1.21E+00 -8.62E-03 393.17 1.40E-02 6.56E-03 2.05E-02 0.26 0.11 1.97 6.40 5.00E+00 1.20E+00 -7.70E-03 349.64 1.47E-02 7.65E-03	4.20	4.10E+00	1.25E+00	-6.89E-03	295.32	1.28E-02	6.43E-02	7.71E-02	0.99	0.80	1.10
4.80 4.98E+00 1.23E+00 -7.45E-03 354.64 1.29E-02 4.59E-03 1.75E-02 0.33 0.03 2.16 5.00 6.49E+00 1.22E+00 -9.42E-03 431.86 1.30E-02 5.13E-03 1.81E-02 0.29 0.12 2.11 5.20 6.84E+00 1.22E+00 -9.88E-03 445.73 1.32E-02 5.73E-03 1.90E-02 0.29 0.10 2.06 5.40 7.69E+00 1.22E+00 -1.08E-02 484.78 1.36E-02 6.15E-03 1.97E-02 0.27 0.09 2.00 5.60 5.56E+00 1.21E+00 -8.34E-03 383.70 1.39E-02 6.35E-03 2.02E-02 0.27 0.14 1.98 5.80 5.76E+00 1.21E+00 -8.62E-03 393.17 1.40E-02 6.56E-03 2.05E-02 0.26 0.11 1.97 6.00 6.32E+00 1.21E+00 -9.31E-03 421.74 1.41E-02 6.91E-03 2.11E-02 0.25 0.15 1.95 6.40 5.00E+00 1.20E+00 -7.70E-03 349.64 1.47E-02 7.65E-03	4.40	4.02E+00	1.23E+00	-6.14E-03	284.67	1.28E-02	4.27E-03	1.71E-02	0.27	0.10	2.26
5.00 6.49E+00 1.22E+00 -9.42E-03 431.86 1.30E-02 5.13E-03 1.81E-02 0.29 0.12 2.11 5.20 6.84E+00 1.22E+00 -9.88E-03 445.73 1.32E-02 5.73E-03 1.90E-02 0.29 0.10 2.06 5.40 7.69E+00 1.22E+00 -1.08E-02 484.78 1.36E-02 6.15E-03 1.97E-02 0.27 0.09 2.00 5.60 5.56E+00 1.21E+00 -8.34E-03 383.70 1.39E-02 6.35E-03 2.02E-02 0.27 0.14 1.98 5.80 5.76E+00 1.21E+00 -8.62E-03 393.17 1.40E-02 6.56E-03 2.05E-02 0.26 0.11 1.97 6.00 6.32E+00 1.21E+00 -9.31E-03 421.74 1.41E-02 6.91E-03 2.11E-02 0.25 0.15 1.95 6.40 5.00E+00 1.20E+00 -7.70E-03 349.64 1.47E-02 7.65E-03 2.24E-02 0.23 0.09 1.88 6.80 4.52E+00 1.19E+00 -7.12E-03 316.29 1.56E-02 8.74E-03 2.44E-02 0.20 0.05 1.79	4.60	4.30E+00	1.23E+00	-6.47E-03	310.10	1.26E-02	4.17E-03	1.67E-02	0.29	0.14	2.24
5.20 6.84E+00 1.22E+00 -9.88E-03 445.73 1.32E-02 5.73E-03 1.90E-02 0.29 0.10 2.06 5.40 7.69E+00 1.22E+00 -1.08E-02 484.78 1.36E-02 6.15E-03 1.97E-02 0.27 0.09 2.00 5.60 5.56E+00 1.21E+00 -8.34E-03 383.70 1.39E-02 6.35E-03 2.02E-02 0.27 0.14 1.98 5.80 5.76E+00 1.21E+00 -8.62E-03 393.17 1.40E-02 6.56E-03 2.05E-02 0.26 0.11 1.97 6.00 6.32E+00 1.21E+00 -9.31E-03 421.74 1.41E-02 6.91E-03 2.11E-02 0.25 0.15 1.95 6.40 5.00E+00 1.20E+00 -7.70E-03 349.64 1.47E-02 7.65E-03 2.24E-02 0.23 0.09 1.88 6.80 4.52E+00 1.19E+00 -7.12E-03 316.29 1.56E-02 8.74E-03 2.44E-02 0.20 0.05 1.79	4.80	4.98E+00	1.23E+00	-7.45E-03	354.64	1.29E-02	4.59E-03	1.75E-02	0.33	0.03	2.16
5.40 7.69E+00 1.22E+00 -1.08E-02 484.78 1.36E-02 6.15E-03 1.97E-02 0.27 0.09 2.00 5.60 5.56E+00 1.21E+00 -8.34E-03 383.70 1.39E-02 6.35E-03 2.02E-02 0.27 0.14 1.98 5.80 5.76E+00 1.21E+00 -8.62E-03 393.17 1.40E-02 6.56E-03 2.05E-02 0.26 0.11 1.97 6.00 6.32E+00 1.21E+00 -9.31E-03 421.74 1.41E-02 6.91E-03 2.11E-02 0.25 0.15 1.95 6.40 5.00E+00 1.20E+00 -7.70E-03 349.64 1.47E-02 7.65E-03 2.24E-02 0.23 0.09 1.88 6.80 4.52E+00 1.19E+00 -7.12E-03 316.29 1.56E-02 8.74E-03 2.44E-02 0.20 0.05 1.79	5.00	6.49E+00	1.22E+00	-9.42E-03	431.86	1.30E-02	5.13E-03	1.81E-02	0.29	0.12	2.11
5.60 5.56E+00 1.21E+00 -8.34E-03 383.70 1.39E-02 6.35E-03 2.02E-02 0.27 0.14 1.98 5.80 5.76E+00 1.21E+00 -8.62E-03 393.17 1.40E-02 6.56E-03 2.05E-02 0.26 0.11 1.97 6.00 6.32E+00 1.21E+00 -9.31E-03 421.74 1.41E-02 6.91E-03 2.11E-02 0.25 0.15 1.95 6.40 5.00E+00 1.20E+00 -7.70E-03 349.64 1.47E-02 7.65E-03 2.24E-02 0.23 0.09 1.88 6.80 4.52E+00 1.19E+00 -7.12E-03 316.29 1.56E-02 8.74E-03 2.44E-02 0.20 0.05 1.79	5.20	6.84E+00	1.22E+00	-9.88E-03	445.73	1.32E-02	5.73E-03	1.90E-02	0.29	0.10	2.06
5.80 5.76E+00 1.21E+00 -8.62E-03 393.17 1.40E-02 6.56E-03 2.05E-02 0.26 0.11 1.97 6.00 6.32E+00 1.21E+00 -9.31E-03 421.74 1.41E-02 6.91E-03 2.11E-02 0.25 0.15 1.95 6.40 5.00E+00 1.20E+00 -7.70E-03 349.64 1.47E-02 7.65E-03 2.24E-02 0.23 0.09 1.88 6.80 4.52E+00 1.19E+00 -7.12E-03 316.29 1.56E-02 8.74E-03 2.44E-02 0.20 0.05 1.79	5.40	7.69E+00	1.22E+00	-1.08E-02	484.78	1.36E-02	6.15E-03	1.97E-02	0.27	0.09	2.00
6.00 6.32E+00 1.21E+00 -9.31E-03 421.74 1.41E-02 6.91E-03 2.11E-02 0.25 0.15 1.95 6.40 5.00E+00 1.20E+00 -7.70E-03 349.64 1.47E-02 7.65E-03 2.24E-02 0.23 0.09 1.88 6.80 4.52E+00 1.19E+00 -7.12E-03 316.29 1.56E-02 8.74E-03 2.44E-02 0.20 0.05 1.79	5.60	5.56E+00	1.21E+00	-8.34E-03	383.70	1.39E-02	6.35E-03	2.02E-02	0.27	0.14	1.98
6.40 5.00E+00 1.20E+00 -7.70E-03 349.64 1.47E-02 7.65E-03 2.24E-02 0.23 0.09 1.88 6.80 4.52E+00 1.19E+00 -7.12E-03 316.29 1.56E-02 8.74E-03 2.44E-02 0.20 0.05 1.79	5.80	5.76E+00	1.21E+00	-8.62E-03	393.17	1.40E-02	6.56E-03	2.05E-02	0.26	0.11	1.97
6.80 4.52E+00 1.19E+00 -7.12E-03 316.29 1.56E-02 8.74E-03 2.44E-02 0.20 0.05 1.79	6.00	6.32E+00	1.21E+00	-9.31E-03	421.74	1.41E-02	6.91E-03	2.11E-02	0.25	0.15	1.95
6.80 4.52E+00 1.19E+00 -7.12E-03 316.29 1.56E-02 8.74E-03 2.44E-02 0.20 0.05 1.79	6.40	5.00E+00	1.20E+00	-7.70E-03	349.64	1.47E-02	7.65E-03	2.24E-02	0.23	0.09	1.88
	6.80	4.52E+00	1.19E+00	-7.12E-03	316.29	1.56E-02	8.74E-03	2.44E-02		0.05	
1.20 4 .21-100 1.10-400 40.00-03 253.00 1.12-02 1.07-02 2.75-02	7.20	4.27E+00	1.18E+00	-6.88E-03	295.08	1.72E-02	1.07E-02	2.79E-02	0.19	0.14	1.69

7.60	4.86E+00	1.18E+00	-7.85E-03	328.29	1.81E-02	1.26E-02	3.07E-02	0.18	0.11	1.63
8.00	6.97E+00	1.18E+00	-1.05E-02	436.90	1.84E-02	1.38E-02	3.22E-02	0.15	80.0	1.58
							mean	0.48	0.35	1.35
							median	0.43	0.30	1.12

Table A-6 Set 2, Ground type C

Regression coefficients for the whole database set

T [s]	a	b	С	h	σ_{r}^{2}	${\sigma_e}^2$	σ^2	MEANNR	MEDNR	STDNR
0.00	0.00E+00	0.00E+00	0.00E+00	0.00	0.00E+00	0.00E+00	0.00E+00	0.00	0.00	0.00
0.10	6.00E-01	5.54E-01	-6.25E-04	129.47	6.79E-03	2.27E-02	2.95E-02	0.30	0.22	1.91
0.20	1.07E+00	5.62E-01	-2.23E-04	88.30	1.06E-02	7.57E-03	1.82E-02	0.02	0.07	2.07
0.30	1.49E+00	5.93E-01	-7.12E-04	107.03	9.79E-03	6.52E-03	1.63E-02	0.13	0.45	2.17
0.40	1.54E+00	6.52E-01	-4.13E-04	89.97	1.05E-02	1.83E-02	2.88E-02	0.11	0.00	1.86
0.50	1.68E+00	6.63E-01	-5.18E-04	88.80	1.12E-02	9.01E-03	2.02E-02	0.13	0.30	2.37
0.60	1.78E+00	6.93E-01	-5.89E-04	80.92	1.19E-02	5.07E-03	1.70E-02	0.40	0.30	2.57
0.70	1.79E+00	7.07E-01	-4.11E-04	83.48	1.25E-02	5.56E-03	1.80E-02	0.31	0.43	2.47
0.80	1.80E+00	7.27E-01	-3.70E-04	78.42	1.20E-02	5.22E-03	1.73E-02	0.22	0.16	2.46
0.90	1.78E+00	7.16E-01	-1.79E-04	67.86	1.40E-02	1.01E-02	2.41E-02	0.20	0.14	2.07
1.00	1.68E+00	7.37E-01	3.97E-04	49.10	1.62E-02	1.11E-02	2.73E-02	0.16	0.20	1.92
1.10	1.72E+00	7.61E-01	2.92E-04	52.17	1.51E-02	8.40E-03	2.34E-02	0.17	0.11	1.99
1.20	1.74E+00	7.76E-01	2.23E-04	50.73	1.40E-02	1.38E-02	2.78E-02	0.19	0.04	1.82
1.30	1.77E+00	7.94E-01	3.64E-05	54.10	1.24E-02	1.76E-02	3.01E-02	0.18	0.03	1.74
1.40	1.78E+00	8.17E-01	-3.44E-05	53.45	1.33E-02	1.53E-02	2.86E-02	0.17	0.09	1.75
1.50	1.76E+00	8.45E-01	-5.91E-06	51.19	1.16E-02	1.26E-02	2.42E-02	0.11	0.13	1.86
1.60	1.78E+00	8.50E-01	-1.12E-04	51.36	1.11E-02	1.11E-02	2.22E-02	0.05	0.19	1.90
1.70	1.76E+00	8.50E-01	-6.77E-05	49.08	1.19E-02	1.28E-02	2.47E-02	0.01	0.17	1.77
1.80	1.77E+00	8.45E-01	-9.95E-05	50.80	1.22E-02	1.28E-02	2.51E-02	0.01	0.12	1.75
1.90	1.76E+00	8.39E-01	-1.15E-05	51.63	1.25E-02	1.78E-02	3.03E-02	0.04	0.19	1.62
2.00	1.77E+00	8.35E-01	-5.95E-05	52.03	1.35E-02	1.95E-02	3.30E-02	0.02	0.29	1.55
2.10	1.79E+00	8.30E-01	-9.92E-05	56.85	1.35E-02	1.93E-02	3.28E-02	0.02	0.24	1.57
2.20	1.79E+00	8.25E-01	-1.08E-04	54.39	1.26E-02	2.13E-02	3.39E-02	0.07	0.30	1.54
2.30	1.81E+00	8.23E-01	-2.27E-04	54.84	1.19E-02	2.18E-02	3.37E-02	0.10	0.20	1.53
2.40	1.83E+00	8.23E-01	-3.33E-04	59.46	1.10E-02	2.24E-02	3.35E-02	0.10	0.21	1.53
2.50	1.84E+00	8.21E-01	-3.87E-04	62.62	1.03E-02	2.33E-02	3.37E-02	0.11	0.29	1.52
2.60	1.84E+00	8.24E-01	-4.04E-04	63.20	9.80E-03	2.62E-02	3.60E-02	0.13	0.30	1.46
2.70	1.83E+00	8.30E-01	-4.20E-04	62.61	1.00E-02	2.89E-02	3.89E-02	0.14	0.28	1.41
2.80	1.83E+00	8.31E-01	-4.24E-04	62.26	9.71E-03	3.12E-02	4.09E-02	0.17	0.32	1.38
2.90	1.83E+00	8.39E-01	-4.69E-04	63.38	9.72E-03	2.88E-02	3.85E-02	0.18	0.33	1.42
3.00	1.85E+00	8.52E-01	-5.16E-04	68.42	9.52E-03	2.82E-02	3.77E-02	0.16	0.27	1.42

_										
3.10	1.86E+00	8.62E-01	-5.39E-04	70.77	9.59E-03	2.76E-02	3.72E-02	0.15	0.20	1.43
3.20	1.86E+00	8.66E-01	-5.37E-04	72.09	9.82E-03	2.71E-02	3.69E-02	0.15	0.24	1.46
3.30	1.86E+00	8.66E-01	-5.55E-04	72.95	9.94E-03	2.71E-02	3.70E-02	0.15	0.24	1.49
3.40	1.87E+00	8.68E-01	-5.89E-04	74.14	1.03E-02	2.73E-02	3.76E-02	0.15	0.23	1.50
3.50	1.89E+00	8.72E-01	-6.62E-04	76.40	1.06E-02	2.60E-02	3.66E-02	0.15	0.25	1.53
3.60	1.90E+00	8.72E-01	-7.29E-04	78.94	1.07E-02	2.59E-02	3.66E-02	0.15	0.21	1.53
3.70	1.92E+00	8.70E-01	-7.93E-04	82.01	1.08E-02	2.66E-02	3.75E-02	0.16	0.21	1.53
3.80	1.93E+00	8.67E-01	-8.19E-04	84.46	1.09E-02	2.80E-02	3.89E-02	0.17	0.23	1.51
3.90	1.91E+00	8.66E-01	-7.44E-04	84.54	1.11E-02	3.00E-02	4.11E-02	0.17	0.29	1.48
4.00	1.88E+00	8.62E-01	-5.74E-04	80.94	1.11E-02	3.29E-02	4.40E-02	0.20	0.31	1.44
	l .			-	-		mean	0.13	0.21	1.63
							median	0.15	0.21	1.53

Table A-7 Set 3, Ground type B

T [s]	a	b	С	h	σr ²	${\sigma_e}^2$	σ^2	MEANNR	MEDNR	STDNR
0.00	0.00E+00	0.00E+00	0.00E+00	0.00	0.00E+00	0.00E+00	0.00E+00	0.00	0.00	0.00
0.10	1.43E+00	5.98E-01	-3.25E-03	224.33	5.84E-03	4.06E-02	4.65E-02	0.01	0.04	1.29
0.20	3.20E+00	6.21E-01	-5.52E-03	312.78	6.43E-03	3.00E-02	3.64E-02	0.44	0.57	1.37
0.30	N/A	N/A	N/A	N/A	N/A	N/A	N/A	N/A	N/A	N/A
0.40	N/A	N/A	N/A	N/A	N/A	N/A	N/A	N/A	N/A	N/A
0.50	N/A	N/A	N/A	N/A	N/A	N/A	N/A	N/A	N/A	N/A
0.60	N/A	N/A	N/A	N/A	N/A	N/A	N/A	N/A	N/A	N/A
0.70	N/A	N/A	N/A	N/A	N/A	N/A	N/A	N/A	N/A	N/A
0.80	3.33E+00	9.46E-01	-4.76E-03	261.74	1.47E-02	7.55E-02	9.02E-02	0.36	0.36	0.93
0.90	2.46E+00	9.80E-01	-2.59E-03	158.90	1.40E-02	7.16E-02	8.56E-02	0.07	0.03	0.94
1.00	2.64E+00	9.95E-01	-2.99E-03	169.84	1.35E-02	8.51E-02	9.86E-02	0.15	0.16	0.91
1.10	2.73E+00	1.03E+00	-3.16E-03	173.61	1.36E-02	9.37E-02	1.07E-01	0.20	0.20	0.90
1.20	2.72E+00	1.07E+00	-3.18E-03	167.72	1.50E-02	8.80E-02	1.03E-01	0.19	0.26	0.90
1.30	2.87E+00	1.09E+00	-3.56E-03	189.49	1.62E-02	7.31E-02	8.94E-02	0.06	0.25	0.94
1.40	3.05E+00	1.10E+00	-3.92E-03	214.40	1.58E-02	6.95E-02	8.53E-02	0.04	0.11	0.95
1.50	3.07E+00	1.12E+00	-4.00E-03	214.14	1.54E-02	6.30E-02	7.84E-02	0.06	0.02	0.98
1.60	2.84E+00	1.13E+00	-3.50E-03	187.09	1.54E-02	5.70E-02	7.24E-02	0.01	0.11	1.01
1.70	2.72E+00	1.14E+00	-3.22E-03	174.56	1.46E-02	5.14E-02	6.60E-02	0.04	0.10	1.04
1.80	2.70E+00	1.15E+00	-3.16E-03	174.39	1.40E-02	4.79E-02	6.20E-02	0.03	0.07	1.07
1.90	2.63E+00	1.16E+00	-3.01E-03	166.20	1.38E-02	4.48E-02	5.87E-02	0.03	0.14	1.08
2.00	2.78E+00	1.16E+00	-3.47E-03	178.88	1.41E-02	4.44E-02	5.85E-02	0.01	0.05	1.08
2.10	2.95E+00	1.16E+00	-3.91E-03	196.78	1.40E-02	4.49E-02	5.89E-02	0.07	0.00	1.06
2.20	3.06E+00	1.17E+00	-4.16E-03	207.11	1.30E-02	4.53E-02	5.83E-02	0.08	0.00	1.06
2.30	2.92E+00	1.17E+00	-3.82E-03	193.05	1.21E-02	4.67E-02	5.88E-02	0.02	0.08	1.06
2.40	2.78E+00	1.18E+00	-3.47E-03	179.59	1.16E-02	4.79E-02	5.95E-02	0.01	0.10	1.07

	1									
2.50	2.67E+00	1.18E+00	-3.19E-03	167.80	1.25E-02	4.93E-02	6.18E-02	0.02	0.10	1.08
2.60	2.58E+00	1.18E+00	-2.95E-03	158.59	1.29E-02	4.91E-02	6.21E-02	0.03	0.13	1.09
2.70	2.57E+00	1.18E+00	-2.88E-03	159.65	1.34E-02	4.79E-02	6.13E-02	0.03	0.11	1.10
2.80	2.63E+00	1.18E+00	-3.04E-03	168.58	1.35E-02	4.83E-02	6.18E-02	0.02	0.09	1.11
2.90	2.58E+00	1.18E+00	-2.89E-03	166.53	1.38E-02	4.83E-02	6.21E-02	0.02	0.10	1.12
3.00	2.55E+00	1.18E+00	-2.78E-03	165.02	1.44E-02	4.73E-02	6.17E-02	0.02	0.10	1.13
3.10	2.52E+00	1.18E+00	-2.73E-03	161.64	1.49E-02	4.69E-02	6.18E-02	0.01	0.06	1.13
3.20	2.51E+00	1.17E+00	-2.72E-03	159.83	1.49E-02	4.72E-02	6.21E-02	0.01	0.02	1.15
3.30	2.50E+00	1.17E+00	-2.72E-03	159.36	1.46E-02	4.75E-02	6.22E-02	0.01	0.03	1.15
3.40	2.49E+00	1.17E+00	-2.70E-03	158.85	1.45E-02	4.80E-02	6.24E-02	0.01	0.03	1.15
3.50	2.47E+00	1.17E+00	-2.62E-03	156.61	1.45E-02	4.85E-02	6.30E-02	0.01	0.03	1.15
3.60	2.45E+00	1.17E+00	-2.58E-03	156.91	1.44E-02	4.85E-02	6.29E-02	0.00	0.04	1.15
3.70	2.48E+00	1.17E+00	-2.64E-03	161.49	1.43E-02	4.86E-02	6.30E-02	0.01	0.01	1.16
3.80	2.54E+00	1.16E+00	-2.80E-03	169.90	1.40E-02	4.87E-02	6.27E-02	0.04	0.01	1.17
3.90	2.62E+00	1.16E+00	-3.00E-03	181.41	1.37E-02	4.94E-02	6.31E-02	0.07	0.01	1.17
4.00	2.68E+00	1.16E+00	-3.14E-03	189.85	1.35E-02	5.02E-02	6.37E-02	0.09	0.00	1.17
							mean	0.06	0.09	1.07
							median	0.03	0.08	1.08

Table A-8 Set 3, Ground type C

References

- Akkar, S. (2016, Noiembrie 28). *Utility Software for Data Processing*. Retrieved from USDP: http://web.boun.edu.tr/sinan.akkar/usdp1.html
- Akkar, S., & Bommer, J. (2007). Empirical Prediction Equations for Peak Ground Velocity Derived from Strong-Motion Records from Europe and the Middle East. *Bulletin of the Seismological Society of America*, 511-530.
- Allen, T., & Wald, D. (2007). Topographic Slope as a Proxy for Seismic Site-Conditions (Vs 30) and Amplification Around the Globe. *U.S. Geological Survey Open-File Report* 2007-1357, 69p.
- ATC-40. (1996). *Seismic evaluation and retrofit of concrete buildings*. Redwood City, California: Applied Technology Council.
- BIGSEES. (2017, July 7). *Bigsees Earthquake Catalogue*. Retrieved from INFP BIGSEES: http://infp.infp.ro/bigsees/Results.html
- Boore. (2004). Estimating Vs30 (or NEHRP classes) from shallow Velocity Models (Depths<30m). *Bulletin of the Seismological Society of America*, 591-597.
- Boore, D. (2017, Iulie 13). *Data Online*. Retrieved from David Boore: http://www.daveboore.com/data_online.html
- Boore, D., Joyner, W., & Fumal, T. (1997). Equations for Estimating Horizontal Response Spectra and Peak Acceleration from Western North American Earthquakes: A Summary of Recent Work. *Seismological Research Letters*, 128-153.
- Borcia, I. S. (2008). *Procesarea Înregistrărilor Mișcărilor Seismice Vrâncene Puternice*. Iași: Editura Societății Academice Matei-Teiu Botez.
- Cauzzi, C., & Faccioli, E. (2008). Broadband (0.05 to 20 s) prediction of displacement responsespectra based on worldwide digital records. *Journal of Seismology*, 12, 453-475.
- CEN. (2004). European Standard EN 1998-1:2004 Eurocode 8: Design of structures for earthquake resistance, Part 1: General rules, seismic actions and rules for buildings. Brussels: Comite Europeen de Normalisation.
- Chopra, A. K. (2012). Dynamics of Structures Theory and Applications to Earthquake Engineering, 4th Edition. Upper Saddle River: Prentice Hall.
- Chopra, A. K., & Goel, R. K. (2001). Direct Displacement-Based Design: Use of Inelastic Design Spectra Versus Elastic Design Spectra. EERI.
- Crăciun, I., Văcăreanu, R., & Pavel, F. (2016). Spectral Displacement Demands for Strong Ground Motions Recorded During Vrancea Intermediate-Depth Earthquakes. *The 1940 Vrancea Earthquake*. *Issues, Insights and Lessons Learnt* (pp. 169-188). București: Springer Natural Hazards.

- Craifăleanu, I. (2005). *Modele neliniare cu un grad de libertate în inginereia seismică*. Bucharest: MatrixRom.
- Damian, I. (2014). *Aplicarea metodelor bazate pe deplasare la proiectarea seismică a structurilor de hale parter cu stâlpi în consolă de beton armat.* București: Teză de doctorat, UTCB.
- Douglas, J. (2016). *Ground motion prediction equations 1964-2016*. Glasgow, United Kingdom: Department of Civil and Environmental Engineering, University of Strathclyde.
- Faccioli, E., Cauzzi, C., Paolucci, R., Vanini, M., Villani, M., & Finazzi, D. (2007). Long Period Strong Ground Motion and its Use as Input to Displacement Based Design. *Earthquake Geotechnical Engineering*, 4th Conference (pp. 23-51). Thessaloniki: Springer.
- Faccioli, E., Paolucci, R., & Rey, J. (2004). Displacement Spectra for Long Periods. *Earthquake Spectra, Earthquake Engineering Research Institute*, 347-376.
- Frohlich, C. (2006). *Deep Earthquakes*. Cambridge: University Press.
- Goda, K., & Atkinson, G. (2009). Seismic Demand Estimation of Inelastic SDOF Systems for Earthquakes in Japan. *Bulletin of the Seismological Society of America*, 3284–3299.
- Gutunoi, A., & Zamfirescu, D. (2013). Study on Relation Between Inelastic and Elastic Displacement for Vrancea Earthquakes. *Mathematical Modelling in Civil Engineering*, Doi:10,2478/mmce-2013-0016.
- INFP. (2017, July 7). Seismicitatea României. Retrieved from INFP: http://www.infp.ro/desprecutremure/#ch 8
- Ismail-Zadeh, A., Mueller, B., & Schubert, G. (2005). Three-dimensional numerical modeling of contemporary mantle flow and tectonic stress beneath the earthquake-prone southeastern Carpathians based on integrated analysis of seismic, heat flow, and gravity data. *Physics of the Earth and Planetary Interiors*, 81-98.
- Joyner, W., & Boore, D. (1993). Methods for Regression Analysis of Strong-Motion Data. *Bulletin of the Seismological Society of America*, 469-487.
- Joyner, W., & Boore, D. (1994). Errata Methods for Regression Analysis of Strong-Motion Data. Bulletin of the Seismological Society of America, 955-956.
- Kashima, T. (2016, Noiembrie 27). *ViewWave*. Retrieved from ViewWave v 2.2.2.0: http://smo.kenken.go.jp/~kashima/viewwave
- Lungu, D., & Ghiocel, D. (1982). *Metode Probabilistice în Calculul Construcțiilor*. București: Editura Tehnică.
- Lungu, D., Aldea, A., Arion, C., & Văcăreanu, R. (2003). Hazard, Vulnerabilitate și Risc Seismic. In D. Dubină, & D. Lungu, Construcții amplasate în zone cu mișcări seismice puternice. Hazard, vulnerabilitate și risc seismic. Structuri performante din oțel pentru clădiri amplasate în zone seismice (pp. 21-157). Timișoara: Editura Orizonturi Universitare.

- Lungu, D., Văcăreanu, R., Aldea, A., & Arion, C. (2000). *Advanced Structural Analysis*. Bucharest: Conspress.
- MDRAP. (2013). *P100-1/2013*. București, România: Ministerul Dezvoltării Regionale și a Administrației Publice.
- Michel, C., Lestuzzi, P., & Lacave, C. (2014). Simplified non-linear seismic displacement demand prediction for low period structures. *Bulletin of Earthquake Engineering*, DOI 10.1007/s10518-014-9585-1.
- Miranda, E., & Ruiz Garcia, J. (2003). Inelastic displacement ratios for evaluation of existing structures. *Earthquake Engineering and Structural Dynamics*, 1237-1258.
- Miranda, E., & Ruiz-Garcia, J. (2007). Probabilistic estimation of maximum inelastic displacement demands for performance-based design. *Earthquake Engineering and Structural Dynamics*, 1235–1254.
- NASA. (2002, October 6). *Digital Tectonic Activity Map*. Retrieved from Visible Earth în iulie 2017: https://visibleearth.nasa.gov/view.php?id=88415
- Neagu, C., Arion, C., Aldea, A., Văcăreanu, R., & Pavel, F. (2017). Ground Types for Seismic Design in Romania. 6th National Conference on Earthquake Engineering & 2nd National Conference on Earthquake Engineering and Seismology Proceedings (pp. 345-352). București: Publishing Conspress.
- Priestley, M., Calvi, G., & Kowalsky, M. (2007). *Displacement-Based Seismic Design Of Structures*. Pavia, Italy: IUSS Press.
- Scherbaum, F., Delavaud, E., & Riggelsen, C. (2009). Model Selection in Seismic Hazard Analysis: An Information-Theoretic Perspective. *Bulletin of the Seismological Society of America*, 3234-3247.
- Seismosoft. (2016, Noiembrie 28). *Seismosignal 2016*. Retrieved from Seismosoft: http://www.seismosoft.com/seismosignal
- Strong Motion Seismograph Networks (K-NET, KiK-net). (2017, Ianuarie 30). Retrieved from National Research Institute for Earth Science and Disaster Resilience: http://www.kyoshin.bosai.go.jp/
- Sucuoglu, H., & Akkar, S. (2014). *Basic Earthquake Engineering. From Seismology to Analysis and Design.* Springer International Publishing Switzerland.
- Trendafiloski, G., Wyss, M., Rosset, P., & Marmureanu, G. (2009). Constructing City Models to Estimate Losses Due to Earthquakes Worldwide: Application to Bucharest, Romania. *Earthquake Spectra*, 22p.
- USGS. (2017, Iulie 13). Vs30 Data. Retrieved from USGS: https://earthquake.usgs.gov/data/vs30/
- Văcăreanu, R., Pavel, F., Aldea, A., Arion, C., & Neagu, C. (2015). *Elemente de analiză a hazardului seismic*. București: Conspress.

- Veletsos, A. S., Newmark, N. M., & Chelapati, C. V. (1965). Deformation Spectra for Elastic and Elastoplastic Systems Subjected to Ground Shock and Earthquake Motions. *Proc. 3rd World Conference on Earthquake Engineering*, (pp. 663-682). New Zealand.
- Wells, D. L., & Coppersmith, K. J. (1994). New Empirical Relationships among Magnitude, Rupture Length, Rupture Width, Rupture Area, and Surface Displacement. *Bulletin of the Seismological Society of America*, 974-1002.